UiT The Arctic University of Norway

Faculty of Biosciences, Fisheries and Economics
Department of Arctic and Marine Biology

Molecular adaptations to diving-induced hypoxia

Diurnal variations in cellular and mitochondrial hypoxia tolerance in the hooded seal (*Cystophora cristata*)

Chiara Ciccone

A dissertation for the degree of Philosophiae Doctor

July 2024

Molecular adaptations to diving-induced hypoxia

Diurnal variations in cellular and mitochondrial hypoxia tolerance in the hooded seal (*Cystophora cristata*)

Chiara Ciccone

A dissertation for the degree of Philosophiae Doctor – July 2024

UiT – The Arctic University of Norway

Faculty of Biosciences, Fisheries and Economics

Department of Arctic and Marine Biology

Arctic Chronobiology and Physiology Research Group

Cover photo: Fredrik Markussen

Or poserai per sempre,
Stanco mio cor.
Perì l'inganno estremo,
Ch'eterno io mi credei. Perì.
Ben sento,
In noi di cari inganni,
Non che la speme, il desiderio è spento
Posa per sempre. Assai
Palpitasti.
Non val cosa nessuna
I moti tuoi, né di sospiri è degna
La terra.
Amaro e noia
La vita, altro mai nulla; e fango è il mondo.
T'acqueta ormai. Dispera
L'ultima volta. Al gener nostro il fato
Non donò che il morire. Omai disprezza
Te, la natura, il brutto
Poter che, ascoso, a comun danno impera,
E l'infinita vanità del tutto.

A se stesso
G. Leopardi, 1835

Table of contents

I. Acknowledgements

It is a life of hopes and disappointments, and yet a life not without pleasant memories for many of us.

Fridtjof Nansen, "The first crossing of Greenland"

Finally, the end. Two cancelled fieldworks, uncountable failed western blots, millions of dead cells, and not so few tears later, finally here I am. At certain times I thought this moment would never arrive and now that it's here I still can't believe it. This almost 5 years have been a rollercoaster of emotions and I always thought that I was going to fill in a "list of complaints" rather than some acknowledgments but now, looking back, I recognise that there is so much I have to be grateful for.

First of all, my supervisors: each one of you, in your own way, has given me more than any other PhD student could hope for. Lars, thank you for all the support over the years, from my first day coming to your office as a master student until now, and for always being there: I have learned so much from you and I can't even explain how grateful I am to have had you as supervisor for these many years. Shona, thank you for being such a great example of what women in science can do and for always making sure that my imposter syndrome was not taking over. Most importantly, I will never forget our victory taco on the Helmer Hansen! David, for always being my most critical reviewer number 2 and for always asking those uncomfortable questions. Alex, thank you not only for all the incredible help in the lab but also for all the times I've come to your office in tears, and you always found the time to listen to me: without your support probably most of the experiments in this thesis wouldn't have happened at all.

To my officemates Jayme and Fredrik for all the little chats in the office, the loud typing, and the silent company. To Daniel and Fernando, for listening to me complaining about writing and for always telling me that everything was going to be fine. To all my fellow PhD students Anna, Jana, Vebjørn, and Therese: you have all been wonderful companions in this amazing journey. Barbara, thank you for all our "bus talks", they have been of great help especially in the last months.

To all my students, for showing me that patience is indeed one of my qualities. A special shout out to Fayiri: for your enthusiasm towards science, for the nights spent working with the Oroboros and for never disappearing despite being far away.

To my friends here and back home. Sandra and Alicia, thank you for always believing in me even when I didn’t. Veronica and Simona, thank you for supporting me even from very far away and for being the sisters I never had.

To Annalisa, Caterina, Daniele, Domenico, Emanuel, Giacomo, Giulia, Maurizio, Sara and the little Helene and Viola. For your friendship and for making me miss my family a little bit less.

Freddy, for how unexpectedly you arrived in my life and for everything you do every day.

Lastly, I would like to thank everyone in my family. Particularly my cousin Sara, for being my big sister and for always listening. And finally my mum: for everything you did for me over the years and, most of all, for having shared some of your mitochondria with me.

II. Thesis abstract

Hypoxia may be defined as a state of O_2 deficiency in which cellular energetic homeostasis is challenged. Prolonged exposure to hypoxia can lead to a bioenergetic collapse as it induces a switch from mitochondrial oxidative metabolism to a mainly glycolytic one, which is not sustainable over time. Recent evidence shows that mitochondrial metabolic response to hypoxia also depends on the circadian clock. Although most species are not able to tolerate hypoxia over time, some live permanently or periodically under hypoxic conditions. Breath-hold diving mammals, like the deep-diving hooded seal (*Cystophora cristata*), display a set of systemic and cellular/molecular adaptations that convey them enhanced hypoxia tolerance. It has been hypothesised that the hooded seal brain is endowed with alternate metabolic pathways between neurons and astrocytes, in which neurons may periodically rely on glycolysis, with astrocytes metabolising the produced lactate, enabling their brain to tolerate repeated exposure to severely hypoxic conditions. The objectives of this thesis were to investigate 1) mitochondria-clock interactions in this hypoxia-tolerant species and 2) the role of mitochondrial oxidative metabolism in hooded seal neurons and astrocytes.

In **paper I**, we show that hooded seals display diurnal variation in diving behaviour, with longer dives during day than night. Further, by using primary skin fibroblasts we characterised the hooded seal circadian clock: two core clock genes displayed circadian expression which was maintained also under constant conditions. Finally, we show the presence of a clock-mediated change in mitochondrial metabolic efficiency, possibly in coordination with daily changes in diving efforts. In **paper II**, we found that adult hooded seal astrocytes have higher mitochondrial density than seal neurons, which is opposite to the situation in mice. In addition, via high resolution respirometry of primary astrocytic and neuronal cultures, we show that mitochondria of hooded seal astrocytes have a similar or possibly higher oxidative capacity than neurons. Finally, in **paper III**, we present three cell lines immortalised from hooded seal primary astrocytes that may serve as *in vitro* models in future studies into brain function and hypoxia tolerance in diving mammals. High resolution respirometry showed that these astrocytic cell lines have the capacity to oxidise both glucose and lactate for mitochondrial energy production.

Overall, the results presented in this thesis work highlight the importance of regulation of mitochondrial oxidative metabolism in hypoxia tolerance physiology and add new knowledge on some of the various hypoxia-induced adaptations in a remarkable species such as the hooded seal.

III. List of papers

Paper I

Circadian coupling of mitochondria in a deep diving mammal

Chiara Ciccone, Fayiri Kante, Lars P. Folkow, David G. Hazlerigg, Alexander C. West, Shona H. Wood

Arctic Seasonal Timekeeping Initiative (ASTI), Arctic Chronobiology and Physiology research group, Department of Arctic and Marine Biology, UiT – The Arctic University of Norway, Tromsø NO-9037, Norway.

Journal of Experimental Biology, 2024: jeb246990 doi: 10.1242/jeb.246990

Paper II

The metabolic roles of neurons and astrocytes in the diving brain

Chiara Ciccone[1], Sari Elena Dötterer[1], Cornelia Geßner[2], Alexander C. West[1], Shona H. Wood[1], David G. Hazlerigg[1], Lars P. Folkow[1]

Arctic Chronobiology and Physiology research group, Department of Arctic and Marine Biology, UiT – The Arctic University of Norway, Tromsø NO-9037, Norway.

[2]Institute of Forest Genetics, Thünen Institute, Braunschweig, Germany

Advanced manuscript

Paper III

AstroSel: a stable astrocytic cell line to study hypoxia tolerance and lactate oxidation in the brain of an Arctic pinniped

Chiara Ciccone, Shona H. Wood, David G. Hazlerigg, Lars P. Folkow, Alexander C. West

Arctic Seasonal Timekeeping Initiative (ASTI), Arctic Chronobiology and Physiology research group, Department of Arctic and Marine Biology, UiT – The Arctic University of Norway, Tromsø NO-9037, Norway.

Advanced manuscript

Authors Contributions

	Paper I	**Paper II**	**Paper III**
Concept and idea	CC, DGH, ACW, SHW	LPF, CC, SED	CC, ACW
Study design and methods	CC, FK, ACW, SHW, LPF	CC, SED, ACW, DGH, LPF	CC, ACW, LPF
Data gathering and interpretation	CC, FK, ACW, SHW	CC, SED, CG, LPF, SHW	CC, ACW, LPF
Manuscript preparation	CC, DGH, FK, LPF, ACW, SHW	CC, SED, LPF, SHW, CG, DGH, ACW	CC, ACW, LPF, SHW, DGH

CC = Chiara Ciccone
SHW = Shona H. Wood
ACW = Alexander C. West
FK = Fayiri Kante
LPF = Lars P. Folkow
DGH = David G. Hazlerigg
CG = Cornelia Geßner
SED = Sari E. Dötterer

IV. Abbreviations

Acetyl-CoA	Acetyl coenzyme A
ADL	Aerobic Dive Limit
ADP	Adenosine diphosphate
ANLS	Astrocyte-neuron lactate shuttle hypothesis
ATP	Adenosine triphosphate
Bmal1	Brain and Muscle ARNT-like 1 (gene)
BMAL1	Brain and Muscle ARNT-like 1 (protein)
Clock	Circadian Locomotor Output Cycles Kaput (gene)
CLOCK	Circadian Locomotor Output Cycles Kaput (protein)
CM	Cristae membrane
CO_2	Carbon dioxide
Cry	Cryptochrome Circadian regulator (gene)
CRY	Cryptochrome Circadian regulator (protein)
e^-	Electrons
EMM	External mitochondrial membrane
ETS	Electron transport system
$FAD^{2+}/FADH_2$	Oxidised/reduced flavin adenine nucleotide
Fe-S	Iron-sulfur clusters
FMN	Flavin mononucleotide
GTP	Guanosine triphosphate
H^+	Proton
Hb	Hemoglobin
Hct	Haematocrit
Hif-1 α/β	Hypoxia inducible factor 1 subunit α/ subunit β (gene)
Hif-1 α/β	Hypoxia inducible factor 1 subunit α/ subunit β (mRNA)
HIF-1 α/β	Hypoxia inducible factor 1 subunit α/ subunit β (protein)
HRR	High Resolution Respirometry
IBM	Inner boundary membrane
IMM	Internal mitochondrial membrane
LDH	Lactate dehydrogenase
M1/M2	Mortality stage 1/2
MAS	Malate-aspartate shuttle
Mb	Myoglobin
MCT	Monocarboxylate transporter
NAD^+/NADH	Oxidised/reduced nicotinamide adenine dinucleotide
Ngb	Neuroglobin
O_2	Oxygen
OXPHOS	Oxidative phosphorylation
P_aO_2	Arterial O_2 pressure
PDH	Pyruvate dehydrogenase
Pdk1	Pyruvate dehydrogenase kinase 1 (gene)
Pdk1	Pyruvate dehydrogenase kinase 1 (mRNA)
PDK1	Pyruvate dehydrogenase kinase 1 (enzyme)
Per2	Period Circadian Regulator 2 (gene)
PER2	Period Circadian Regulator 2 (protein)
PFK1	6-phospofructo-1-kinase

PFK2	6-phospofructo-2-kinase
PHD	Prolyl hydroxylase
rANLS	Reverse Astrocyte-Neuron Lactate Shuttle hypothesis
RET	Reverse Electron Transfer
SCN	Suprachiasmatic nucleus
SRDL	Satellite Relay Data Loggers
SV40	Simian virus 40
TCA cycle	Tricarboxylic acid cycle
TTFL	Transcription-translational feedback loop
UQ	Ubiquinone
UQH_2	Ubiquinol (reduced ubiquinone)

1 Introduction

1.1 Energy needs and metabolism

All animals require energy to maintain their functions. To understand why, it is necessary to go back to the laws of thermodynamics. According to its second law, every system in the universe is inclined towards a greater disorder unless it receives energy from the outside, where energy can be interpreted as the capacity required to increase order (Chandel, 2021). Animals obtain this energy through the ingestion of food. By breaking down chemical bonds contained in the food, the processes of digestion and cellular respiration release the food chemical energy. The first law of thermodynamics (i.e., law of conservation of energy) states that energy cannot be created or destroyed, but only converted to one form to the other to ensure equilibrium (Chandel, 2021). Therefore, the chemical energy obtained from the food must be used by the organism to perform physiological work, which includes the maintenance processes required for homeostasis (Hill et al., 2012).

There are three major types of physiological work: (1) *chemical work* or *biosynthesis*, for growth and synthesis of new constituents (e.g. proteins); (2) *transport work*, to maintain molecules concentration gradients across membranes; (3) *mechanical work*, to generate movement. Whenever the food chemical energy is used to perform any of these functions, some of it is released as heat. The first to prove that animals can exploit energy in food, turn it into heat, and depend on oxygen in air to do so, was Antoine Lavoisier (1743-1794). He built the first direct calorimeter which consisted of a sealed cage containing a guinea pig, surrounded by a layer of ice placed, in turn, in an isolated chamber. Since the guinea pig was completely isolated, by measuring the amount of melting water, Lavoisier was able to measure the amount of heat it was producing (Duveen and Klickstein, 1954). Although the first law of thermodynamics implies that energy should remain constant, by being a low-grade ('disordered') form of energy, heat cannot be used to perform any type of physiological work or be converted back into other forms of energy (Hill et al., 2012). This implies that heat energy cannot be recycled and, therefore, animals need to meet their energetic needs by regularly ingesting food.

The set of reactions converting the food chemical energy into energy for physiological work constitutes the organism's metabolism. At the cellular level, there are two major forms of

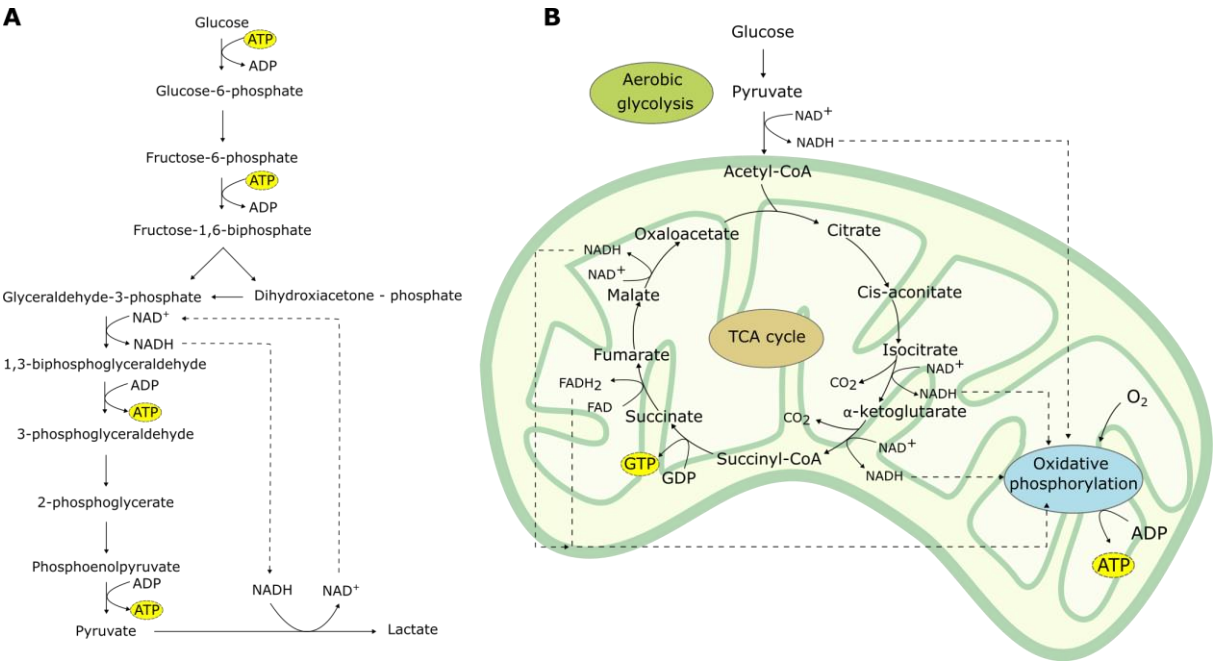

Figure 1. Anaerobic vs aerobic catabolic metabolism of glucose. A) Anaerobic glycolysis. The end-product pyruvate is converted into lactate, which allows the re-oxidation of NADH into NAD^+. This guarantees a continuous supply of reducing agents (NAD^+) for glycolysis to continue over time. **B)** Aerobic glycolysis and tricarboxylic acid (TCA) cycle. The glycolytic end-product, pyruvate, is converted into Acetyl coenzyme A (Acetyl-CoA) which enters the mitochondria and takes part in the TCA cycle. Aerobic glycolysis and TCA cycle produce the substrates NADH and $FADH_2$, both used for the process of oxidative phosphorylation which consumes O_2 to produce ATP. Illustration by C. Ciccone.

metabolism: *catabolism*, converting nutrients into simple molecules and generating energy, and *anabolism*, converting simple molecules to bigger structures, in a process that consumes energy (Chandel, 2021). In the cell, the energy is provided in the form of phosphorylated organic compounds, of which adenosine triphosphate (ATP) is considered as the universal energy carrier. The cellular energetic equilibrium is, thus, determined by the rate at which ATP is synthesized and consumed (Suarez, 2012). The catabolic pathways that synthesize ATP can be *aerobic*, which require oxygen (O_2), or *anaerobic*, which can function without O_2. Anaerobic glycolysis is a classic example of a catabolic pathway which does not need O_2 to produce ATP (Figure 1A). This is a series of 10 enzymatic reactions taking place in the cytoplasm of the cell that convert a molecule of glucose into 2 molecules of pyruvate. Although using 2 molecules of ATP, glycolysis produces 4 molecules of ATP, therefore its net energy yield is 2 ATP per each molecule of glucose. For anaerobic glycolysis to sustain itself overtime, it is necessary to have enough of the reducing agent nicotinamide adenine dinucleotide (NAD^+). NAD^+ is converted to its reduced form (NADH) during the oxidation of glyceraldheyde-3-phosphate into 1,3-biphosphoglyceraldheyde (Figure 1A). To avoid NADH accumulation and NAD^+ shortage, the end-product, pyruvate, is typically converted to lactate, a reaction involving the re-oxidation of NADH into NAD^+ (Figure 1A).

As Lavoisier discovered (Duveen and Klickstein, 1954), organisms also need O_2 in order to combust (i.e., oxidise) the ingested food. Using O_2, the aerobic catabolic pathway yields 30-32 molecules of ATP per glucose: 15-16 times more energy than anaerobic glycolysis. There are three major groups of metabolic reactions involved in the aerobic production of ATP: (1) aerobic glycolysis, (2) tricarboxylic acid (TCA) cycle and (3) oxidative phosphorylation (OXPHOS) (Figure 1B). The aerobic glycolysis consists of the same 10 enzymatic reaction of anaerobic glycolysis (Figure 1A), but pyruvate is now shuttled to the mitochondria and converted into Acetyl coenzyme A (Acetyl-CoA), allowing the reduction of NAD^+ to NADH. In the mitochondria, Acetyl-CoA reacts with oxaloacetate and enters the enzymatic reactions of the TCA cycle (Figure 1B). Four products are obtained from the TCA cycle: carbon dioxide (CO_2), guanosine triphosphate (GTP), NADH and flavin adenine nucleotide ($FADH_2$). GTP can donate its phosphate group to a molecule of adenosine diphosphate (ADP), thereby contributing to ATP production. NADH and $FADH_2$ are used in the OXPHOS process where, at the expense of a molecule of O_2, ATP is synthesized. However, before entering the details of OXPHOS, it is important to describe the organelles where it all takes place: the mitochondria.

1.1.1 Mitochondria

Classic textbooks define the mitochondria as the "powerhouse of the cell" since they are the organelles where ATP is produced. These subcellular organelles were first identified in the 1890s (Altmann, 1894), but it was not until the 1950s that their ultrastructure was described (Palade, 1952; Palade, 1953). Mitochondria are double-membraned organelles with an external mitochondrial membrane (EMM) and an internal mitochondrial membrane (IMM), separated by the intermembrane space (Palade, 1952; Smoly et al., 1970) (Figure 2). The IMM folds into ridges named *cristae mitochondriales* and it contains the so-called mitochondrial *matrix* (Palade, 1953). More recent analysis have shown that the IMM is sub-compartmentalized into the inner boundary membrane (IBM) and the cristae membrane (CM), identified as the main site of OXPHOS (Vogel et al., 2006) (Figure 2).

As already mentioned, OXPHOS is dependent on the NADH and $FADH_2$, produced by aerobic glycolysis and by the TCA cycle, to convert chemical energy into its useful format, ATP.

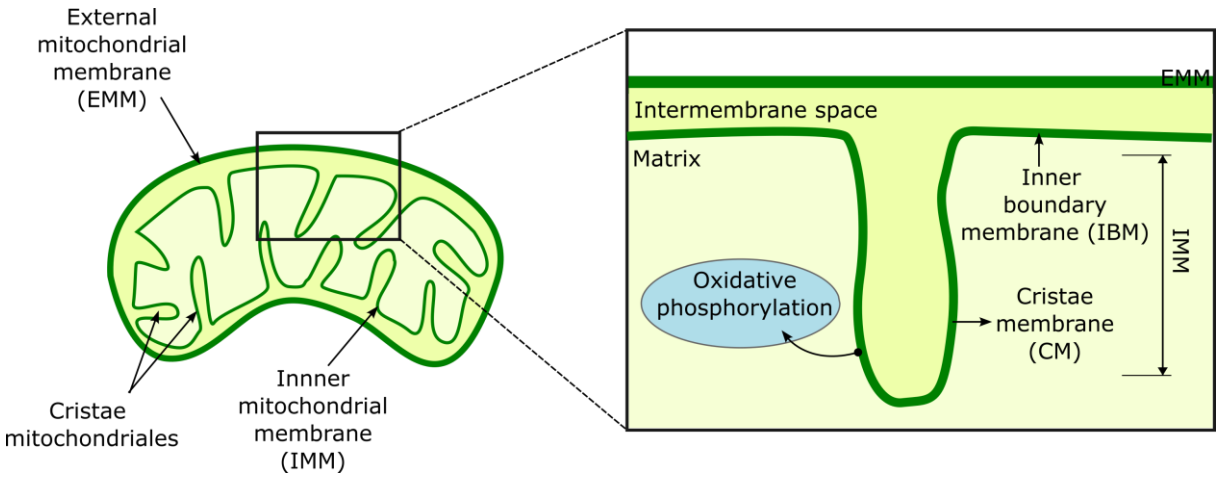

Figure 2. Mitochondrial ultrastructure. On the left: schematic representation of a mitochondrion surrounded by a double membrane consisting of the external mitochondrial membrane (EMM) and the internal mitochondrial membrane (IMM). In the rectangle: schematic representation of the IMM sub-compartments. The intermembrane space is enclosed between the EMM and IMM, while the matrix is delimited by the IMM which folds into the so-called cristae mitochondriales. The IMM may be said to consist of the inner boundary membrane (IBM) and the cristae membrane (CM), where most of the electron transport system (ETS) complexes are located, making it the major site of oxidative phosphorylation (OXPHOS). Illustration by C. Ciccone.

NADH and $FADH_2$ are re-oxidised to NAD^+ and FAD^{2+} by a group of enzymes located on the IMM, which together are referred to as the electron transport system (ETS). The ETS is composed of 4 enzymes (complexes I to IV) that, by oxidising NADH and $FADH_2$, carry electrons (e^-) along the IMM until they are transferred to their final acceptor: O_2 (Figure 3).

Complex I, consisting of 45 subunits, is the largest membrane-bound enzyme in the ETS (Brandt, 2006; Carroll et al., 2006). It is a NADH ubiquinone oxidoreductase with the role of oxidising the NADH into NAD^+ while transferring electrons within the IMM (Figure 3). The enzyme contains a noncovalently bound flavin mononucleotide (FMN) which receives e^- through the oxidation of NADH. These electrons are then transferred through an iron-sulfur clusters (Fe-S) to ubiquinone (UQ), a lipid-soluble compound also known as coenzyme Q (Walker, 1992). While transporting e^- across the IMM, complex I also transfers 4 protons (H^+) from the mitochondrial matrix to the intermembrane space.

Just like complex I, complex II also has the role of transferring e^- to UQ (Figure 3). Complex II is a succinate-ubiquinone oxidoreductase composed by 4 subunits (SDHA, SDHB, SDHC and SDHD) and it has a role in both the TCA cycle and the ETS (Van Vranken et al., 2015). In the mitochondrial matrix, the SDHA subunit takes part in the TCA cycle by converting succinate into fumarate while reducing FAD^{2+} into $FADH_2$. The subunit SDHB contains an Fe-

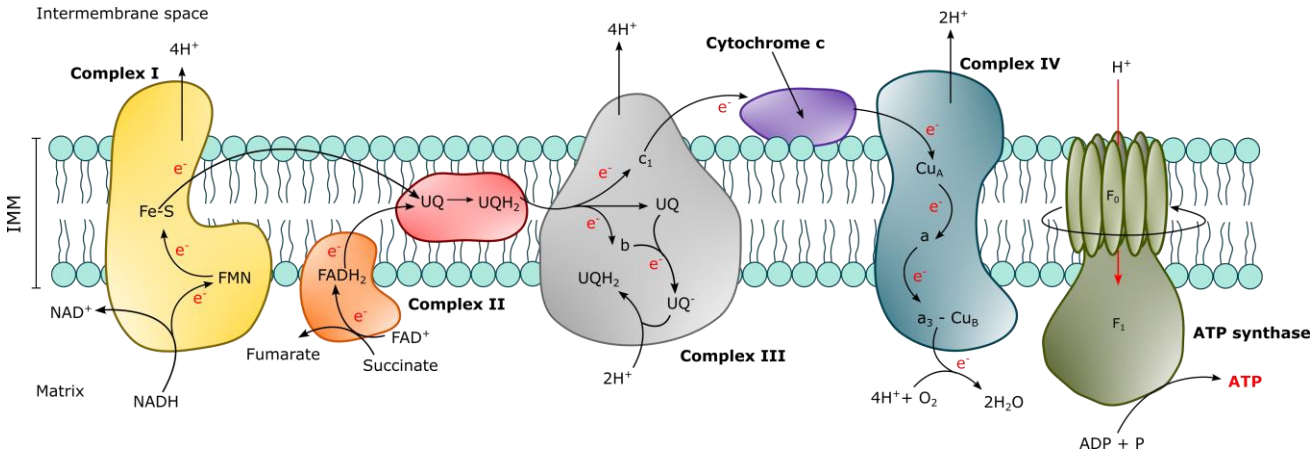

Figure 3. The mitochondrial electron transport system (ETS). The ETS is located in the inner mitochondrial membrane (IMM) and consists of 4 enzymatic complexes. Complexes I and II transport electrons (e^-) to ubiquinone (UQ) through a series of oxidations and reductions. These e^- are then transferred through an H^+-linked transport to complex III which passes them to complex IV through cytochrome c. At complex IV, O_2 can act as final electron acceptor and be reduced to water. While transporting e^-, complexes I, III and IV create a gradient of H^+ across the membrane, from the intermembrane space and inwards, to the matrix. The gradient is used by ATP synthase (also referred to as complex V) to combine ADP with a phosphate group (P) to generate ATP. Illustration by C. Ciccone.

S which acts as anchor mediating translocation of e^- to the membrane-bound subunits SDHC and SDHD. From here, the reoxidation of $FADH_2$ into FAD^{2+} ensures the transfer of e^- to UQ (Van Vranken et al., 2015). The e^- from complexes I and II are transferred to UQ through an H^+-linked transport which reduces UQ to ubiquinol (UQH_2). To be re-oxidised and be ready to receive new H^+ and e^-, UQH_2 transfers e^- to complex III, also known as cytochrome *b*-c_1 (Rieske, 1976). The e^- from UQH_2 are passed to the cytochrome *b* unit generating oxidised UQ and another molecule of UQH_2 by using $2H^+$ from the mitochondrial matrix; instead, the e^- passed to the cytochrome c_1 unit are transferred to cytochrome *c* while $4H^+$ are pumped into the intermembrane space (Figure 3). Cytochrome *c* is a water-soluble compound which passes e^- to complex IV, the cytochrome *c* oxidase. In mammals, complex IV is composed of 13 subunits and is considered to be the key enzyme regulating OXPHOS, since it is where O_2 is consumed (Capaldi, 1990; Li and Deng, 2006). Here, e^- are passed first to the Cu_A centre and then to heme centre *a*. The further passage of e^- to the heme centre $a_3 - Cu_B$ causes the reduction of molecular O_2, the final electron acceptor (Figure 3). The last reaction requires $4H^+$ from the mitochondrial matrix to generate 2 molecules of H_2O (Capaldi, 1990).

In addition to transporting e^- along the IMM, complexes I, III and IV also pump H^+ into the intermembrane space (Figure 3). This generates an electrochemical gradient of H^+ across the IMM which is used by an ATP synthase (often referred to as complex V) to generate ATP. The ATP synthase has two main regions: F_0 in the IMM and F_1 in the matrix. F_0 is composed of a

rotating subunit which dissipates the H^+ gradient while the interaction between F_0 and F_1 ensures the binding of ADP with a phosphate group (P) to generate ATP (Boyer, 1993).

1.2 Brain metabolism

O_2, thus, plays a key role in generating cellular ATP. This is valid for all types of mammalian cells and tissues but some of them are more heavily relying on O_2 than others, especially the brain. In humans, despite its small size relative to the total body mass, the brain accounts for up to 20% of the total bodily O_2 consumption (Erecińska and Silver, 2001). The reason is that the brain is where synaptic signalling occurs. This process ensures that information is processed and passed on between the neurons, but it has a high energetic cost (Harris et al., 2012). During synaptic signalling, large amounts of ATP are used by the sodium/potassium pump (Na^+/K^+ ATPase) and the calcium (Ca^{2+}) ATPase, both transporting ions in and out of the cellular membrane to enable the generation of action potentials and the vesicular release of neurotransmitters (Harris et al., 2012).

Neurons, being the cells capable of synaptic signalling, are the major users of ATP. It has been estimated that neuronal signalling accounts for ~80% of the total neuronal energy requirements, while ~20% is destined for nonsignaling mechanisms (e.g., maintenance of membrane resting potential) (Yu et al., 2018). Most of this substantial energetic demand is met by carbohydrate metabolism, through the aerobic oxidation of glucose (Figure 1B). Substrates other than glucose can also be used, like ketone bodies, lactate and pyruvate, although their use is related to special (e.g., starvation, intense exercise) or pathological conditions (e.g. diabetes) (Magistretti and Allaman, 2022). Therefore, glucose is a key substrate to ensure ATP production and it is considered the major energy source of the brain (Dienel, 2019; Sokoloff, 1977).

1.2.1 The astrocyte-neuron lactate shuttle (ANLS) hypothesis

Although neurons are major consumers of ATP, an increase in neuronal activity typically leads to an enhanced glucose uptake not in neurons, but in astrocytes, the most abundant type of glia cell in the brain (Chuquet et al., 2010). Accordingly, the Astrocyte-Neuron Lactate Shuttle (ANLS) hypothesis that was introduced in 1994 states that the high rate of neuronal aerobic metabolism is sustained through metabolic coupling between neurons and astrocytes (Pellerin and Magistretti, 1994).

To illustrate this, let us consider the example of a glutamatergic synapse (Figure 4): When an action potential arises, the presynaptic neuron releases glutamate, which binds to glutamatergic receptors on the postsynaptic membrane, causing depolarization that may allow the signal to continue. Accumulation of glutamate in the extracellular space can be toxic for the cells, therefore glutamate is removed by astrocytes, through co-transport with Na^+ along its concentration gradient, into the cell. Here, glutamate is converted into glutamine, which is transported to the neurons where it is recycled into new glutamate, to be reused for synaptic signalling. The uptake of glutamate by the astrocytes is known to increase the cellular glycolytic rate (Azarias et al., 2011; Pellerin and Magistretti, 1994). This is because the co-transport of glutamate and Na^+ creates an ion imbalance across the astrocytic cellular membrane, which is resolved by Na^+/K^+ ATPase (Figure 4, step 5). The immediate need for ATP by the Na^+/K^+ ATPase increases the rate of astrocytic glycolysis which - although not being as productive as OXPHOS – can produce ATP at a faster rate. The pyruvate from glycolysis in the astrocytes is converted into lactate. This lactate is shuttled to the neurons via monocarboxylate transporters (MCTs) (Figure 4). Here, by being converted back into pyruvate, lactate may be used as main fuel for OXPHOS, instead of glucose. The final result of this metabolic coupling is that astrocytes rely mainly on glycolysis, while neurons rely mainly on OXPHOS (Almeida and Medina, 1997; Pellerin and Magistretti, 1994). Of course, this hypothesis does not exclude that both cell types are still capable of using both metabolic pathways, when needed.

This subdivision of metabolic work implies differences in the distribution of lactate dehydrogenase (LDH) isoenzymes between the two cell types (Bittar et al., 1996). LDH is a tetrameric enzyme that may convert pyruvate into lactate, or lactate back into pyruvate (Dawson et al., 1964). Five different isoforms are known - LDH1 to LDH5 - whose catalytic activity depends on the ratio of the two subunits A and B that constitute them (Cahn et al., 1962). For example, the LDH1 isoenzyme is composed of 4 subunits B, it has a high affinity for lactate and is typically active in aerobic tissues, while LDH5 is made up of 4 subunits A, has a higher affinity for pyruvate and is usually found in lactate-producing tissues (e.g., skeletal muscle; Cahn et al., 1962). Analysis of LDH isoenzymes distribution between neurons and astrocytes have shown that mammalian neurons are typically enriched for LDH1 (Figure 4), supporting the idea of a predominantly aerobic metabolism, as predicted by the ANLS (Bittar et al., 1996).

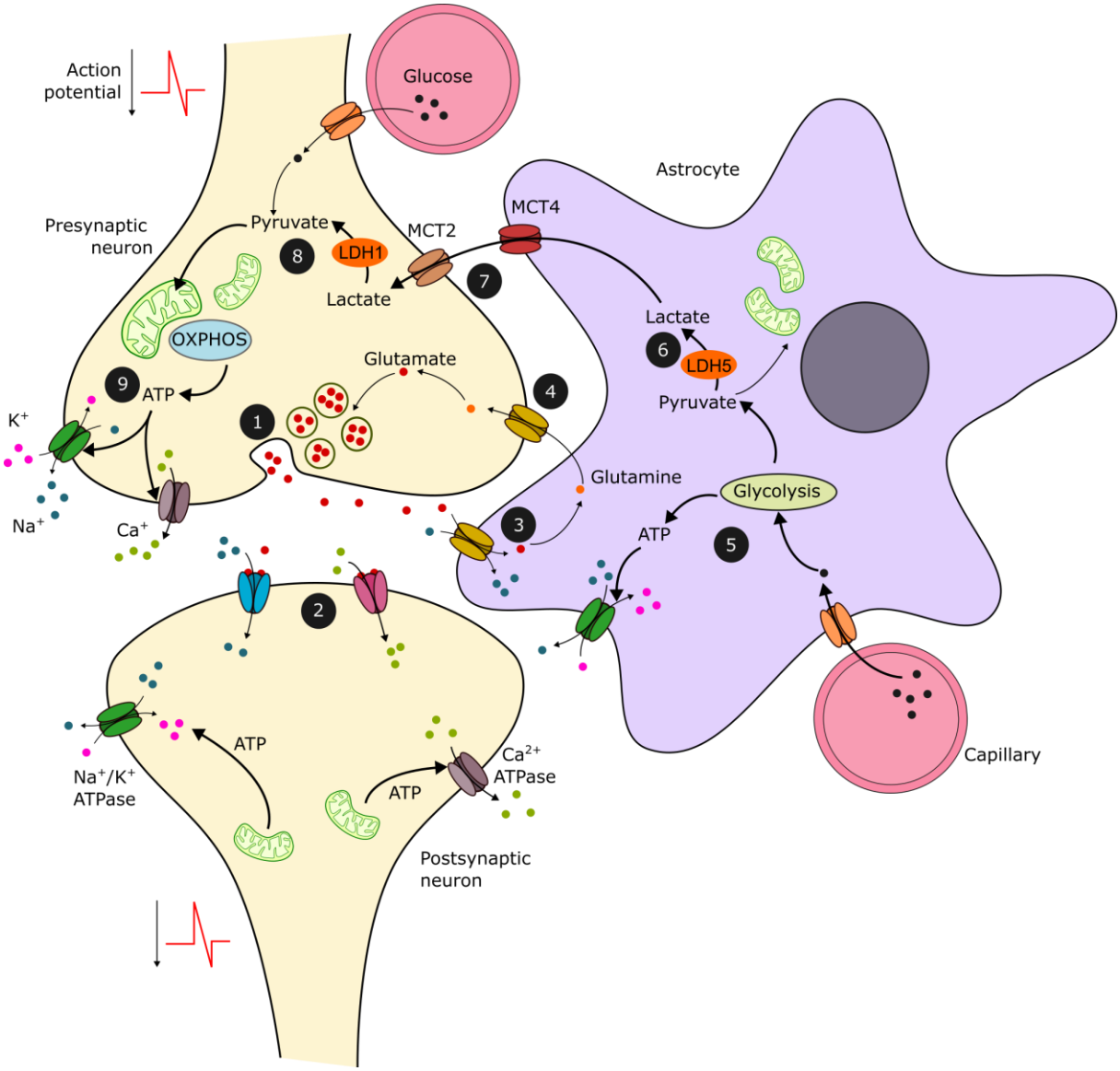

Figure 4. Astrocyte-Neuron Lactate Shuttle (ANLS) hypothesis. Schematic representation of the metabolic coupling between neurons and astrocytes at a glutamatergic synapse. **1)** An action potential arises and causes the release of glutamate (red dots) from the presynaptic neuron. **2)** The glutamate activates the receptors of the postsynaptic neuron, causing inflow of sodium (Na^+, blue dots) and calcium (Ca^{2+}, green dots), which triggers a new action potential. **3)** Glutamate is removed by astrocytic Na^+-glutamate co-transporters. **4)** In the astrocyte, glutamate is converted into glutamine (orange dot) which is transported back to the neuron, to be recycled into new glutamate. **5)** The uptake of glutamate increases the activity of the Na^+/K^+ ATPase which pumps Na^+ out of the astrocyte, in exchange of K^+ (purple dots). The ATP needed for the Na^+/K^+ ATPase activity is supplied by an increased rate of astrocytic glucose uptake (black dots) and glycolysis. **6)** The pyruvate is converted by LDH5 to lactate that **(7)** is shuffled out of the astrocyte via monocarboxylate transporter MCT4 and into the neuron, through MCT2. **8)** In the neuron, lactate is converted by LDH1 into pyruvate, which can enter the TCA cycle and fuel OXPHOS. **9)** This will provide energy to maintain both Na^+/K^+ ATPase and Ca^{2+} ATPase functional and ensure that a new action potential can be triggered.
Thicker arrows represent the preferred metabolic pathways of both cell types according to ANLS: anaerobic glycolysis in astrocytes and OXPHOS for neurons. This does not exclude that both cell types can still produce ATP through alternative metabolic pathways when needed (thinner arrows: glycolysis in neurons and OXPHOS in astrocytes). Black dots: glucose; red dots: glutamate; blue dots: Na^+; green dots: Ca^{2+}; orange dots: glutamine; purple dots: K^+. Redrawn by C. Ciccone from Pellerin and Magistretti (1994) and Harris et al. (2012).

These findings were supported also by a later study showing that astrocytes are enriched for LDH5 (which is absent in neurons), while neurons also showed a high concentration of pyruvate dehydrogenase (PDH), the enzyme converting pyruvate into Acetyl-CoA (Figure 1B) and indicative of a high aerobic metabolism (Laughton et al., 2007).

Another piece of evidence supporting the ANLS theory is given by the distribution of monocarboxylate transporters (MCTs) (Pierre and Pellerin, 2005). These are membrane carriers responsible for the cellular import or export of monocarboxylates compounds, i.e. lactate, pyruvate or ketone bodies (Pierre and Pellerin, 2005). There are 14 different MCT isomers, of which MCT1, MCT2 and MCT4 are localized in the brain (Halestrap and Meredith, 2004; Pierre and Pellerin, 2005). Specifically, MCT1 is localized on endothelial cells and glia cells (including astrocytes), while MCT2 is exclusively expressed by neurons and MCT4 only by astrocytes (Pierre et al., 2000; Pierre et al., 2002; Rafiki et al., 2003). MCT4 is the isoform with the highest affinity for lactate and it is usually expressed by cells with a high rate of lactate export (e.g., muscle), while MTC2 has a lower affinity and is associated with import of lactate (Contreras-Baeza et al., 2019). Therefore, the distribution of MCT2 and MCT4 between neurons and astrocytes also points towards an enhanced export of lactate from the astrocytes (via MCT4) and an enhanced import of lactate into neurons (via MCT2) (Figure 4). This hypothesis has also been confirmed by *in vivo* evidence of a lactate flux in mouse cortex (Mächler et al., 2016).

The most important concept introduced by the ANLS is that the main fuel for oxidative metabolism in neurons is lactate and not glucose (Magistretti and Allaman, 2018). Over the years the hypothesis has been highly debated (e.g., Bak and Walls, 2018; Dienel, 2012), with the main argument being that there is not enough evidence to declare that lactate is the preferred neuronal substrate, when there is, in fact, evidence in favour of neuronal glucose utilization (Dienel, 2012; Tang, 2018). The higher glycolytic rate and lactate production reported for astrocytes has been connected to the higher levels of the regulatory enzyme 6-phospofructo-2-kinase (PFK2) (Herrero-Mendez et al., 2009; Itoh et al., 2003). PFK2 is responsible for the production of fructose-2,6-biphosphate, which acts as allosteric activator of 6-phospofructo-1-kinase (PFK1) (Van Schaftingen et al., 1982), a rate-limiting enzyme of the glycolytic pathway. PFK2 is instead continuously degraded in neurons, technically making them uncapable of increasing their glycolytic rate (Herrero-Mendez et al., 2009). Although this is apparently in favour of the ANLS, many studies have shown that, during activation, neurons are instead

capable of increasing both their glucose uptake and glycolytic rate, while astrocytes show a higher lactate uptake from the extracellular space (Gandhi et al., 2009).

Recent *in vivo* analysis suggests instead that the ANLS mechanism could be functional during rest periods but not during neuronal activation (Díaz-García et al., 2017). Indeed, inhibition of MCTs causes a reduction of neuronal cytosolic NADH at rest, while it does not reduce the transient spike in cytosolic NADH after activation. This supports the hypothesis that during stimulation neurons still predominantly rely on the use of glucose, while the shuttling of lactate from astrocytes to neurons might be taking place only during resting periods (Díaz-García et al., 2017). Moreover, neurons have been shown to change their cell-specific MCTs expression after an ischemic insult, demonstrating that they possess the capacity to either release or take up lactate (Rosafio et al., 2016). Therefore, it is important to understand that ANLS is not to be interpreted as an "all or nothing" mechanism, but, taken together with other lines of evidence, it highlights the versatility of neurons and their ability to use different substrates according to the situation (e.g., cerebral ischemia, brain injury, etc.) (Tang, 2018). As will be discussed later, this ability may play a key role in how some animals and their tissues have adapted to tolerate hypoxia, through related adjustments in cellular substrate use.

1.3 Circadian clocks

To efficiently produce energy, cellular metabolism does not only depend on substrate supply and O_2 availability, but it also needs to be coordinated with the needs of the whole organism. Organisms temporally organise their behaviour and physiology to ensure efficient energy usage on a daily (circadian) and seasonal timescale (Hazlerigg et al., 2023). This temporal organisation extends to the cellular and mitochondrial level (Reinke and Asher, 2019). Therefore, it is important to also consider the temporal mechanisms coordinating cellular metabolism and ATP production.

The rotation of the Earth on its orbit around the Sun exposes our planet to changes in light conditions resulting in an alternating day/night rhythm of 24 hours. Most animals have evolved to adapt both their behaviour and physiology to the Earth's daily and seasonal rhythms. Behavioural and physiological daily rhythms of animals can persist also under constant conditions, with an approximately circadian cycle, indicating that these are not simply driven by the surrounding environmental changes but also rely on an internal system. This is an

endogenous oscillating system which orchestrates the circadian rhythms of an organism: the circadian clock. Circadian rhythms of organisms have three fundamental properties: (1) they are based on an endogenous self-sustained rhythm and therefore persist under constant conditions, (2) they are independent of temperature and (3) they must be able to synchronise to environmental cues (i.e., they must be entrainable). Environmental cues are usually referred to as "Zeitgeber" ("time-giver" in German), which can be of different nature (Dunlap et al., 2004; Johnson et al., 2003). For animals, the most important Zeitgeber is light.

In mammals, information about environmental light is perceived by the eyes' photoreceptors, which then inform the suprachiasmatic nucleus (SCN) in the hypothalamus (Buhr and Takahashi, 2013). The SCN is considered as the *master synchronizer* as it uses the light information to synchronize the endogenous clocks of individual cells and tissues (Buhr and Takahashi, 2013). In the cell, the molecular core of the circadian clock is based on a transcription-translation feedback loop (TTFL) that appears to be well preserved among species (Paranjpe and Sharma, 2005). The mammalian TTFL involves a positive and a negative limb (Figure 5). The positive limb is a heterodimer formed by the genes *Clock* and *Bmal1* (the latter also referred to as *Arntl*). The CLOCK/BMAL1 protein complex binds DNA elements called E-boxes, through which they activate the genes encoding for the negative limb of the TTFL: *Per2* and *Cry* (Buhr and Takahashi, 2013). The formation and accumulation of the PER/CRY protein complex in the cytoplasm inhibits the transcriptional activity of CLOCK/BMAL1 which will result also in lower expression of *Per2* and *Cry* (Figure 5). The subsequent suppression of the PER2/CRY complex activity will give start to a new cycle (Buhr and Takahashi, 2013). This loop is continuously repeated with a period of approximately 24-hours.

The presence of an internal clock gives an organism the ability to survive in its environment, as the entrainment to environmental cycles gives the possibility not only to adapt, but also to anticipate and prepare for changing conditions (Sharma, 2003). For example, by determining patterns of either daily or night activity (e.g. feeding schedule), the ability to avoid predators or competition will increase, together with the chances for survival (Cloudsley-Thompson, 1960). It is clear that the circadian organisation of both behavioural patterns and physiological processes is fundamental for a species' survival (Sharma, 2003).

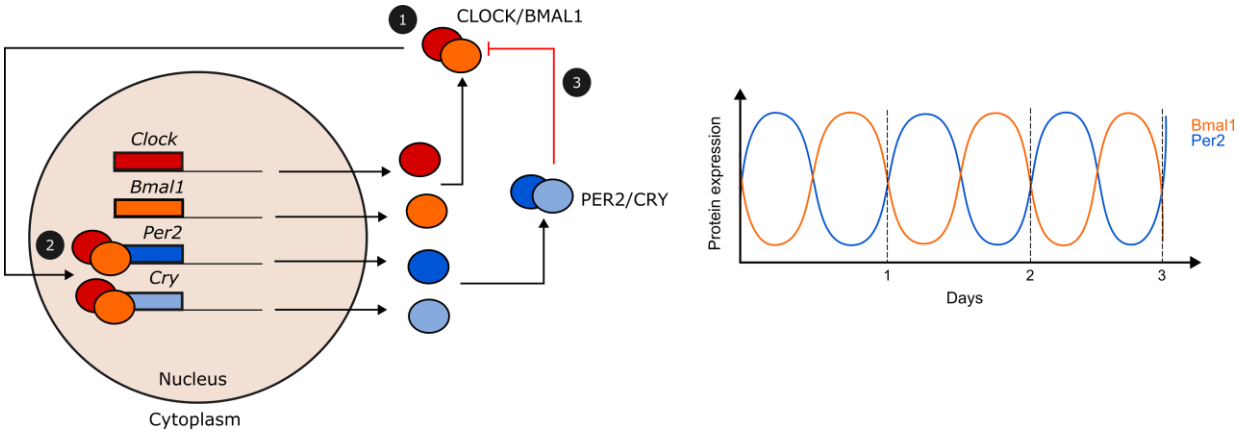

Figure 5. The mammalian transcriptional-translational feedback loop (TTFL). Left panel**: 1)** The two genes *Clock* and *Bmal1* are transcribed and translated into functional proteins and dimerize to form the positive limb of the TTFL**. 2)** The CLOCK/BMAL1 heterodimer translocates into the nucleus where it stimulates the expression of *Per2* and *Cry*, the negative limb of the TTFL. **3)** The PER2/CRY heterodimer inhibits the activity of CLOCK/BMAL1, thereby acting as a repressor of its own gene expression. When the levels of PER2 and CRY reach low enough values, the cycle will start again, with a period of ca. 24 hours. Right panel: schematic representation of the cyclic protein expression of BMAL1 and PER2: both proteins have an expression cycle of 24 hours, but they are in antiphase. Illustration by C. Ciccone.

1.3.1 Circadian clocks and mitochondrial metabolism

In most mammals, several parameters show circadian rhythmicity: body temperature, blood pressure, expression of hormones and also metabolism (Buhr and Takahashi, 2013). Indeed, if feeding activity is subject to a circadian control, the metabolism of the organism will also have to adjust accordingly, in order to maintain metabolic homeostasis (Takahashi et al., 2008). Therefore the synchronization of catabolism and anabolism is also under control of the circadian clock (Asher and Schibler, 2011; Takahashi et al., 2008). For example, the expression of most genes encoding for key metabolic enzymes in the mouse liver has been shown to be under circadian control, and timed according to feeding and fasting time so as to optimize absorption and storage of nutrients for energy production (Panda et al., 2002).

The circadian regulation of metabolism is the result of the circadian regulation of mitochondrial activity which, in turn, is connected to rhythms in both mitochondrial composition and morphology (Manella and Asher, 2016). A large fraction of mitochondrial proteins, thus, presents a circadian expression profile and some of these have a key role in regulating mitochondrial oxidative activity. One example is PDH, which, by transforming pyruvate into Acetyl-CoA, dictates the rate of OXPHOS (Neufeld-Cohen et al., 2016). Mitochondrial function is also related to mitochondrial size and shape, which are both results of the

equilibrium between mitochondrial fusion and fission (Wai and Langer, 2016). The rate of mitochondrial fusion and fission (mitochondrial dynamics) is regulated by specific proteins whose expression is also under circadian control (Jacobi et al., 2015). The synchronization of both mitochondrial protein expression and mitochondrial dynamics results in a fine regulation of mitochondrial activity where, for example, at certain times of the day a larger ratio of mitochondria will be fused, promoting increased OXPHOS, possibly also through concomitant rhythmic changes in PDH levels (Neufeld-Cohen et al., 2016; Wai and Langer, 2016). Further evidence for the importance of the clock-mitochondria interaction comes from studies on clock gene mutations or knock-out studies, which usually result in mitochondrial dysfunctions and disorganization of both OXPHOS and glycolytic rate (Ameneiro et al., 2020; Peek et al., 2013; Peek et al., 2017).

Thus, an imbalance in the circadian organization of mitochondrial activity could cause a desynchronization between anabolism (storage of nutrients) and catabolism (consumption of nutrients) which, in the case of glucose metabolism, for example, could cause the development of metabolic syndromes (e.g., obesity, hyperglycaemia, hypoinsulinemia, etc.) (Takahashi et al., 2008; Turek et al., 2005). The equilibrium between catabolism and anabolism and, therefore, the amount of ATP produced, relies on circadian synchronisation but also on the availability of oxygen.

1.4 Metabolism under hypoxic conditions

As final electron acceptor of the ETS, O_2 availability is critical for mitochondrial OXPHOS. There are, however, situations in which the O_2 availability and delivery to cells and tissues can be impaired. Hypoxia may be defined as the *"state in which oxygen is not available in sufficient amounts at the tissue level to maintain adequate homeostasis"* (Bhutta et al., 2022). Cells and tissues can experience episodes of *physiological hypoxia* during which O_2 levels might temporarily drop, from the normal ~38 mmHg to 15 mmHg or less, and the cellular hypoxic response is initiated (McKeown, 2014). For example, during exercise, skeletal muscle O_2 content might decrease to ~4 mmHg (Richardson et al., 2001), which triggers a series of hypoxia-induced responses, allowing the maintenance of ATP levels for the duration of the exercise (Mason et al., 2004). Brief periods of physiological hypoxia, like the one induced by exercise, allow for restoration of cellular homeostasis and bioenergetic balance once the O_2 content increases back to normal levels. However, prolonged periods of poor oxygenation can

lead to *pathological hypoxia*, a condition instead involved in numerous diseases, like stroke, Alzheimer's, Parkinson's and cancer (Eales et al., 2016; Ogunshola and Antoniou, 2009).

The hypoxia-induced responses involves the adjustment of cellular metabolism via a series of regulatory pathways, some of which are mediated by the hypoxia inducible factor 1 (HIF-1) (Lee et al., 2020; Wheaton and Chandel, 2011). One key effect of the HIF-1-mediated hypoxia response is the lowering of the cellular ATP demands so as to decrease the need for O_2 and avoid a *bioenergetic collapse* and, eventually, cellular death (Lee et al., 2020; Lenihan and Taylor, 2013; Wheaton and Chandel, 2011). One way to reduce oxygen consumption during an hypoxic episode, and thereby prevent the bioenergetic collapse, would be to reduce ETS activity and rather use glycolysis to produce ATP (Kierans and Taylor, 2021; Lee et al., 2020). But, although glycolysis could initially meet the ATP needs of the cell, its very low efficiency compared to OXPHOS, and the accumulation of its product lactate, would eventually lead to energy deficiency, especially during prolonged and repeated hypoxic episodes (Boutilier, 2001; Lee et al., 2020). A lack of ATP would cause the ATPases along the cellular membrane to stop working (e.g., NA^+/K^+ ATPase). This would create an imbalance in the ion distribution across the two sides of the cellular membrane, leading to loss of membrane potential and depolarisation. A depolarisation, in turn, would cause an influx of extracellular Ca^{2+} that would eventually activate a series of proteases and phospholipases, leading to cellular death (Boutilier, 2001; Drew et al., 2004).

1.4.1 The HIF-1 pathway and its role in mitochondrial metabolism regulation

HIF-1 is a heterodimeric protein composed of two subunits: HIF-1α and HIF-1β. Both genes, *Hif-1α* and *Hif-1β*, are routinely transcribed into mRNA at normal O_2 levels, but, while Hif-1β is translated into a functional protein, the HIF1-α protein is hydrolysed by prolyl hydroxylases (PHD). The hydroxylation promotes the binding to the von Hippel-Lindau (VHL) protein, leading to ubiquitination and degradation of HIF-1α (Jaakkola et al., 2001). PHD activity is regulated by O_2 availability and is inhibited during hypoxia (Fong and Takeda, 2008). Therefore, at low O_2 levels, HIF-1α is free to accumulate and dimerize with HIF-1β (Wang et al., 1995). The dimer, HIF-1, acts as a transcription factor and promotes the expression of several genes, among them pyruvate dehydrogenase kinase 1 (*Pdk1*) (Kim et al., 2006; Semenza et al., 1994; Wang and Semenza, 1993). PDK1 inhibits PDH, the enzyme responsible for the conversion of pyruvate into Acetyl-CoA, which will cause a reduction in OXPHOS (Kim et al.,

2006; Papandreou et al., 2006). At the same time, HIF-1 upregulates the expression of glucose transporters (e.g., GLUT1) and some key glycolytic enzymes, like 6-phosphofructo-1-kinase (PFK1) (Semenza et al., 1994), thereby promoting increased glycolytic rate (Henderson, 1969).

The HIF-1 mediated PDK1 activation is also responsible for a reduction in mitochondrial production of reactive oxygen species (ROS) (Kim et al., 2006). Even in normoxia, mitochondria are the major source of ROS, which, at low levels, can act as signalling molecules, but can cause cellular injuries if produced at high rates (Mazat et al., 2020; Reczek and Chandel, 2015). Hypoxic episodes are usually accompanied by a dramatic increase in ROS production by complex III in the ETS (Figure 6) (Bell et al., 2007). This increase in ROS is fundamental for the stabilisation of HIF-1α, which, once dimerised into HIF-1, will decrease OXPHOS via PDK1 activation and bring ROS back to low and unharmful levels (Bell et al., 2007; Kim et al., 2006).

At the same time, the increased complex III-linked ROS production also contributes to the hypoxia-induced reduction in ATP demands. Mitochondrial ROS are indeed partially responsible for the increased intracellular Ca^{2+} levels, typically reported during hypoxic conditions (Bell et al., 2007; Waypa et al., 2002). The elevated Ca^{2+} levels lead to stabilisation of the AMP-activated protein kinase (AMPK), which promotes the endocytosis of the Na^{+}/K^{+} ATPase (Hawley et al., 2005). Since Na^{+}/K^{+} ATPase is the major consumer of cellular ATP, its endocytosis further contributes to decreased energy requirements during hypoxia (Figure 6).

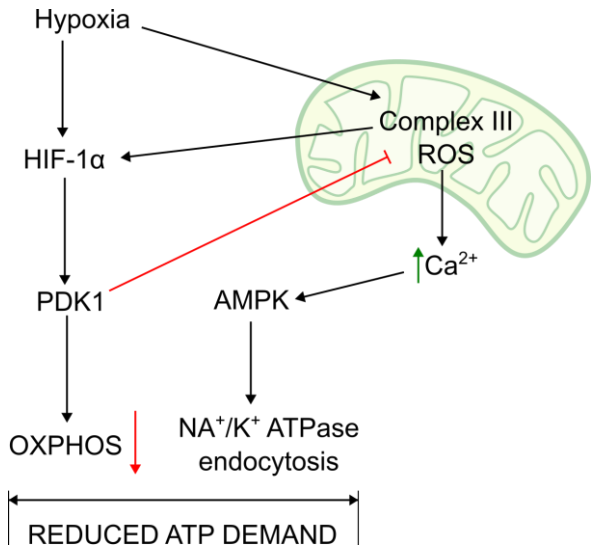

Figure 6. Hypoxia effects on mitochondrial ROS production and ATP demand. The onset of hypoxia causes an increase in complex III ROS production. ROS contribute to the stabilisation of HIF-1α and to the increase in intracellular levels of Ca^{2+}. After dimerization with HIF-1β, HIF-1α can act as a transcription factor and activate PDK1 which, in turn, causes a reduction of OXPHOS-related O_2 consumption. The increased calcium levels activate the AMPS-activated protein kinase (AMPK) which stimulates endocytosis of Na^{+}/K^{+}-ATPase. Both mechanisms contribute to a reduction of cellular ATP needs during hypoxia. Redrawn by C. Ciccone after Wheaton and Chandel (2011) and Lee et al. (2020).

The decrease in OXPHOS in hypoxic cells is also connected to the role of HIF-1 in the molecular reprogramming of the ETS (Lee et al., 2020; Solaini et al., 2010; Wheaton and Chandel, 2011). For instance, HIF-1 promotes the expression of NDUFA4L2, a mitochondrial protein which decreases O_2 consumption via inhibition of complex I activity (Tello et al., 2011). Additionally, HIF-1 induces a switch in one of the complex IV subunits, from the COX4|1 isoform to the COX4|2 isoform (Fukuda et al., 2007). This switch is considered a critical adaptive response to hypoxia, as COX4|2 – unlike COX4|1 – can work more efficiently in conditions of low O_2 availability (Douiev et al., 2021; Fukuda et al., 2007; Pajuelo Reguera et al., 2020). In addition, complex II is known to revert the activity of its SDHA subunit during ischemic episodes, thereby causing succinate accumulation which contributes to HIF-1α stabilisation (Chouchani et al., 2014; Selak et al., 2005).

1.4.2 The clock-mitochondria interaction during hypoxia

At the tissue level, O_2 concentration can fluctuate daily depending on the organism's activity pattern (Adamovich et al., 2022). Normal physiological O_2 partial pressure (P_{O2}) in tissue (i.e., physoxia) is around 38 mmHg (5%), but can vary depending on the tissue (e.g., alveoli can reach up to 110 mmHg (~14%)) (McKeown, 2014). However, P_{O2} has been shown to fluctuate in rat renal tissue between ~19 (2.6%) and ~25 (3.6%) mmHg (Adamovich et al., 2017). These daily fluctuations can act as a resetting cue for molecular clock re-synchronisation via the intermediate action of HIF-1α (Adamovich et al., 2017; Peek et al., 2017). Considering that O_2 tissue levels between 1% and 5% are already considered as physiological hypoxia (McKeown, 2014), and that different tissues show a time-of-day dependency in their hypoxia response, it is logical to think that there might be an intricate crosstalk between the molecular clock and the HIF signalling pathway (Manella et al., 2020).

A transcriptional regulatory loop exists between HIF-1α and the clock genes, due to the similarities between the promoter regions of the hypoxia-activated genes, also called hypoxia responsive elements, and the E-boxes regulating the activation of the clock genes. Interactions of HIF-1α with the clock genes promoters, and of BMAL1 with the HIF-1α promoter, have indeed been documented in different studies (Peek et al., 2017; Wu et al., 2017). Both HIF-1α and the clock proteins belong to the same superfamily of PAS domain-containing proteins. The PAS domain is a region of around 120 amino acids typical of eukaryotic transcription factors, able to sense different external stimuli such as light, oxygen and energy levels (Taylor and

Zhulin, 1999). Specifically, HIF-1α and BMAL1 belong to the basic-helix-loop-helix (bHLH)-PAS protein group (Hogenesch et al., 1998; Wang et al., 1995). The presence of the bHLH-PAS determines the need of these proteins to heterodimerise in order to act as transcription factors and this is what determines the physical interaction between BMAL1 and HIF-1α (Hogenesch et al., 1998; Millar, 1997; Wang et al., 1995). The negative limb of the TTFL (Figure 5) has also been shown to interact with HIF-1α. For example, CRY can directly bind HIF-1α, thereby inhibiting its activity (Dimova et al., 2019). Conversely, interaction of PER2 with HIF-1α leads to an increased HIF activity (Kobayashi et al., 2017).

The HIF-1α/BMAL1 interaction allows for integration of information on O_2 levels with the circadian regulatory mechanisms and one of its results is the cyclic regulation of mitochondrial metabolism. For instance, in mouse skeletal muscle, the HIF-1α/BMAL1 complex mediates the metabolic switch from an OXPHOS-based metabolism to a mainly glycolytic one, possibly via enhancement of the expression of the HIF-1α target genes. This is especially beneficial at times of intense activity/exercise that can cause a temporary hypoxic state within some muscles (Peek et al., 2017).

Apart from direct interactions, it has been suggested that HIF-1α and the clock can also indirectly work together to orchestrate "temporal cycling of metabolism" (Peek, 2020). Many studies have shown that the clock has a direct influence on glucose metabolism and the ETS; since many metabolic intermediates affect HIF-1α stabilisation, it is possible that the clock is affecting HIF-1α stability also by controlling different metabolic pathways (Peek, 2020). For example, since production of both ROS and antioxidants molecules is under circadian control, it may be that the clock is controlling HIF-1α stability via regulating mitochondrial nutrient oxidation (Mezhnina et al., 2022; Peek, 2020). In addition, the activity of PHDs (HIF-1α hydroxylases) does not only depend on O_2 levels but also on the presence of α-ketoglutarate, a TCA cycle intermediate (Schofield and Ratcliffe, 2004). The enzymes involved in the production and consumption of α-ketoglutarate both show circadian oscillations. Therefore, it can be hypothesised that also α-ketoglutarate levels can change on a daily basis. The oscillating levels of α-ketoglutarate will then cause diurnal oscillations also in PHD activity and, therefore, in HIF-1α stabilisation (Manoogian and Panda, 2016; Neufeld-Cohen et al., 2016; Peek, 2020). The overall result would be the optimisation of the use of energy substrate through a circadian regulation of mitochondrial activity via indirect cooperation between the clock and the HIF-activation pathway (Peek, 2020).

1.4.3 Animal models of hypoxia – the hooded seal

Although most animals may suffer detrimental effects from exposure to severe hypoxia, there are some species that display impressive tolerance. Thus, species that typically live under oxygen-deficient conditions, either permanently or intermittently, have evolved particular physiological and behavioural strategies to cope with this challenge (Fago, 2022; Larson et al., 2014; Lutz et al., 2003). Among these we find diving mammals, which have evolved to tolerate repeated episodes of acute hypoxia (Blix, 2018; Ramirez et al., 2007; Scholander, 1940). For example, while non-diving mammals experience the bioenergetic collapse within seconds or minutes of hypoxia (Lutz et al., 2003), diving mammals are able to hold their breath during prolonged dives, during which blood oxygen drops to very low levels, without having reported ill effects. Among diving mammals, some species are considered as "champion divers" as they can stay submerged for 1-2 hrs at the time (e.g., southern elephant seal (*Mirounga leonina*), northern elephant seal (*Mirounga angustirostris)*, Weddell seal (*Leptonychotes weddellii*), and hooded seal (*Cystophora cristata*)) (Hassrick et al., 2010; Hindell et al., 1991; Hindell et al., 2002; Vacquie-Garcia et al., 2017). In my thesis work, I have used one of them, the hooded seal, as a model to study evolutionary adaptations to severe hypoxia.

The hooded seal is a deep diving Arctic seal that makes breath-hold dives that last for up to 87 min (Vacquie-Garcia et al., 2017), to depths of more than 1600 m (Andersen et al., 2013). It is distributed in the North Atlantic Ocean (Figure 8) (Folkow et al., 1996) and divided in two main

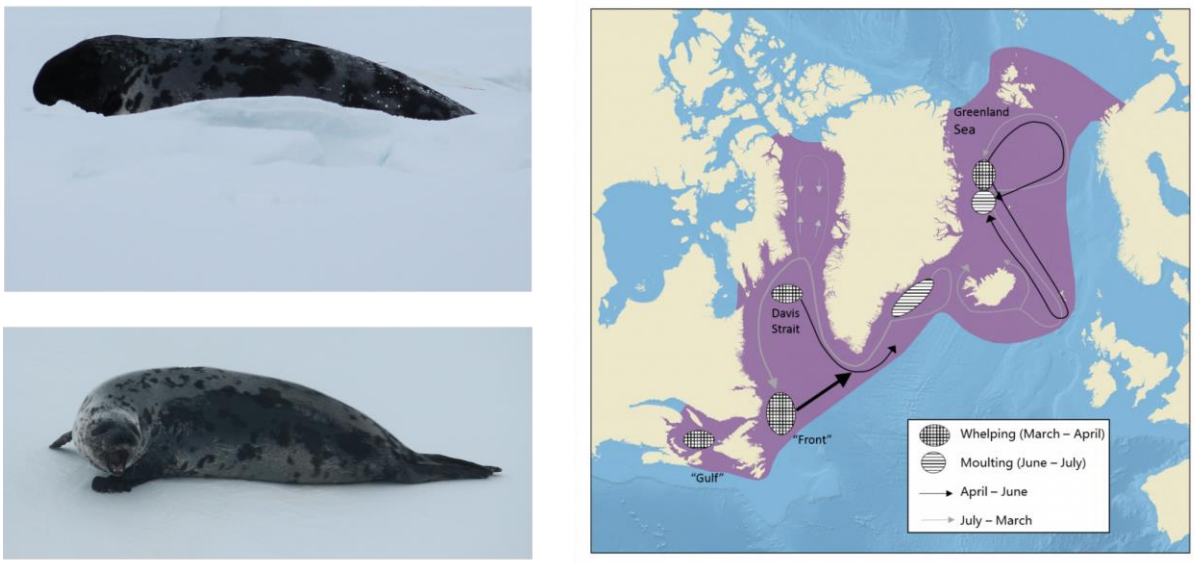

Figure 7. Hooded seals and their distribution. Top left: adult hooded seal male; Bottom left: adult hooded seal female. Both individuals belong to the Greenland Sea population (photos: C. Ciccone). Right: hooded seal distribution in the North Atlantic (picture taken from North Atlantic Marine Mammal Commission, NAMMCO: https://nammco.no/hooded-seal/)

populations, counting altogether some 700,000 individuals (Hammill and Stenson, 2006; ICES, 2023). It is sexually dimorphic, with males weighing ~250-300 kg and females ~150-250 kg (Kovacs and Lavigne, 1986), and with the males being recognized by their nasal sac that can be inflated to a 'hood', which has given the species its name (Figure 7) (Merriam, 1884).

Although hooded seals have been documented to dive very deep and for durations exceeding one hour, their dives appear to usually be within the so-called Aerobic Dive Limit (ADL), i.e. the maximum time a seal can dive without accumulating lactate in blood/tissues (Kooyman et al., 1980) - estimated to be around 20 minutes for the hooded seal (Folkow and Blix, 1999). With reference to the possible interactions between clocks, metabolism and mitochondrial function, hooded seals typically display daily and seasonal variations in their diving behaviour. These variations are in part connected to their life history, but also to daily changes in the vertical distribution of their prey (Folkow and Blix, 1999). Like other seals, hooded seals display a suite of mechanisms and responses that enable them to endure long breath-hold dives (Blix, 2018). These are summarized below.

1.4.4 Systemic hypoxia defense in seals

One major challenge of breath-hold diving is dealing with an ever-decreasing O_2 content and an increasing CO_2 content in the blood (Scholander, 1940). To tolerate prolonged periods of hypoxia, seals present enhanced abilities for storing and carrying O_2: a hooded seal can store up to 90 ml/kg of O_2, in contrast to the average 25 ml/kg that may be stored in the human body (Burns et al., 2007). The enhanced O_2 carrying capacity is due to a very large blood volume: the harbor seal (*Phoca vitulina*) blood volume is 132 ml/kg, almost two times that of humans (~75 ml/kg) (Lenfant et al., 1970). Seals also have an elevated haematocrit (Hct) compared to humans, i.e. the percentage of red blood cells in the blood, which translates into high hemoglobin (Hb) concentrations. The hooded seal Hct was measured to 57.5 ± 1.4 % (and may exceed 63%; Clausen and Ersland, 1969), corresponding to an Hb content of 23.3 ± 0.9 g/dl of blood, while the human Hct is normally around 45%, with 13-17 g Hb/dl of blood (Burns et al., 2007; Packer et al., 1969). The high Hb concentration allows for higher quantities of O_2 to be stored and carried by the blood.

The skeletal muscle of diving mammals has a very peculiar appearance, being very dark (almost black) compared to many non-diving species. This is because it is very rich in myoglobin (Mb):

the Mb concentration of hooded seal muscle is on average 94.8 ± 8.9 mg/g, and 85.9 ± 12.5 mg/g in the harp seal (*Pagophilus groenlandicus*), in contrast to levels of only 10-30 mg/g in man (Burns et al., 2007). Hence, the hooded seal skeletal muscle can store at least 3 times as much O_2 as the human skeletal muscle.

The diving response

These traits allow seals to start a dive with onboard O_2 reserves that are 3-4 times as large as in humans (e.g., Blix 2018). However, as Lawrence Irving stated already in 1939 "*the storage of oxygen is inadequate to provide for its use by all tissues, but differential control of the distribution of oxygen might reasonably serve to maintain the brain, allowing the less sensitive tissues or those with fair capacity for anaerobic metabolism to do without oxygen*" (Irving, 1939). Indeed, another major systemic adaptation to diving is the so-called *diving response*, which is composed of two complementary events: peripheral vasoconstriction and bradycardia.

In pinnipeds, a diving-induced widespread peripheral vasoconstriction results in a selective re-distribution of the blood flow towards the most hypoxia-sensitive tissues, i.e., the brain and the heart (Blix et al., 1983; Zapol et al., 1979). The presence of this response was already noted by Scholander (1940) when, during forced dives experiments, he reported an increase in the arterial blood lactic acid only after the animals had resurfaced. Since lactic acid (i.e., lactate) is the byproduct of anaerobic metabolism (Figure 1A), Scholander assumed that during a dive, muscles were excluded from the circulation and had to rely mainly on anaerobic metabolism, while all the O_2 stored in the blood would be made available for the less hypoxia-tolerant tissues. He verified this idea very directly by cutting the muscle of a diving seal and observed that the cut did not bleed until the animal surfaced.

The redistribution of the blood flow is strictly connected to the observed bradycardia: to maintain a stable arterial pressure, the resistance to flow caused by the massive peripheral vasoconstriction must be accompanied by a substantial reduction of the heart rate (Irving et al., 1942), or blood pressure would surge. During a dive, heart rates lower than 10 beats/min have been reported for the harbor seals and grey seals (*Halichoerus grypus*) (Murdaugh et al., 1961; Thompson and Fedak, 1993). The bradycardia is also a function of dive duration and, usually, the lowest heart rates are associated with the longest dives (Thompson and Fedak, 1993). This dependence on dive duration is given by the fact that the diving response is not an "all-or-

nothing" response and only the longer (and potentially severely hypoxic) dives trigger it to its fullest extent (Blix, 2018).

Studies of freely diving seals have shown that most of their dives are within their predicted ADL, and they presumably primarily rely on aerobic metabolism (Kooyman et al., 1980). However, the "champion divers" (e.g., Weddell seals, hooded seals) appear to sometimes exceed their ADL (Folkow and Blix, 1999; Kooyman et al., 1980), and then probably experience very low arterial O_2 pressures (P_aO_2) levels. Normal values of P_aO_2 are between 120-80 mmHg and non-diving mammals may suffer neural damages already at P_aO_2 of 25-40 mmHg (Erecińska and Silver, 2001), but these seals can routinely experience P_aO_2 of 10-20 mmHg during diving, without any obvious major complications (Meir et al., 2009; Qvist et al., 1986). This shows that these animals must possess additional specific mechanisms that allow them to cope with these extremely low blood oxygen levels.

1.4.5 Cellular and molecular hypoxia defense mechanisms in seals

Knowing how low the P_aO_2 can be during a dive, it is natural to ask how an organ as highly aerobic as the brain can survive it. *In vitro* investigations have revealed that hooded seal neurons maintain stable resting membrane potential, the capacity to produce action potentials, and the ability for synaptic transmission, even after 1 hour or more of severe hypoxia exposure, while neurons of non-diving species stop working under the same conditions (Folkow et al., 2008; Geiseler et al., 2016). This shows that seal neurons must possess endogenous mechanisms that enable them to maintain functional integrity under such conditions.

Metabolic shutdown

One way to meet O_2 deficiency during prolonged diving is through a general *metabolic arrest*, by which seals not only lower the ATP demands of tissues and organs, but also avoid the accumulation of unwanted byproducts of anaerobic metabolism (Hochachka, 1986).

In seals (and other mammals), the brain is presumably a major O_2 consumer in the body, in relation to its size. Therefore, any reduction in brain ATP demand and consumption could be an advantage, especially during long and hypoxic dives (Blix, 2018). Diving seals have been shown to allow brain temperature to drop, by up to 3°C (Blix et al., 2010; Odden et al., 1999). According to the Q_{10} effect concept, a reduction of brain temperature of around 2.5°C could be

expected to cause a ~25% reduction of brain O_2 demand and metabolic rate (i.e., hypometabolism) (Blix et al., 2010).

It has further been hypothesised that via other, cell-specific mechanisms of metabolic shutdown, and by reconfiguration of neuronal networks, some networks (e.g., related to respiration and lung ventilation) may undergo hypometabolic responses during diving, while other networks (that presumably subserve vital functions) remain active, thereby securing both neuroprotection and preservation of cerebral function while diving (Larson et al., 2014; Ramirez et al., 2007). This suggestion was based on *in vitro* studies using hooded seal brain slices, which showed that some spontaneously active neural circuits maintained their activity while others shut down upon exposure to experimental hypoxia, only to reactivate upon reoxygenation (e.g., Czech-Damal et al., 2014; Ramirez et al., 2011).
This hypothesis finds support in a recent study of the hooded seal neuronal transcriptome, which revealed reduced expression of genes related to synaptic activity, compared to mouse neurons (Geßner et al., 2022). Since synaptic activity is the most energy-demanding cerebral function (Harris et al., 2012), its depression during diving would reduce neural ATP requirements, but also drastically decrease cerebral O_2 demands, thereby conveying hypoxia-tolerance (Geßner et al., 2022).

Antioxidants activity

In addition to dealing with prolonged periods of hypoxia, another important challenge imposed by diving is the oxidative stress after resurfacing and reoxygenation. During the hypoxic episodes, large amounts of succinate accumulate (Zhang et al., 2018). Reoxygenation induces a mechanism known as reverse electron transfer (RET), for which succinate is converted again into fumarate by complex II which, at the same time, pushes e^- towards complex I (Chouchani et al., 2014). Complex I then starts working in reverse by transferring the e^- to O_2 and becoming one of the major sources of ROS (Chouchani et al., 2014; Murphy, 2009). The large accumulation of ROS can cause severe oxidative stress and damage, particularly after reperfusion of tissues after ischemia (Schieber and Chandel, 2014). To avoid the detrimental effects connected to oxidative stress and damage, organisms have evolved enzymes that act as ROS scavenger (i.e., antioxidants). A few examples of antioxidant enzymes are the superoxide dismutase (SOD), glutathione reductase (GPX) and glutathione reductase (GR).

Considering that because of their behaviour, diving mammals are often subjected to episodes of hypoxia/reoxygenation, it is logical to think that they have evolved defensive mechanisms against oxidative stress (Vázquez-Medina et al., 2012). Although early studies hypothesised that one possibility might be a reduced production of ROS, soon enough it was discovered that most diving species show instead an increased production of antioxidants (Vázquez-Medina et al., 2012). For example, glutathione (GSH) levels were found to be 3 times higher in the Weddell seal blood than in humans (Murphy and Hochachka, 1981), while ringed seals (*Phoca hispida*) were shown to have higher activities of SOD in both heart and lungs when compared to pigs (*Sus scrofa*) (Vázquez-Medina et al., 2006). A more recent study further corroborated the hypothesis of elevated antioxidant defence in seals, by showing higher activity of GPX and GSH in the hooded seal brain compared to the mouse brain (Martens et al., 2022).

Neuroglobin

In the early 2000s, a new member of the globin family was discovered: neuroglobin (Ngb) (Burmester et al., 2000). Ngb is mainly present in the neurons of the mammalian brain, but also in the retina, thus, typically being associated with highly aerobic tissues. It resembles Mb in terms of both structures and O_2 affinity (Burmester and Hankeln, 2009). One of Ngb's many possible functions is to enhance the cellular O_2 storage capacity of neurons, to ensure enough O_2 supply for mitochondrial OXPHOS (Burmester and Hankeln, 2009).

Because of their predominantly oxidative role, it was hypothesised that, as for Hb in the blood and Mb in the skeletal muscle, seal neurons would also have a higher concentration of Ngb compared to "non-diving neurons". Analysis of Ngb expression in seal, mouse and ferret (*Mustela putorius furo*) brain did not reveal any significance difference between these species (Mitz et al., 2009; Schneuer et al., 2012). However, immunohistochemical analysis of Ngb distribution in the visual cortex of seal and mouse suggested that, while in the mouse Ngb was localized in neurons, as expected, seal Ngb was mainly found in astrocytes (Mitz et al., 2009). The same result was obtained from the analysis of another marker of oxidative metabolism, cytochrome c. These findings led to the first theory of a metabolic reorganization between neurons an astrocytes in the diving brain, and the formulation of the *reverse ANLS* (rANLS) hypothesis (Figure 8) (Mitz et al., 2009).

Do seals have a reversed Astrocyte-Neuron Lactate Shuttle?

The rANLS hypothesis suggests that, as an adaptation to recurrent hypoxia, seal neurons may be equipped to produce ATP through glycolysis during severe incidents of hypoxia (Figure 8). To prevent neuronal lactate overload, this compound may then be shuttled to the astrocytes. Here, lactate could be re-converted to pyruvate upon reoxygenation after surfacing and used for OXPHOS, thus giving the astrocytes a key role in the oxidative metabolism of the seal brain (Mitz et al., 2009).

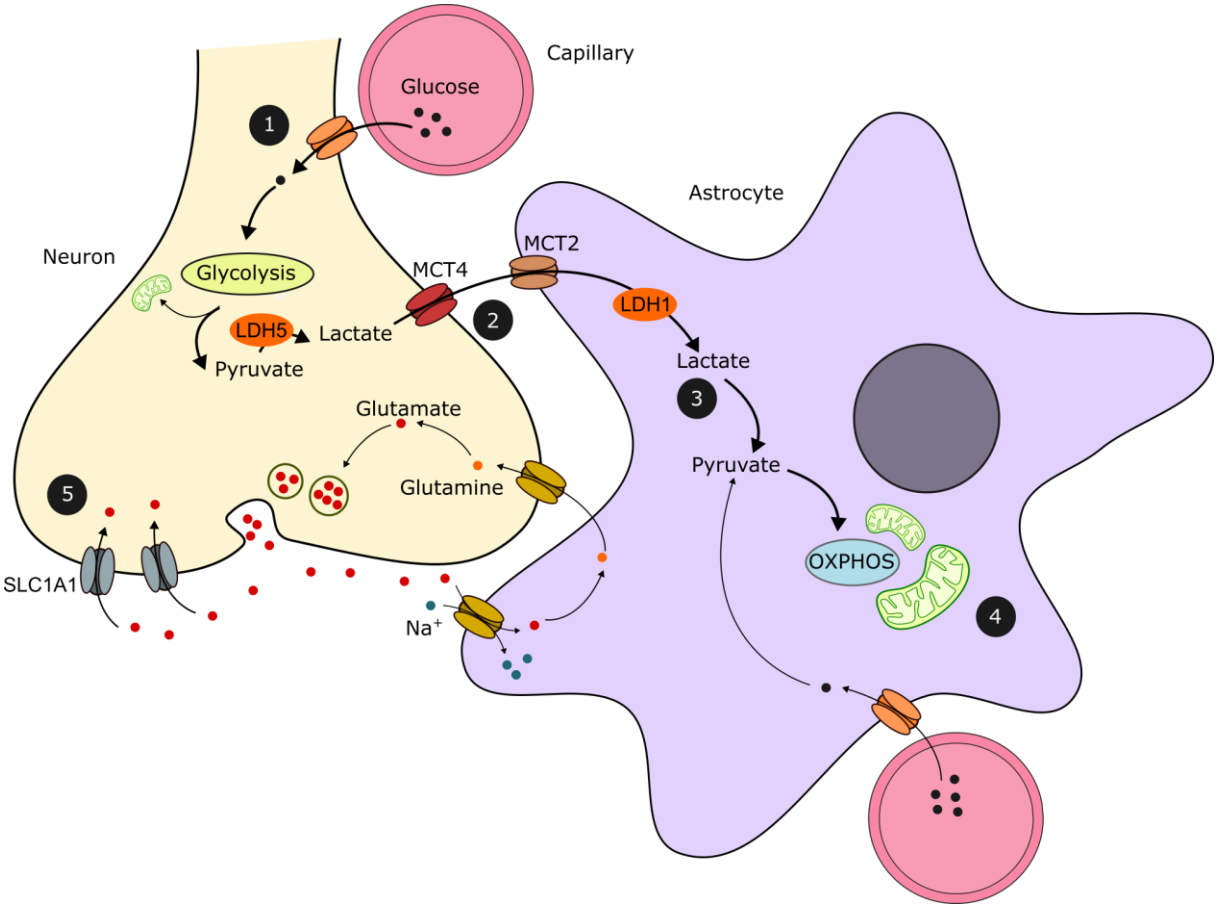

Figure 8. The "reverse ANLS" hypothesis. Schematic representation of the suggested metabolic coupling between astrocytes and neurons in the hooded seal brain. **1)** When required, under severely hypoxic conditions, neurons mainly rely on the use of glucose and glycolysis to generate ATP. The end-product pyruvate is transformed into lactate via LDH5. **2)** The neuronal lactate can be toxic if accumulated in great amounts and it is therefore exported to the extracellular space via MCT4 and shuttled into the astrocytes via MCT2. **3 - 4)** Here, when oxygen again becomes readily available, lactate is converted into pyruvate via LDH1 and used for energy production in the mitochondria. **5)** At the same time, via overexpression of glutamate transporter SLC1A1, seal neurons contribute to the uptake of glutamate from the synaptic cleft.
Thicker arrows represent the preferred metabolic pathways of both cell types, according to rANLS: anaerobic glycolysis in neurons and OXPHOS for astrocytes. This does not exclude that both cell types can still produce ATP through alternative metabolic pathways when needed (thinner arrows: glycolysis in astrocytes and OXPHOS in neurons). Black dots: glucose; red dots: glutamate; orange dots: glutamine; blue dots: Na^+. Illustration by C. Ciccone, based on data from Mitz et al. (2009), Hoff et al. (2016), Geßner et al. (2022).

Such a peculiar subdivision of the metabolic work would relieve neurons from three big challenges (Mitz et al., 2009): (1) maintaining a high OXPHOS-based ATP production under hypoxic conditions, (2) dealing with the potential toxicity from lactate accumulation, and (3) exposure to and handling of a post-dive surge of ROS.

LDH and anaerobic metabolism

Earlier work already suggested that the seals' ability to tolerate hypoxia was due to an elevated anaerobic capacity, based on findings of a high cerebral LDH content (Blix and From, 1971). However, later analysis of the LDH content and distribution in the hooded seal brain showed that, rather than relying on an elevated anaerobic capacity, the ability to withstand hypoxia is due to an unusual distribution of LDH isoenzymes (Hoff et al., 2016). Thus, the hooded seal brain has a high content of the isoforms LDH1 and LDH2, which have a high proportions of the LDHB subunit – as typically found in aerobic tissues converting lactate into pyruvate (Cahn et al., 1962; Hoff et al., 2016). More interestingly, in the hooded seal brain, LDHB was found to be highly co-localized with the astrocytes (Hoff et al., 2016). These results not only show a high capacity of the hooded seal brain for recycling lactate, but also support the rANLS hypothesis, as this suggests that the astrocytes are the main site for cerebral lactate oxidation – instead of them producing lactate, as the ANLS mechanism states (Figure 8).

MCTs distribution

The rANLS hypothesis would also predict a distribution of MCT isozymes that conform with the suggested reversed metabolic roles of neurons vs astrocytes in seals (Figure 8). This would predict that seal neurons are rich in MCT4 (the "normal" astrocytic lactate *exporter*, in ANLS) and that seal astrocytes are rich in MCT2 (the "normal" neuronal lactate *importer*, in ANLS) (Figure 8). Transcriptome analysis has shown that upon exposure to hypoxia/reoxygenation there is an upregulation of MCT4 and a downregulation of MCT2, in whole hooded seal brain tissue (Hoff et al., 2017), but these authors had no means to attribute these changes to either astrocytes or neurons. More recent transcriptome analyses of single hooded seal neurons, isolated by laser capture microdissection, showed an elevated expression of MCT4 in seal neurons compared to in mouse neurons (Geßner et al., 2022), thus favouring the rANLS scenario. But a specific analysis of MCT2 and MCT4 expression profiles in hooded seal neurons vs astrocytes is still missing.

The implication of a rANLS is that neurons would be major consumer of glucose during diving hypoxia, as they would then rely on glycolysis for ATP production. Indeed, the uptake and use of glucose in the brain of diving Weddell seals was shown to increase by about 40% when compared to resting levels (Murphy et al., 1980), while an increase in lactate content in cerebral venous blood was measured in harbor seals at the end of a dive (Kerem and Elsner, 1973) .
A high neuronal use of glucose would be better supported by high local glycogen stores. In non-diving mammals, cerebral glycogen is mainly stored in the astrocytes (Brown and Ransom, 2007), the major site of anaerobic glycolysis. The rANLS hypothesis would instead predict high glycogen stores that are localized in the neurons. Although direct measurements of glycogen content in neurons and astrocytes has not been made in the seal brain, the 4-fold higher glycogen concentration found in the hooded seal brain compared to mouse suggests that diving mammals, depend more heavily on high glucose availability (Czech-Damal et al., 2014). This, together with a maintained or even increased cerebral blood flow during diving (Blix et al., 1983), probably ensure an adequate substrate supply to drive anaerobic glycolysis even during the longest dives.

1.4.6 Current knowledge gaps

Previous transcriptome analyses using hooded seal brain tissue have been unable to separate between cell-specific neuron vs astrocyte adaptation (Fabrizius et al., 2016; Hoff et al., 2017). The only cell-specific transcriptome study employed neurons isolated from hooded seal visual cortex slices by laser capture microdissection (Geßner et al., 2022). This study gave very useful insights on how seal neurons differ from mouse neurons, but still cannot answer some very important questions as to how seal neurons differ from seal astrocytes, and whether such differences are the same as found in non-diving mammals.
Thus, a direct analysis of the metabolic profiles of both seal astrocytes and neurons is necessary to identify any differences in their oxidative and glycolytic capacities that could confirm or affirm the rANLS hypothesis. Also, a characterization of the distribution of MCTs expression profile is still missing, Finally, an astrocyte-specific transcriptome analysis has yet to be done. To do so, either frequent access to fresh seal brain tissue, or the establishment of viable neuron and astrocyte cultures from brain tissue, is needed - both of which are challenging endeavours.

2 Research aims

The interrelationship between mitochondrial function, clock, and hypoxia and how it is regulated is important for the understanding of how homeostasis may be maintained under oxygen-limited conditions. By using the hooded seal as model organism, I have aimed to understand how molecular mechanisms may be employed to optimise metabolic processes in relation to dive behaviour, to tolerate intermittent and recurring exposure to severe hypoxia during diving. I have considered both the circadian regulation of mitochondrial activity and how the metabolic roles of astrocytes and neurons may be adjusted, in relation to variable oxygen availability. Specifically, I aimed to:

1. Characterize the hooded seal molecular clock;
2. Investigate whether there are any clock-driven effects on mitochondrial function in a deep-diving mammal;
3. Study the mitochondrial respiration of hooded seal astrocytes and neurons as a mean to investigate the rANLS theory;
4. Develop a reproducible *in vitro* approach to study metabolic adaptations to variable oxygen availability in the hooded seal brain.

The first two objectives are addressed in **paper I,** where, by using primary skin fibroblast cultures, we verified the presence of core clock genes and investigated changes in mitochondrial activity in different clock phases, in the hooded seal. The third objective is addressed in **paper II,** by investigating mitochondrial abundance in seal neurons and astrocytes and by utilising hooded seal primary astrocyte and neuronal cell cultures to measure mitochondrial O_2 consumption.

Finally, in **paper III**, I sought to develop an *in vitro* methodology to study the roles of astrocytes in the cerebral adaptations of diving mammals without depending on access to fresh brain tissue, which is in line with the 3R's principle in animal research (Russell and Burch, 1959), and also would overcome the logistic and economic challenges of accessing a remotely distributed species (Figure 7) that, moreover, is listed by the IUCN as a vulnerable species (Kovacs, 2016). Three stable cell lines were created from the primary astrocytic cultures I isolated in the field from fresh hooded seal visual cortex. The specific aim of **paper III** was to characterize these cell lines and determine whether they maintained primary cell characteristics that enabled their use in future studies of metabolic or other adaptations of hooded seal astrocytes.

3 Methods

3.1 Studying diving behaviour

Studying physiological mechanisms of an animal without considering how it behaviourally relates to its environment creates data and information that is difficult to put into a context. At the same time, studying animal behaviour without asking ourselves what the physiological limits of that same animal are, will also result in an incomplete understanding. Thus, it is when we combine physiology with ecology that we can obtain the full understanding of *how* and *why* an animal can do what it does (Manning and Dawkins, 2003).

It is becoming more and more evident how mitochondrial physiology has a large impact on organism metabolism and fitness, and thereby on an animal's responses to environmental changes (Heine and Hood, 2020; Koch et al., 2021). Therefore, the integration of mitochondrial analysis and the study of ecological patterns (e.g., behaviour) can give a fuller picture of how cellular processes are connected to the evolution of specific behavioural patterns (Koch et al., 2021). Having this in mind, we decided that, to verify the presence of a functional molecular clock and clock-mitochondria interactions in the hooded seal, it was necessary to relate this to any cyclicity in its diving behaviour.

The diving behaviour of marine mammals is usually studied through biotelemetry, the "*remote measurement of physiological, behavioural or energetic data*" (Cooke et al., 2004). These measurements require the deployment of recording devices that can keep track of the animal, its position, behaviour and possibly physiology, and then have the collected information remotely conveyed to the user. In the early days, time-depth recorders (TDRs) were employed. These devices greatly improved our understanding of the diving behaviour of seals, whales, and diving birds (Kooyman, 2004; Kooyman et al., 1976). However, in order to access data, these units needed to be retrieved (Carter et al., 2016), thus requiring recapture of the tagged individual (Carter et al., 2016; Fedak et al., 2002).

As explained in **paper I**, to analyse the hooded seal diving behaviour we used a pre-existing data set made available by the Norwegian Polar Institute (Vacquie-Garcia et al., 2017). The data were collected through Conductivity-Temperature-Depth Satellite Relay Data Loggers

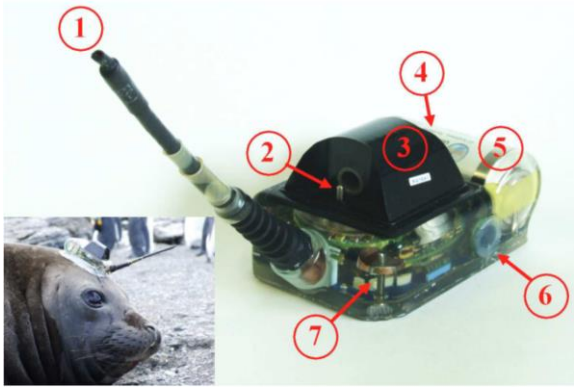

Figure 9. Conductivity-temperature Depth Satellite Data Logger (CTD-SRDL). Bottom left: CTD-SRDL on a southern elephant seal (*Mirounga leonina*). **1)** antenna for satellite transmission; **2)** probe for temperature measurement; **3)** inductive cell; **4)** pressure sensor; **5)** Battery; **6**) communication port; **7)** wet-dry sensor. Picture from Boehme et al. (2009).

(CTD-SRDL) that were glued to the fur of the animals (Figure 9) and that, by enabling relay of data via satellite, represent a big advance from the use of classical data logger devices (Boehme et al., 2009; Fedak et al., 2002). SRDL units transmit the collected data (covering periods of 2 to 6 hours) via the Argos satellite system, which then passes the information to local download stations and servers (Fedak et al., 2002), thus eliminating the problem of having to recapture the animals for data collection. Another advantage is the possibility to pair these devices with other sensors (e.g., CTDs, accelerometers), allowing for collection of behavioural, environmental, and even physiological, data at the same time (Carter et al., 2016). Finally, by introduction of the technique of gluing the units to the fur of seals, an 'automated drop-off' function is used, since the tag will be lost as the animal undergoes its annual moult, thus preventing life-long tagging (Fedak et al., 1983).

Nevertheless, some limitations apply to the use of SRDL devices. For example, the Argos satellite system cannot provide very precise location data (Carter et al., 2016). The data transfer capacity is, moreover, quite limited. Therefore, high resolution data are compressed in various ways using onboard algorithms, e.g., into a time-depth dive profile containing information on maximum depth, depth/time pair points, and total dive duration (Fedak et al., 2002). In addition, the SRDL data transmission depends on the satellite coverage and there is no way to confirm whether a transmission has been successful (Fedak et al., 2002). However, satellite coverage is better in the polar regions, making the SRDL device-Argos satellite a good option for studying the behaviour of polar species, like the hooded seal (Carter et al., 2016).

Despite some limitations, the SRDL devices can still collect enormous amounts of information (dive depth, swimming speed, surface duration, temperature, etc.) and represent a huge step ahead from the old TDRs (Boehme et al., 2009; Fedak et al., 2002).

3.2 Collecting brain samples from hooded seals in the wild

All the hooded seals sampled for this PhD project belonged to the Greenland Sea stock. Seals were live-captured on the ice during their breeding season (late March): this is the only time of the year, apart from during moulting in July, that the hooded seal is relatively easily accessible for live-capture, as the females then spend all time on the ice, nursing their pups (e.g., Folkow et al., 1996).

Adult lactating females were captured by use of hoop-nets and were tranquilized/sedated before being brought on the research vessel. Here, their level of sedation was further secured, so as to allow the animal to be intubated with an endotracheal tube and being fully anesthetised via isoflurane ventilation. Once deeply anaesthetised, seals were euthanised by decapitation and exsanguination via the carotid arteries. The head was placed in a bucket containing freshly made ice-cold artificial cerebrospinal fluid (aCSF). After removing skin and blubber, the skull was cut open from the top using an oscillating orthopaedic saw, to allow the extraction of the brain without damaging it. The extracted brain was immersed in ice-cold aCSF, and slices of visual cortex were cut to be processed, for cell cultures establishment, or for preservation for other uses (e.g., fixation for immunohistology). The entire procedure, from euthanasia to sampling, was completed within ~7 min (Geiseler et al., 2016).

The pup was usually captured together with the female (unless deemed to be in a near fully weaned state, in which case it was left on the ice to fend for itself, as it is fit to do from nature's side), to be used in research, either onboard or in the approved animal facility at UiT.

3.3 Mitochondrial High Resolution Respirometry

The measurement of mitochondrial respiration is fundamental to understand and map the bioenergetic profile of a cell type, or to verify the presence of mitochondria-related injuries and disfunctions (Brand and Nicholls, 2011; Hütter et al., 2006). The use of a system with high sensitivity to O_2 is also decisive, since even small changes in respiration rate can reflect significant defects of the mitochondria themselves, or of mitochondria-associated proteins (Gnaiger, 2008; Hütter et al., 2006; Pesta and Gnaiger, 2012). The basic principle of cellular/mitochondrial respirometry is to measure O_2 concentration in a closed chamber, while it declines as the biological sample consumes O_2 (Gnaiger, 2008). The respiration rate of the sample is then calculated as the negative time derivative of the O_2 concentration (Gnaiger, 2008; Hütter et al., 2006).

In the early days, respirometry measurements were made with a Clark electrode, a polarographic sensor composed of a gold or platinum cathode and a silver (Ag) anode. The O_2 content of the experimental chamber was determined by calculating the rate of anode Ag oxidation and precipitation to the cathode, which created an electric current proportional to the O_2 partial pressure (Gnaiger, 2008). In the 1950s, the Clark electrode for O_2 concentration measurements was replaced by a polarographic sensor equipped with a vibrating platinum electrode (Chance and Williams, 1955). This allowed for a higher accuracy and response speed, as the platinum sensor can detect changes in mitochondrial O_2 consumption within seconds after substrate stimulation (Chance and Williams, 1955). One of the issues associated with the Clark electrode was the time limitation, as O_2 concentration in the experimental chamber would drop quite fast after addition of the sample, especially if added at high concentrations. The shift from the use of microchambers to larger volume ones allowed instead for the development of longer protocols, without the risk of O_2 depletion in the experimental chambers (Gnaiger, 2008). Both these changes constituted the first steps towards modern high resolution respirometry (HRR). Over the years, HRR has proven to be a valuable tool, by enabling the measurement of mitochondrial respiration in quite small samples and at physiological O_2 levels. In addition, HRR guarantees both reliability and quality control through the application of various calibration protocols (Gnaiger, 2008).

Around 30 years ago, the Oroboros Oxygraph-2k (O2k) was introduced, a respirometer designed to study O_2 consumption in different types of mitochondrial preparations (Gnaiger, 2020; Gnaiger et al., 1995). The Oroboros O2k possess two glass chambers within a copper block and stainless-steel structure (Figure 10). O_2 sensors are inserted so to be in contact with the chambers at an optimum angular position (Gnaiger, 2008). The chamber is closed by a stopper equipped with a capillary, into which the needle of a Hamilton micro syringe can be inserted for the injection of different substrates (Figure 10) (Gnaiger, 2008; Pesta and Gnaiger, 2012). All the structures that are in contact with the respiration medium in the chamber are made from materials with low O_2 solubility (e.g., polyvinylidene fluoride (PVDF)), in contrast to the Teflon previously used with the Clark electrode, which has a more than 10-fold higher O_2 solubility. This type of electrode did not allow for high-resolution measurements as any decline in the O_2 concentration could be due to back-diffusion to the material itself (Gnaiger, 2008).

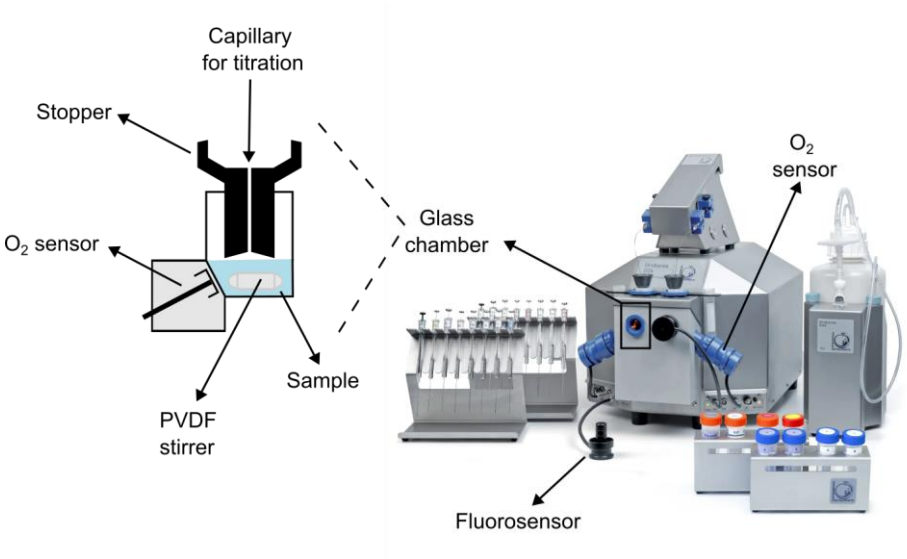

Figure 10. The Oroboros Oxygraph-2k (O2k) for high resolution respirometry (HRR). The sample glass chambers and the O_2 sensors are enclosed in a copper block and a stainless-steel structure. Fluorosensors can be connected to the chambers to allow measurement of ROS production or mitochondrial membrane potential. On the left: schematic representation of the sample glass chamber; within the chamber there is a polyvinylidene fluoride (PVDF) stirrer which secures adequate oxygenation of the whole sample volume. On one side of the chamber, the O_2 sensor is continuously measuring the O_2 concentration inside the chamber. The chamber is sealed with a stopper which also has a capillary for the insertion of the micro syringe needles, for injection of different chemicals. Redrawn by C. Ciccone after Pesta and Gnaiger (2012), Oroboros O2k picture, on the right, from www.oroboros.at.

Mitochondrial preparations

The Oroboros O2k is suitable for measurements of mitochondrial respiration in isolated mitochondria, tissue homogenate, permeabilised cells, intact cells, etc. (Gnaiger, 2020). Each has advantages and disadvantages.

Isolated mitochondria are easy to handle and can be directly treated with substrates in the respirometer (Brand and Nicholls, 2011). Initially, it was thought that the advantage of using isolated mitochondria was associated with the absence of all the cellular and cytoplasmic factors that could influence the results and, therefore, they were considered as “pure” mitochondrial preparations (Hütter et al., 2006). However, the absence of the cellular context represents a great disadvantage, as mitochondria are actively involved in the intracellular dynamics, which, in turn, can influence mitochondrial activity (Brand and Nicholls, 2011; Hütter et al., 2006). In addition, the isolation process requires a large amount of tissue, or cells, and it increases the risk of damaging the mitochondrial membrane (Brand and Nicholls, 2011).

To guarantee the preservation of the cytosolic environment, intact cells can be used for HRR (Brand and Nicholls, 2011; Gnaiger, 2008). Intact cells give the opportunity of measuring mitochondrial respiration in a normal physiological state (e.g., with physiological ions concentrations and distributions), giving results a higher physiological relevance (Brand and Nicholls, 2011; Gnaiger, 2008). One major limitation of using intact cells is that they are not permeable to most of the substrates used in a SUIT protocol and therefore most of the HRR functional assays cannot be performed (Gnaiger, 2008).

One way to meet the advantages of both the isolated mitochondria and the intact cells approach is the use of permeabilised cells. These can be considered as a "subtype" of isolated mitochondria, with the advantage of a faster preparation, since the optimization of the cellular membrane permeabilization is much easier than for mitochondrial isolation (Brand and Nicholls, 2011; Gnaiger, 2008). The process of membrane permeabilization leaves most of the mitochondria-cytosol interactions unharmed and, at the same time, overrides the substrates diffusion restrictions associated with the use of intact cells (Brand and Nicholls, 2011; Gnaiger, 2008).

In both **paper I** and **II**, I used permeabilised cells, as cell-specific mitochondrial properties were to be tested. In both papers, the use of permeabilised cells allowed me to assess the mitochondria respiration without losing its relationship with the cellular environment.
In **paper III**, I opted for using intact cells. This was because one of the objectives of the HRR procedure was to test the rANLS hypothesis, by suppling lactate to the cells. Adding any step of permeabilization would have compromised the cellular membrane and, thereby, the functionality of MCTs, fundamental for uptake/release of lactate.

Manipulating the ETS using substrate-uncoupler-inhibitor titration (SUIT) protocols
Once placed in the chamber, samples can be treated with different chemicals via Hamilton micro syringes injections. Chemicals are added to the chamber following the substrate-uncoupler-inhibitor titration (SUIT) protocols, which consist of a stepwise titration of different substrates linked to the TCA cycle and ETS (substrates in red in Figure 11) (Gnaiger, 2018; Gnaiger, 2020). Adding substrates like pyruvate, malate and glutamate can induce the production of NADH, which stimulates the complex I-linked OXPHOS. Another typical SUIT substrate is succinate, which is the direct substrate of complex II and therefore stimulates complex II-linked OXPHOS. As the SUIT term suggests, not only substrates inducing

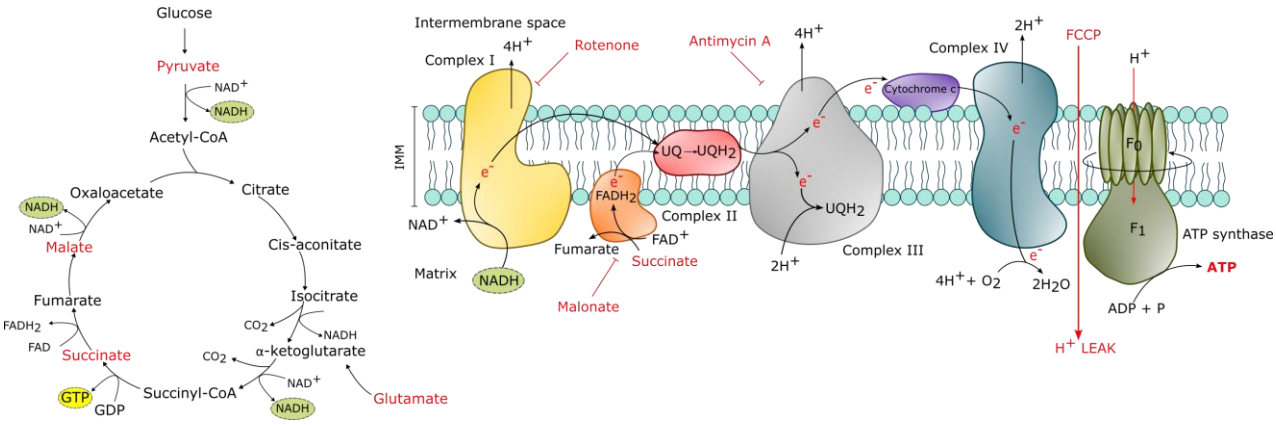

Figure 11. Substrates of the Substrate-Uncoupler-Inhibitor titration (SUIT) protocol and their role in the TCA cycle and ETS. Substrates in red are commonly added to the sample in the Oroboros O2k chamber during a SUIT protocol. Pyruvate, malate, and glutamate stimulate the production of NADH by the TCA cycle. NADH is the main substrate for complex I in the ETS on the IMM. When only these three substrates are supplied (or a combination of two of them), together with ADP, the OXPHOS capacity of complex I can be measured in the respirometer (see main text for definition). Succinate is the direct substrate of complex II and therefore its injection together with ADP allows for measurement of the OXPHOS capacity of complex II, specifically. Substrates for complex I and II can be added together in the presence of ADP to determine the total OXPHOS capacity (complex I + complex II - see main text for definition). Addition of these substrate alone, without ADP, allows instead for measurements of LEAK respiration (see main text for definition). After assessment of total OXPHOS capacity, rotenone can be added to inhibit complex I and indirectly allow the calculation of the OXPHOS capacity of complex II alone. The further addition of malonate can inhibit complex II, leaving only complex III active, which can then be inhibited by injection of Antimycin A. The addition of FCCP dissipates the proton gradient across the IMM and allows for measurement of the ET capacity, that is the maximal mitochondrial respiratory capacity that ETS can reach, independently of the ATP synthase activity. Illustration by C. Ciccone

OXPHOS can be added, but also inhibitors that directly act to inhibit the ETS complexes, like rotenone (complex I inhibitor), malonate (complex II inhibitor) and antimycin A (complex III inhibitor). Finally, also uncouplers can be injected in the chamber. Such chemicals have the role of uncoupling the ETS activity from the phosphorylating action of the ATP synthase and can therefore reveal the maximal respiratory capacity. One example is the carbonyl cyanide 4-trifluoromethoxy phenylhydrazone (FCCP), which dissipates the proton gradient created by the ETS across the IMM (Figure 11) (Benz and Mclaughlin, 1983).

The SUIT protocol allows for measurement of three major respiratory states: OXPHOS capacity, LEAK respiration and ET capacity (Gnaiger, 2020). OXPHOS capacity is measured by injecting substrates for complex I and II, together with ADP, and represents the mitochondrial respiratory capacity in an ADP-activated state. The LEAK respiration is a nonphosphorylating state and represents proton leak across the IMM which is not destined for ATP production. Thus, even though the substrates for both or either of complexes I and II are

supplied, ADP is absent and there is no ATP synthase activity. The ET capacity reflects the maximum flux of the ETS, and it is usually measured after injection of an uncoupler.

It is also possible to test whether the mitochondria are still intact and alive, by injection of cytochrome c in the chamber. Usually, cellular apoptosis and EMM damage are associated with loss of cytochrome c, which causes a decrease in respiration rate. If the addition of cytochrome c causes an increase in respiration, the mitochondria are considered damaged and the respiration previously measured is probably an underestimation (Gnaiger, 2020).

3.4 Primary cell cultures or immortalised cell lines?

Cell cultures have been widely used since the early 1900s in many different fields, e.g. virology, metabolism, intracellular processes, etc (Baydon, 2010; Richter et al., 2021). The very first cell culture was established by Ross Harrison early in the 20th century while studying the development of frog nerves (Harrison, 1906). After that, Alexis Carrel developed the aseptic technique and grew cells from chicken embryos for years (Carrel and Burrows, 1911). Even though it is now confirmed that Carrel's cells growth was due to cross-contamination, he is still considered one of the pioneers in the establishment of "immortal cell lines" and was awarded a Nobel Prize in 1912 (Capes-Davis and Freshney, 2021; Taylor, 2014). In the following years, many efforts were made to optimise his technique until, during the second half of the 1900s, the first mouse fibroblast cell line (Earle, 1943) and first human cell line (HeLa cells) (Gey et al., 1952) were established. This also led to a better understanding of the needs of different cell types, allowing for the development of specific culture media.

Harrison's nerve cells and Gey's HeLa cells are considered two different types of cultures. A culture that is derived directly from the tissue of interest is referred to as a *primary cell culture*, while the HeLa cells is defined as a *cell line*, a subculture of the primary culture, which, after a certain number of divisions, is able to proliferate indefinitely (Baydon, 2010; Capes-Davis and Freshney, 2021).

Primary cell cultures

In research, the use of primary cells is usually preferred since they are assumed to preserve the characteristics of the tissue of origin (Capes-Davis and Freshney, 2021). This approach also allows bulk sampling of rare or unique tissues, e.g. from an organism with a very remote distribution, or a very specific type of tumour (Capes-Davis and Freshney, 2021). Indeed, the

primary culture technique has been crucial for cancer research, since it allowed for tumour cells isolation and better understanding of their physiology (Richter et al., 2021).

The major drawback of working with primary cultures is that they have a very limited lifespan (Hayflick, 1965). After a certain number of cell divisions (usually ~50 cell divisions, i.e. the Hayflick limit), primary cells lose their ability to proliferate and just grow into senescence and apoptosis (Hayflick, 1965). Although once isolated primary cells can be cryopreserved for later use, both their metabolism and phenotype might be influenced if they are exposed to more than one freezing-thawing cycle (Anderson et al., 2019). Therefore, to conduct a long-term research based on primary cultures, the continuous access to fresh tissue is required. In addition, having to periodically isolate cells increases the risk of variations from one cell preparation to another, limiting the possibility of comparing results from different experiments and/or clinical trials (Stacey and Macdonald, 2001; Voloshin et al., 2023).

Immortalized cells

Over the years many methods have been developed for the creation of "immortal" lines from primary cultures. The process of *cell immortalisation* has several advantages: (1) it increases the amount of cells that can be grown over longer periods of time; (2) it abolishes the donor-to-donor variability; (3) it is convenient for genetic modification studies (Voloshin et al., 2023). Immortalisation is achieved by changing the expression profile of the genes involved in cellular aging (Voloshin et al., 2023).

One way to do this is through ectopic expression of telomerase, or of its catalytic subunit telomerase reverse transcriptase (TERT) (Maqsood et al., 2013). This enzyme is usually inactive in normal cells, but it has a high degree of activity in cancerous cells. The telomerase role is to prevent the shortening of the telomeres (i.e., the tips of the chromosomes) after each cell division, which is thought to be one of the main mechanisms behind cellular aging (Dahse et al., 1997). Therefore, by treating the cells with ectopic telomerase, it is possible to maintain elongated telomeres and active proliferation (Maqsood et al., 2013).

Another way to achieve immortalisation is by introducing oncogenes via viral infection (Maqsood et al., 2013). The simian virus 40 (SV40) is one of the most widely used vectors for immortalisation (Figure 12) (Jha et al., 1998; Pereira-Smith and Smith, 1988). Cells infected with SV40 integrate the viral DNA into their own genome, leading to the expression of the SV40 large T-antigen (LT), responsible for the immortalisation process (Shay et al., 1991). Cellular mortality has two different phases, "mortality state 1" (M1) and "mortality state 2" (M2), whose disruption is necessary for immortalisation to happen (Dahse et al., 1997). The SV40 LT deactivates two growth regulators involved in M1, namely p53 and pRB (Dahse et al., 1997; Shay et al., 1991). This attenuates senescence and maintains proliferation, until the M2 stage is activated (Ozer et al., 1996; Shay et al., 1991). At this point the cells will reach a "crisis" with a high rate of cellular death, after which only a few of them will survive (Ozer et al., 1996). The survivors are the immortal cells which express LT and will keep proliferating (Ozer et al., 1996; Shay et al., 1991). In addition, the cells that become immortal show a higher activity of the telomerase enzyme, further indicating that maintenance of telomeres length is fundamental for proliferation (Counter et al., 1992).

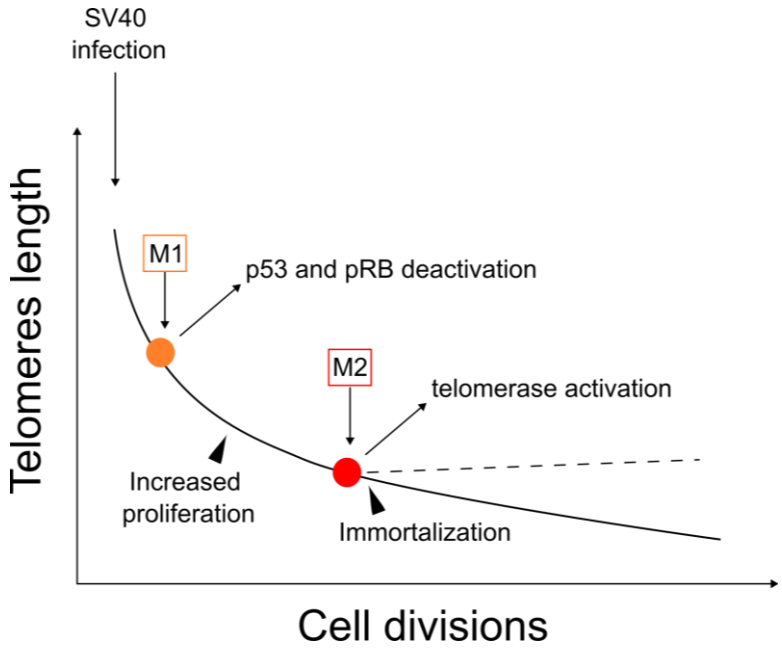

Figure 12. Schematic representation of immortalization via simian virus 40 (SV40) infection. After each cell division, the telomeres length at the tip of the chromosomes decreases. After infection with SV40, cells enter the process of cellular death which has two mortality stages (M1 and M2). The genes involved in M1 and responsible for growth suppression (p53 and pRB) are inactivated by the SV40 antigen. Therefore, the cells enter a stage of increased proliferation, after which they reach a growth crisis. At this stage (M2), most of the cells will reach apoptosis but some of them will keep dividing and reach immortalization by activation of telomerase. This enzyme ensures that the telomeres length is maintained even during further cell divisions, avoiding the process of cellular aging. Redrawn by C. Ciccone after Dahse et al. (1997).

Although there are several advantages in using immortalised cell lines for research, the immortalization process increases the risk for malignant transformations (e.g., tumours) and for drastic changes in the cellular phenotype (Voloshin et al., 2023). Given that both primary cultures and immortalized cells have advantages and disadvantages, it is important to consider which one best applies to specific research questions.

In both **paper I** and **paper II**, I used primary cell cultures (skin fibroblasts, astrocytes, and neurons). Indeed, to verify my hypothesis it was important for the cells to represent the physiology of their tissue of origin as closely as possible. Given the inaccessibility of hooded seals and considering the 3R's in animal research (Russell and Burch, 1959), I decided to focus on the establishment and characterisation of an immortalized cell line derived from primary hooded seal astrocytes, in **paper III**.

4 Results

4.1 Paper I: Circadian coupling of mitochondria in a deep-diving mammal

Paper I is published in "Journal of Experimental Biology" (doi: 10.1242/jeb.246990). The objective of this paper was to characterise the hooded seal molecular clock and determine its possible role in regulating daily mitochondrial activity.

The first step was to analyse the hooded seal diving behaviour and verify and describe the presence of circadian rhythmicity. In accordance with previous results (Folkow and Blix, 1999), our analysis confirmed the presence of a diurnal pattern in the hooded seal diving behaviour, with dives being consistently deeper and longer during the day and shallower and shorter at night, throughout the year. Although these diurnal variations are probably linked to the similar daily pattern in the vertical distribution of prey species (Folkow and Blix, 1999), we wondered whether they could also be connected to a functional molecular clock. To verify this, we established cultures of primary hooded seal skin fibroblasts and entrained them by temperature cycling. Temperature can indeed act as a resetting cue for the mammalian molecular clock and it has been previously used for clock entrainment (Brown et al., 2002; Buhr et al., 2010). We found that, when exposed to temperature cycles (12 hours at 36.5°C and 12 hours at 39.5°C), hooded seal skin fibroblasts displayed circadian expression of two core clock genes, *Bmal1* (indicated as *Arntl* in the paper) and *Per2*. Importantly, *Bmal1* and *Per2* expression continued to cycle in a constant temperature, demonstrating that there was an endogenous circadian clock operating in the hooded seal. We also monitored fibroblast mitochondrial activity via respirometric O_2 consumption measurements. Principal component analysis revealed that there was a significant difference in the LEAK state linked to complex I at the two timepoints where *Bmal1* was at its approximate peak and trough.

Because of how the experiment was designed, our initial mitochondrial O_2 consumption measurements did not cover the exact peak and trough phases of *Bmal1* expression. Therefore, to predict the exact clock phase, we used cells transfected with a Bmal1:luciferase reporter and again synchronised through temperature cycling (12 hours at 36.5°C and 12 hours at 39.5°C). This allowed us to perform respirometry at the exact peak and trough phases of *Bmal1*. The results confirmed the presence of a clock-dependent change in complex I efficiency, being

higher at *Bmal1* trough, probably in synchrony with the daily changes in the hooded seal diving efforts.

To summarise, in **paper I** we were able to characterize for the first time, the hooded seal molecular clock and to show that it is involved in regulation of mitochondrial activity via changes in complex I efficiency.

4.1.1 Extension to paper I

Hypoxia and clocks in a deep-diving mammal

Having established the presence of a functional clock and its relation to mitochondrial activity in hooded seal fibroblasts, we also wanted to investigate whether cellular responses to hypoxia show cyclic diurnal variation. Therefore, we also monitored the gene expression profiles of *Hif-1α* and *Pdk1* in the same set of experiments as in **paper I**. To analyse rhythmicity, we used the Jonckheere–Terpstra–Kendall (JTK) cycle, a non-parametric algorithm designed to detect cyclic patterns (Hughes et al., 2010). In contrast to previous reports (Wu et al., 2017), there was no significant circadian rhythmicity in the expression of *Hif-1α* either under temperature cycling or under constant temperature (Figure 13A and B). This may be seen as evidence of that, also in the hooded seal, Hif-1α is always expressed, and if any type of circadian regulation exists, it most likely takes place at the protein level (Adamovich et al., 2017).

As already mentioned, *Pdk1* is one of the HIF-1 dimer target genes and its product inhibits the conversion of pyruvate into Acetyl-CoA, contributing to a switch towards a glycolysis-centred metabolism (Kim et al., 2006). Even though Hif-1α expression did not show rhythmicity, Pdk1 expression was oscillating with a period of ~24 hours both under temperature cycling and constant temperature (JTK $p<0.001$ and $p<0.05$, respectively; Figure 13A and B). In previous studies on mice transcriptomics, Pdk1 was not found to be oscillating (Neufeld-Cohen et al., 2016). Nevertheless, the circadian oscillation of Pdk1 expression reported here can be considered as a species-specific mechanism that may regulate a daily switch from a more OXPHOS-based metabolism to a mainly glycolytic metabolism, in concomitance with the longer and deeper dives at daytime.

We also wanted to test whether hypoxia induction had any effect on the clock genes expression profile in a diving mammal, as fluctuations in O_2 levels have been reported to act as a resetting cue (i.e., Zeitgeber) for the molecular clock in non-diving species (Adamovich et al., 2017).

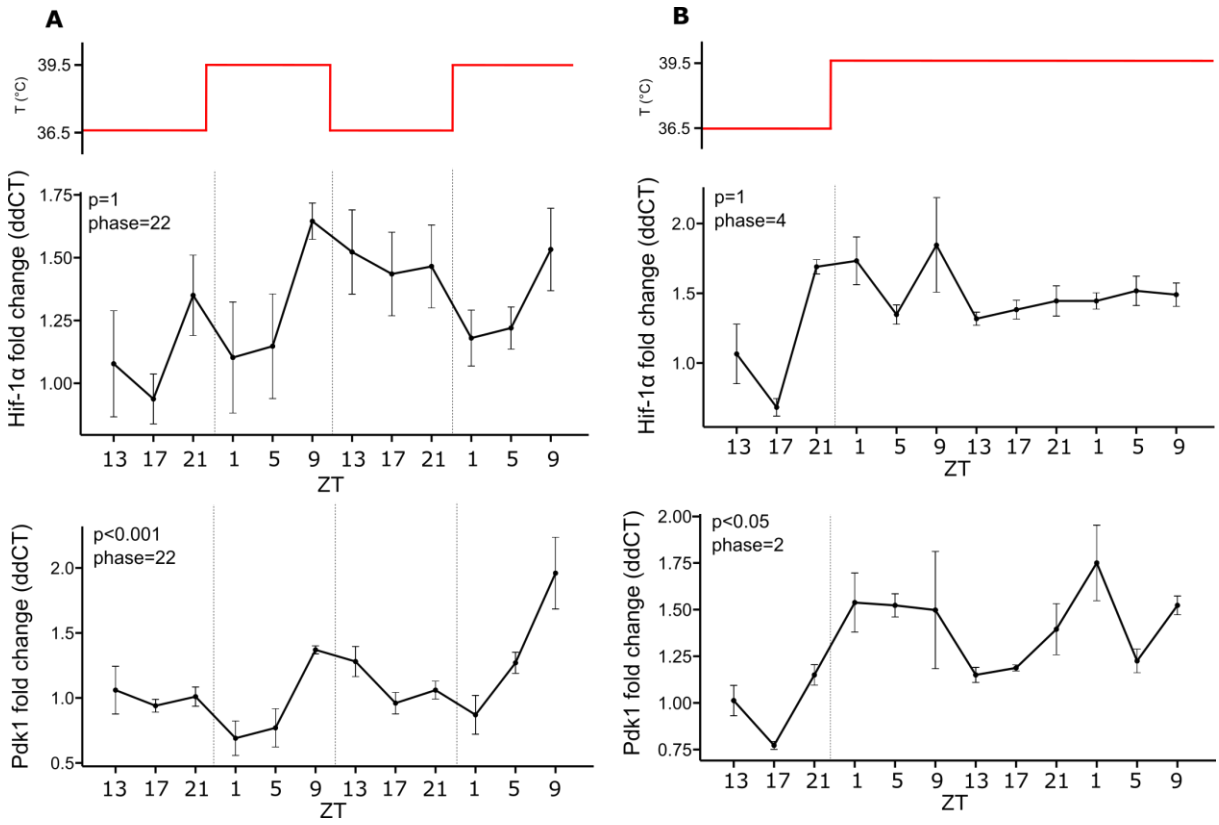

Figure 13. Expression profile of hypoxia inducible factor 1-α (Hif-1α) and pyruvate dehydrogenase kinase 1 (Pdk1). A) mRNA expression of Hif-1α and Pdk1 in hooded seal fibroblasts synchronised by temperature cycle, as shown in the upper panel. Hif-1α expression does not show circadian oscillations, while Pdk1 expression oscillates with a roughly 24 hours period. P-values and phases were calculated through JTK cycle analysis (n=4). **B)** mRNA expression of Hif-1α and Pdk1 in hooded seal fibroblasts synchronised by temperature cycle and then kept under constant temperature, as shown in the upper panel. Hif-1α expression does not have circadian oscillations, while Pdk1 maintains its ~24 hours period also under constant conditions. P-values and phases were calculated through JTK cycle analysis (n=4). Data are expressed as mean ± s.e.m.

To do so, we exposed hooded seal skin fibroblast to "chemical hypoxia", through incubation with dimethyloxalylglycine (DMOG). DMOG inhibits PHD and therefore stabilises HIF-1α at normal O_2 levels, mimicking the cellular response to hypoxia (Ogle et al., 2012). We demonstrated that we could induce HIF-1α stabilisation via DMOG in hooded seal skin fibroblast (Figure 14A), using human embryonic kidney 293T (HEK 293T) cells as a positive control (Ciminera et al., 2021).

Using hooded seal skin fibroblasts transfected with a Bmal1:luciferase reporter and synchronised with dexamethasone for 30 minutes (Du and Brown, 2021) and treated with either 500 µM DMOG, or with 1% dimethyl sulfoxide (DMSO) as control, we measured the reporter activity in a photomultiplier tube for 4 days (Figure 14B). Incubation with DMOG caused a reduction of the cycle amplitude and, though not significant, a lengthening of the period (Figure 14B, C and D), in accordance with previous studies in two widely used cell lines, human

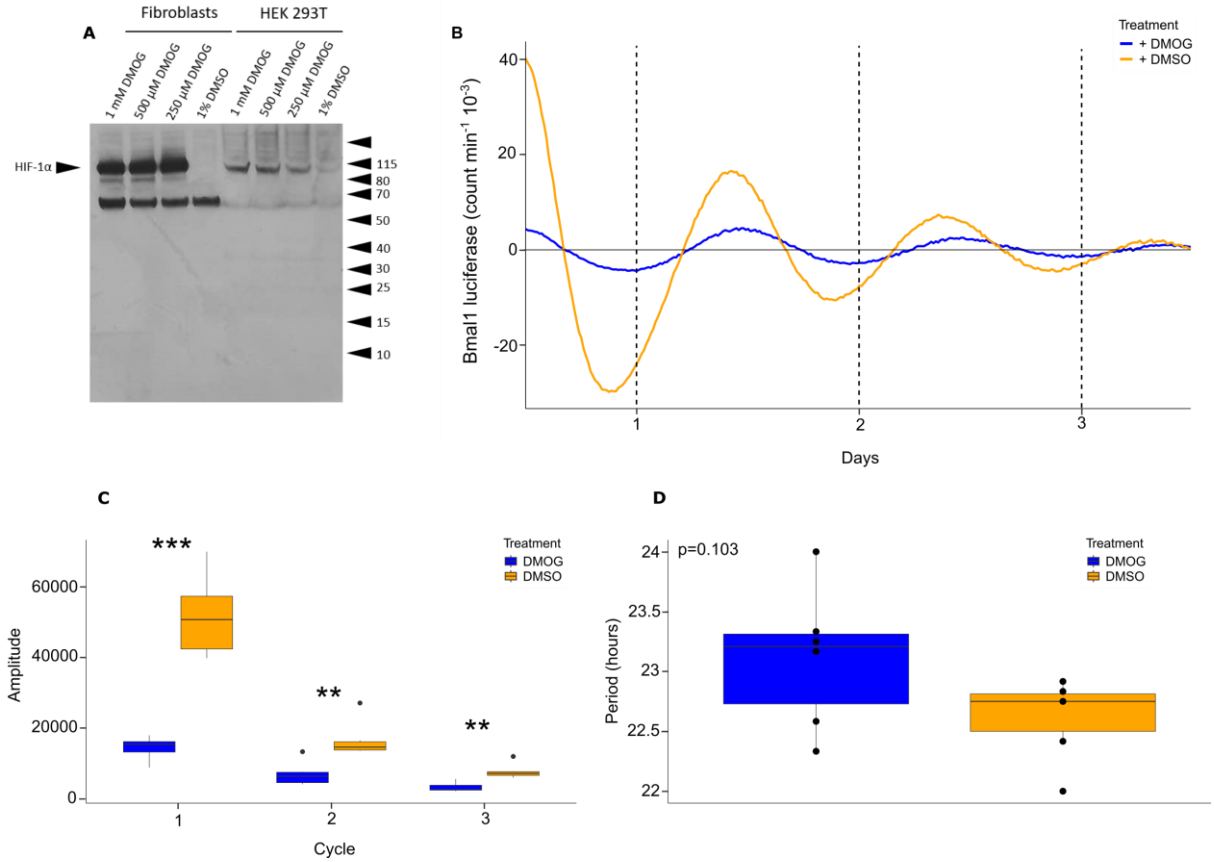

Figure 14. Dimethyloxalylglycine (DMOG) effect on hooded seal skin fibroblasts. A) Western blot showing HIF-1α protein accumulation in hooded seal skin fibroblasts and HEK 293T cells after incubation with 1% DMSO (control), 250 µM, 500 µM and 1 mM DMOG for 2 hours. **B)** Photon multiplier tube recordings of hooded seal skin fibroblasts transfected with Bmal1 luciferase reporter synchronised with dexamethasone and incubated with 1% DMSO (control group - orange) and 500 µM DMOG (blue). **C)** Average amplitude for each cycle reported in B. Data expressed as mean ± s.d. (n=6) **D)** Period length calculation based on the recordings shown in B. Data expressed as mean ± s.d. (n=6). ***p<0.001, **p<0.01 (One-way ANOVA analysis).

osteosarcoma cells (U2OS) and mouse myotubes (C2C12) (Peek et al., 2017; Wu et al., 2017). Since hypoxia is known to cause tissue-specific clock misalignments (e.g., period lengthening in the liver or shortening in the kidneys) (Manella et al., 2020), it seems logical to assume that the phase shifting seen in hooded seal fibroblasts might be connected to the DMOG-linked induction of HIF-1α stabilisation. However, more studies are needed to verify the presence of a molecular interaction between HIF-1α and the clock machinery in hooded seal.

Overall, these data show a possible connection between the HIF-1-singalling pathway and the clock genes also in hypoxia-tolerant mammals. But these data also highlight the difficulties in interpretating the direction of causation when considering the interactions between clock-mitochondria and hypoxia.

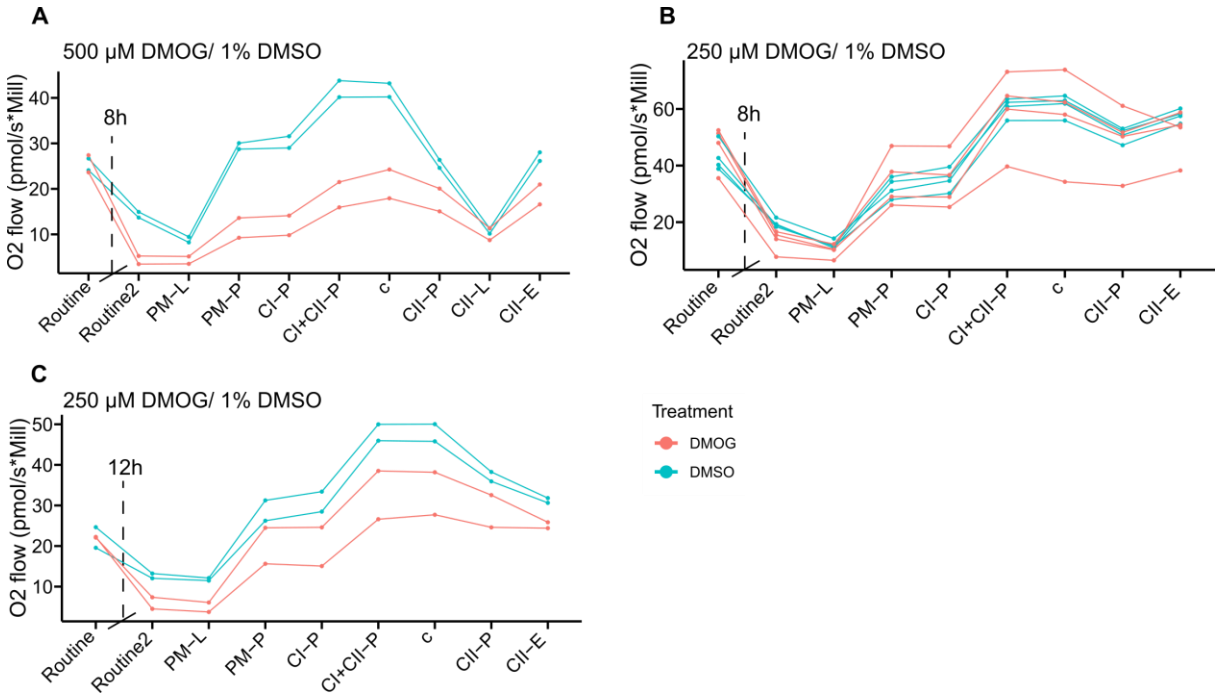

Figure 15. O_2 consumption of human embryonic kidney cells (HEK 293T) incubated with DMOG in the Oroboros oxygraphic chamber. A) HEK 293T cells incubated with 1% DMSO (control - blue) and 500 µM DMOG (red) for 8 hours in the oxygraphic chamber. Every mitochondrial state measured showed reduction in O_2 flow, but cells did not pass the cytochrome c test. **B)** HEK 293T cells incubated with 1% DMSO (control - blue) and 250 µM DMOG (red) for 8 hours in the oxygraphic chamber. Even though the cells passed the cytochrome c test, results were not clear: only one experimental chamber showed a reduction in O_2 flow. **C)** HEK 293T cells incubated with 1% DMSO (control - blue) and 250 µM DMOG (red) for 12 hours in the oxygraphic chamber. Every mitochondrial state measured showed reduction in O_2 flow and the cells passed the cytochrome c test. *Mitochondrial states measured*: basal respiration before incubation (Routine), basal respiration after incubation period (Routine2), complex I leak (PM-L), complex I OXPHOS with pyruvate and malate (PM-P), complex I OXPHOS with pyruvate, malate and glutamate (CI-P), complex I and II OXPHOS (CI+CII-P), cytochrome c test (c) complex II OXPHOS (CII-P) complex II leak (CII-L), complex II uncoupled state (CII-E).

HRR in simulated hypoxic conditions

A hypoxia response was induced in the oxygraphic chamber by injecting DMOG, previously shown to effectively induced HIF-1α stabilisation in HEK 293T cells (Ciminera et al., 2021). Following Fets et al. (2018), HEK 293T cells were suspended in respiration medium and then introduced into the oxygraphic chambers. Basal respiration (Routine) was measured and treatments to optimise the concentration and duration of DMOG were applied, then we proceeded following the same protocol as for the HRR measurements described in **paper I** (Figure 15).

Long incubation times with DMOG were used prior to the full SUIT protocol because within the first 1 hour of DMOG treatment there are effects on mitochondrial respiration, independent of HIF-1α activation (Zhdanov et al., 2015) and protein HIF-1α stabilisation does not occur

until after ~ 4 hours, while effects on HIF-1α target gene are not seen until 7 hours later (Zhdanov et al., 2015). We also removed oligomycin from the SUIT protocol because it is a potent inhibitor that is quite difficult to remove from the oxygraphic chamber and that could negatively affect any subsequent measurements (source: https://www.bioblast.at/index.php/Oligomycin).

The results (Figure 15) provide a protocol to test the effects of chemical hypoxia in the Oroboros. We show that: (1) the DMOG response is both concentration and time dependent, (2) long incubation times in the oxygraphic chamber are possible, and (3) it is possible to chemically induce a hypoxic response in the Oroboros. This protocol remains to be tested on cells derived from hooded seals.

4.2 Paper II: The metabolic roles of neurons and astrocytes in the diving brain

Paper II is provided as a manuscript. The aim was to investigate the rANLS hypothesis (Mitz et al., 2009) (Figure 8). Specifically, our proposition, based on rANLS, was that seal neurons would possess less mitochondria and a reduced OXPHOS capacity compared to seal astrocytes, essentially the reverse of what has been observed in rodents (Alano et al., 2007; Wong-Riley, 1989).

To investigate this, we needed to isolate hooded seal astrocytes and neurons, to investigate mitochondria number and size in both cell types, in a comparison between mice and seals, and to conduct cell specific HRR measurements of mitochondrial respiratory capacity. Our analysis using cell-specific immunohistochemistry revealed that adult hooded seal astrocytes had higher mitochondrial counts compared to seal neurons, which is the opposite to our observations in mice and which supports the rANLS hypothesis. However, we also found an age-related difference in mitochondrial number and size between juvenile and adult seals, with juveniles appearing “mouse-like” in the distribution of mitochondria. This may be related to developmental changes in diving behaviour, from less numerous and shallower dives in the first year of living (particularly for our captive seals), to more frequent and deeper dives as adults (Folkow et al., 2010; Folkow & Blix 1999).

The respirometry data suggest that hooded seal astrocytes have an O_2 consumption capacity at least equal to seal neurons, which seems to be in line with the rANLS hypothesis. The relative

contribution of complexes I to total respiration was however significantly lower in astrocytes than in neurons. Considering that complex I is the major producers of ROS at reoxygenation, a reduction in astrocytic complex I contribution to total O_2 consumption might also be regarded as an hypoxia-induced adaptation (Ravasz et al., 2024). In addition, the analysis of existing hooded seal neuron-specific transcriptome data (Geßner et al., 2022) revealed that seal neuron might show decreased O_2 consumption in connection to specific molecular rearrangements in the mitochondrial ETS.

In summary, the results presented in **paper II** support the rANLS by showing higher mitochondria density in hooded seal astrocytes than in neurons, and that astrocytes present an equal or higher O_2 consumption capacity as hooded seal neurons.

4.3 Paper III: AstroSel: a stable astrocytic cell line to study hypoxia tolerance and lactate oxidation in the brain of an Arctic pinniped

Paper III is presented as a manuscript. The aim of this paper was to validate the use of an immortalised cell line, AstroSel, as a substitute for the primary astrocytic cultures derived from the hooded seal visual cortex. The costs of the immortalisation process were covered by a grant awarded to me from the Nansenfondet in 2023. The immortalised cells were also used to determine the ability of seal astrocyte to use lactate as energy fuel, as is predicted by the rANLS (Mitz et al., 2009).

The analysis of previously established astrocytic and neuronal markers (Steuernagel et al., 2022), showed an increased expression for astrocytic markers in the immortalised cells, similar to the expression pattern reported for the primary cultures. The positive stain for the glia marker GFAP further confirmed the identity and purity of the cell lines.
We also looked at metabolic markers whose expression profile might be of key importance for the rANLS: LDHA, LDHB, MCT2 and MCT4. Our analysis showed similar results between the primary cells and the immortalised cells: all of them presented high expression levels of both LDHA and LDHB, showing that seal astrocytes are capable of not only reducing pyruvate to lactate, but also oxidising lactate to pyruvate. Further, we report high levels of MCT2 and low levels of MCT4 in both the astrocytic cell lines, which is the opposite of what is expected for mammalian astrocytes (Pierre and Pellerin, 2005). High levels of MCT2 indicate that seal astrocytes possess the ability to import lactate and, presumably, use it as fuel for energy.

Indeed, our HRR measurements of cells supplied with either glucose or lactate show that these cells can maintain their normal OXPHOS rate independently of which substrate is supplied. To further prove that the cells were importing lactate, we also treated the cells with an MCT2 inhibitor, which showed to have a negative effect on the respiration in two of the cell lines incubated only with lactate.

To summarise, in **paper III** we show that the AstroSel cell lines can be used as an alternative to primary astrocytic cultures, making the study of cellular hypoxia-induced adaptations in the hooded seal brain more accessible. Further, we show that hooded seal astrocytes might possess the ability to adjust their metabolism according to available substrate and that they may be actively involved in the elevated capacity for lactate oxidation in the brain of this species (e.g., Czech-Damal et al., 2014).

5 Discussion and conclusions

5.1 General discussion

One of the key requirements for life on Earth is the presence of O_2 in adequate amounts Although reduction in O_2 levels may have severe consequences for the energy state, and even survival, of most species, some have evolved a series of behavioural and physiological adaptation that enable them to cope with many of the challenges that follow from hypoxia, or even anoxia (Fago, 2022; Larson et al., 2014). Among vertebrates, some species, have adapted to chronically hypoxic (e.g., the naked mole rat, *Heterocephalus glaber*), or seasonally anoxic (e.g., the freshwater turtle, *Trachemys scripta*; the crucian carp, *Carassius carassius)* environments (Fago, 2022; Larson et al., 2014). Although for shorter periods, also diving mammals, like pinnipeds, are regularly exposed to reduced O_2 availability that has been shown to cause severe hypoxemia, as a result of their breath-hold diving behaviour (Larson et al., 2014; Ramirez et al., 2007). Among pinnipeds the hooded seal is considered quite remarkable as it performs some of the longest and deepest dives recorded (Andersen et al., 2013; Vacquie-Garcia et al., 2017).

In the following paragraphs I will discuss the most common adaptations to hypoxia and anoxia, focusing on how these are shared between different species. I will then focus on how the findings of this thesis add new knowledge to the present literature on hypoxia-tolerance.

5.2 Adaptations to hypoxia: common strategies in different species

Hypoxia-tolerant species share many adaptations, of which the most pronounced is hypometabolism (Boutilier, 2001; Hochachka, 1986). Suppressing the metabolic rate decreases the cellular and tissue's demand for ATP, allowing some organisms to rely only on glycolysis for energy production. In the brain of the anoxia-tolerant freshwater turtle (genera *Trachemys* and *Chrysemys*) a comatose-like state is achieved by decreasing the activity rate of the ion-motive ATPases, which, alone, are responsible for the consumption of almost 50% of the ATP produced (Rolfe and Brand, 1996). This is possible because the onset of hypoxia also causes a reduction in ion-channel density, allowing for fewer ions to leak through the cellular membrane (Hochachka, 1986). This mechanism, referred to as *channel arrest*, allows for a reduction in membrane permeability making the maintenance of membrane potentials less energy demanding (Hochachka, 1986). The channel arrest is also accompanied by a *synaptic arrest* consisting of decreased levels of the excitatory neurotransmitter glutamate and increased

release of the inhibitory neurotransmitter gamma-aminobutyric acid (GABA) (Nilsson and Lutz, 1993b). The increase in GABA concentration contributes to brain hypometabolism by binding to its $GABA_A$ receptors (also upregulated during anoxia) and causing neuronal hyperpolarisation (Nilsson and Lutz, 1993b; Pamenter et al., 2011).

Although the evidence for channel arrest and synaptic arrest come mainly from species of turtles and fish, the possibility that a similar mechanism might also take place in the mammalian brain should not be excluded. Indeed, the reduced synaptic activity that is implied by transcriptome data from seal neurons (Geßner et al., 2022) might indicate that also the seal brain can enter a hypometabolic state, presumably by actively suppressing synaptic signalling. In accordance with this hypothesis, spontaneous activity and synaptic transmission in hooded seal visual cortex slices was shown to decrease during hypoxia incubation and to be restored after reoxygenation (Czech-Damal et al., 2014; Geiseler et al., 2016; Ramirez et al., 2011). Similar results were also obtained for the naked-mole rat hippocampus after exposure to both hypoxia and anoxia (Larson and Park, 2009). Considering that, in contrast to the anoxic turtles, seals must remain active (e.g., hunting for food) during potentially hypoxic dives, a complete shutdown of neuronal signalling would not be beneficial. This rather suggests that a controlled shut-down of neural activity might be taking place in some cerebral circuits but not in others, so to maintain neuronal function (Ramirez et al., 2007). Indeed, also in the crucian carp, which remains relatively active even during anoxia, brain energy consumption is decreased only by ~30% (Johansson et al., 1995), in contrast to the 95% reported for anoxic turtles (Jackson, 1968; Perez-Pinzon et al., 1992).

The lower ATP demand of this hypometabolic state also ensures substrates conservation during the entire anoxic/hypoxic period (Hochachka, 1986). As the main source of glucose for glycolysis during O_2 deprivation is glycogen, a slower metabolism will also allow for a slower depletion of the glycogen stores (Hochachka, 1986). Although this is not as much of a problem to the diving brain, since it receives an unchanged or even elevated blood glucose supply during the dive (Blix et al., 1983), it is nevertheless a common characteristic of hypoxia- and anoxia-tolerant species to have elevated glycogen stores (Lutz et al., 2003). Usually, the larger the glycogen stores the longer is the anoxic survival time (Bundgaard et al., 2020; Warren et al., 2006).

Elevated glycogen stores were also found in the hooded seal brain (Czech-Damal et al., 2014). Although this was initially thought to be possibly connected to an increased glycolytic metabolism, it was later found that the anaerobic capacity of the hooded seal brain does not differ markedly from that of the brain of ferret or mouse (Hoff et al., 2016). This led to the conclusion that the difference between the seal brain and the non-diving brain is in the ability of dealing with the potentially toxic end-product of glycolysis: lactate (Hoff et al., 2016). Indeed, not only the capacity of relying on anaerobic metabolism for prolonged periods of time, but also the ability to deal with its end products, is a typical trait of hypoxia- and anoxia-tolerant species (Bundgaard et al., 2020; Fago, 2022; Lutz et al., 2003).

A great example is the crucian carp. By having one of the largest glycogen stores among vertebrates (Hyvärinen et al., 1985), the crucian carp heavily relies on glycolytic ATP while overwintering in anoxic ice-covered lakes (Lutz and Nilsson, 1997). The high glycolytic rate can potentially lead to toxic levels of lactate and protons. However, in the crucian carp the enzyme PDH possesses an additional catalytic component which allows for conversion of pyruvate into acetaldehyde which, in turn, is transformed into ethanol by the enzyme alcohol dehydrogenase (Fagernes et al., 2017; Shoubridge and Hochachka, 1980). The ethanol can then be expelled by the organism through the gills, avoiding lactate accumulation (Shoubridge and Hochachka, 1980).

As well as dealing with maintaining energetic homeostasis during the hypoxic period, some hypoxia-tolerant species must deal with reoxygenation. It is at reoxygenation that most of the ROS are produced by the mitochondria (Murphy, 2009). Some species, like pinnipeds, counteract the increase in ROS production by maintaining an efficient antioxidant defence (e.g., Pablo Vázquez-Medina et al., 2012). By contrast, turtles of the genus *Trachemys* are known to avoid production of ROS at reoxygenation, probably by preventing accumulation of succinate during hypoxia (Bundgaard et al., 2019a). Indeed, succinate oxidation to fumarate by complex II via RET is the major cause of ROS production by complex I upon reoxygenation (Murphy, 2009), therefore, avoiding succinate accumulation can reduce the probability of RET taking place. Elevated succinate concentrations are instead found in the liver of anoxic crucian carps (Dahl et al., 2021). A recent hypothesis suggests that during anoxia, the succinate produced in the brain might be transported to the liver, where the consequent production of ROS might be less damaging because of the higher regenerative capacity of the hepatic tissue compared to that of the brain (Dahl et al., 2021; Lefevre and Nilsson, 2023).

In the past 20 years, more and more attention has been given to mitochondria and their role in conveying hypoxia and anoxia tolerance (Lefevre and Nilsson, 2023). By being the source of the increased intracellular Ca^{2+} during anoxia, mitochondria are one of the major contributors of the hypoxia-induced hypometabolism (Buck and Bickler, 1995). The onset of anoxia activates the mitochondrial potassium channel (K_{ATP}), allowing for K^+ ions to accumulate in the mitochondria. The subsequent depolarisation of the mitochondrial membrane leads to Ca^{2+} in the cytosol. Here, the interaction of Ca^{2+} with calmodulin appears to contribute to the decreased activity of two glutamatergic receptors, AMPA and NMDA (Buck and Bickler, 1995; Buck and Pamenter, 2018; Pamenter et al., 2008), contributing to the overall decrease of neuronal activity.

In addition, mitochondria can drastically decrease their respiration rate upon hypoxia exposure. This was found to be true both for the red-eared turtle, (*Trachemys scripta elegans*), the goldfish (*Carassius auratus*) and the naked-mole rat (Bundgaard et al., 2019a; Farhat et al., 2021; Pamenter et al., 2018). This suppression of mitochondrial respiration is not accompanied by a change in mitochondrial shape, distribution or density in the cardiac tissue of the red-eared turtle or in the skeletal muscle of the naked-mole rat (Bundgaard et al., 2019a; Marks de Chabris et al., 2023), indicating that in these species, hypoxia more likely induces changes in mitochondrial substrates oxidation rather than in their morphology. However, it has been hypothesised that the reduced mitochondrial complex IV activity reported in goldfish might be concomitant to a reduction in mitochondrial density (Farhat et al., 2021).

There are, therefore, both similar and different ways in which evolution has allowed different organisms to adapt to the lack of O_2 and survive. However, if these organisms were just "waiting" for the hypoxic or anoxic insult to start, the onset of all these adaptations might be too late to have an effect. After all, it is also the ability to trigger hypometabolism in a "*regulated fashion*" which confers these species their remarkable survival skills (Boutilier, 2001).

5.3 The importance of "timing" in O_2 usage

Evidence from early studies show that pinnipeds possess a variety of adaptations, from an enhanced O_2 carrying and storing capacity to drastic rearrangement of the circulatory function while submerged (Blix, 2018). The scope of these adaptations is obviously to guarantee that

enough O_2 is supplied to the hypoxia-sensitive tissues to maintain metabolic homeostasis. Evidence gathered in more recent studies suggests that it is not only the quantity of O_2 but also the efficiency with which O_2 is used that plays a crucial role (Geßner et al., 2022). Indeed, a more efficient use of O_2 does not only delay O_2 depletion but also ensures metabolic homeostasis without the accumulation of harmful metabolic byproducts (e.g., lactate, ROS). In addition, as already pointed out by Boutilier (2001), an increased efficiency of the energy producing pathways also contributes to the hypoxia-induced hypometabolism. One way to ensure a more efficient use of O_2 is for the organisms to be able to predict when the O_2 levels will drop and prepare for this situation.

As described in **paper I** and in previous studies (Folkow and Blix, 1999), the hooded seal shows a circadian rhythmicity in its diving behaviour, with dives being longer and deeper during the day and shorter and shallower at night. This implies that, possibly, the entity of the hypoxic challenge these seals must face will change with a period of approximately 24-hour. The results presented in **paper I** show that the ability of the hooded seal to predict and adapt to these challenges relies on the presence of a functional endogenous clock, which among other things, may be responsible for synchronising mitochondrial activity according to diving effort.
Particularly, my analyses suggest that the clock is responsible for a change in complex I efficiency, which may be extremely beneficial as it can either cause a reduction in ROS production by the mitochondria (Brand, 2000; Cadenas, 2018), or a switch from an OXPHOS-based metabolism towards a less oxygen-dependent one. In both cases, the clock-mediated metabolic adjustments are likely small parts in a larger range of adaptive responses that altogether have enabled hooded seals to cope with their deep-diving lifestyle. Indeed, by enhancing the efficiency of mitochondrial O_2 use when the dives are longer (i.e., during the day), the seal will be able to spend more time underwater when it is more convenient, i.e., when also its prey is found deeper in the water column (e.g. redfish (Torsvik et al., 1995) and squid (Kristensen, 1984)).

By contrast, the circadian clock of another hypoxia-tolerant mammal, the plateau pika (*Ochotona curzoniae*), was found to be disrupted (Liu et al., 2022). The plateau pika is a small mammal living at high altitude and therefore adapted to chronic hypoxia. The two different types of hypoxic challenges that a seal and a pika must face (intermittent vs chronic) might be the reason why clock function is preserved in one but not in the other. As already mentioned, one of the advantages of possessing a functional clock is the ability to predict environmental

changes and adapt to them. However, the pika inhabits a very unstable habitat where environmental changes are difficult to predict. Thus, in this case, a functional clock might actually be more detrimental then helpful (Liu et al., 2022). Interestingly, disruption of clock function in the pika occurs via a mutation of the Epas1 protein, i.e. hypoxia inducible factor 2 (HIF-2), further highlighting the role of the hypoxia-clock interaction in determining a species adaptations and survival in their own environment (Liu et al., 2022).

High altitude-induced hypoxia also affects the clock gene expression in humans, together with the expression of genes related to the immune response (Manella et al., 2022). Although the effect of both the circadian clock and high altitude hypoxia on the immune response have been described separately (Pham et al., 2021; Scheiermann et al., 2013), the hypoxia-clock interaction effects on the immune response have been poorly investigated (Manella et al., 2022). The understanding of the coordinated regulation of the immune response via both the hypoxia signalling pathway and the clock might be beneficial for the development of strategies against pathologies that have both a hypoxic and a circadian component (e.g., obstructive sleep apnea) (Gabryelska et al., 2022).

5.4 Possible role of complex I in brain hypoxia-tolerance

Considering that seals spend ~90% of their time underwater, most molecular adaptations to hypoxia have probably evolved to be graded adaptations, rather than *on and off* mechanisms. This is the case with the diving response itself, and probably concerns all levels of adaptations to their (primarily submerged) lifestyle.

The hooded seal brain has a remarkable ability to maintain integrity, even after long exposure to hypoxia. *In vitro* recordings in cortical slices of maintained membrane potential and ability to produce action potentials in neurons, and maintained synaptic transmission in the hippocampus during exposure to severe hypoxia for 1-3 hours, demonstrate that this feature in part is due to intrinsic mechanisms of hypoxia tolerance (Folkow et al., 2008; Geiseler et al., 2016). One possible mechanisms is the rANLS hypothesis (Figure 8) which suggests that seal astrocytes have a high oxidative capacity, possibly to support anaerobic neuronal ATP-production, when that is needed (Hoff et al., 2016; Mitz et al., 2009). This hypothesis is corroborated by the results presented in **paper II** where, adult seal astrocytes not only show a higher number of mitochondria compared to neurons, but also appear to have an OXPHOS

capacity equal to that of neurons. Analysis of hooded seal neuronal transcriptome datasets further suggest that the low neuronal OXPHOS rate is related to molecular rearrangement of the ETS possibly involving deactivation of complex I.

Given the involvement of complex I in both tumour biology and hypoxia (Iommarini et al., 2013; Tello et al., 2011), it is interesting to note that the results of both **paper I** and **II** suggest the presence of a complex I-linked adaptation to hypoxia. In cancer cells, defects in the complex I assembly are indeed related to the induction of the Warburg effect, a switch towards enhanced glycolytic metabolism even when O_2 is not limiting (Desquiret-Dumas et al., 2019; Warburg, 1956). In diving seals, which frequently encounter hypoxia, such a switch could be beneficial and promote neuronal survival, especially if occurring in combination with the decreased OXPHOS rate proposed in **paper II**. As the latter confers enhanced efficiency to the oxidative metabolism, the two mechanisms together could contribute to a slower depletion of the available O_2 while guaranteeing adequate ATP supply. In addition, a switch from complex I active form to the deactive form is known to be stimulated by hypoxia exposure in rodent models; a passage that is of crucial importance for reduction of ROS production and oxidative damage upon reoxygenation (Stepanova et al., 2019). Indeed, complex I is one of the major producers of ROS via RET when, at reoxygenation, complex II starts transferring electrons to complex I (Murphy, 2009). The presence of a deactive form of complex I has been connected to a reduced and slower production of ROS after reoxygenation (Stepanova et al., 2019). Such a mechanism would be extremely beneficial to a diving mammal that is frequently experiencing episodes of hypoxia and reoxygenation.

5.5 Glutamate catabolism in hypoxia tolerance

Glutamate is an important excitatory neurotransmitter in the brain and plays an active role in the metabolic coupling of astrocytes and neurons in the non-diving brain (Figure 4).
Normally, glutamate is taken up from the extracellular space by the astrocytes, where it stimulates aerobic glycolysis. Glutamate is also shuttled back to neurons in the form of glutamine (Figure 4) (Azarias et al., 2011; Pellerin and Magistretti, 1994). However, recent analysis of hooded seal neuron transcriptome suggests that, in the seal brain, neurons might also have an important direct role in glutamate uptake, implying that cerebral glutamate dynamics might also differ between diving and non-diving mammals (Geßner et al., 2022).

Considering this and the differential expression of the complex II subunits SDHA and SDHB reported for seal neurons in **paper II**, the possibility of an increased glutamate catabolism should not be excluded. An enhancement of glutamate catabolism upon hypoxia exposure has been hypothesised for another hypoxia-tolerant mammal, the naked-mole rat (Cheng et al., 2022), as well as for the anoxia-tolerant crucian carp and freshwater turtle (Bundgaard et al., 2019b; Dahl et al., 2021). The advantage of switching to glutamate catabolism would be the preservation of the activity of mitochondrial dehydrogenases and of ATP production, when O_2 is limiting. Indeed, during hypoxia, glutamate can undergo a deamination reaction together with pyruvate, which results in the production of alanine and α-ketoglutarate. The latter is a TCA cycle intermediate (Figure 1B) from which succinyl-coenzyme A is generated which, in turn, is transformed into succinate (Figure 1B). The conversion of succinyl-coenzyme A into succinate also generates GTP, which can be used to produce ATP. It has been demonstrate that this metabolic pathway is one of the major sources of ischemic succinate accumulation (Zhang et al., 2018).

The last reactions of the TCA cycle, from succinate to oxaloacetate (Figure 1B), are all reversible. In hypoxia, the generation of α-ketoglutarate from glutamate also contributes to the formation of oxaloacetate (Figure 1B) via the malate-aspartate shuttle (MAS). In the turtle heart, the increased concentration of oxaloacetate pushes the TCA cycle "in reverse" towards the formation of malate, fumarate and finally succinate (Figure 1B) (Bundgaard et al., 2019b). Other than contributing to the succinate accumulation, this pathway also reduces the cellular "reductive stress". The latter is one of the consequences of the hypoxia-induced decreased mitochondrial respiration rate: specifically, the lower complex I activity will decrease the rate at which NADH is oxidised to NAD^+, therefore causing an increase in NADH concentration (i.e., high NADH/NAD^+ ratio) and a lack of useful reducing agents for the glycolysis and the TCA cycle (Figure 1) (Xiao and Loscalzo, 2020). As the formation of malate from oxaloacetate requires the oxidation of NADH to NAD^+, this would restore the "reductive equilibrium" of the cells, which is in turn needed for the maintenance of glycolysis. At the same time, the MAS also guarantees the maintenance of glutamate levels which, indeed, have been found not to be changing after hypoxia exposure, in either the turtle heart or the hooded seal brain (Bundgaard et al., 2019b; Martens et al., 2023).

Although investigating glutamate dynamics was beyond the scope of this thesis, it is interesting to note how this might be of relevance in determining the hypoxia tolerance of different species.

However, more directed studies are needed to understand how and if glutamate is involved in the hooded seal brain hypoxia tolerance.

5.6 The role of lactate in the hooded seal brain

As already discussed above, one of the most important adaptations of hypoxia- and anoxia-tolerance species is the ability to rapidly eliminate the byproducts of anaerobic metabolism, especially lactate. The lactate levels in the hooded seal visual cortex are known to decrease after hypoxia and reoxygenation (Martens et al., 2023). This decrease might happen in connection with the increased export of lactate via cerebral venous blood at the end of a dive (Kerem and Elsner, 1973), or due to an increase in astrocytic lactate import (via MCT2) and metabolism, on reoxygenation. In the non-diving brain, neurons are known to increase MCT2 expression after ischemia (Rosafio et al., 2016) and also astrocytic MCT4 expression is known to be O_2 dependent (Rosafio and Pellerin, 2014). According to the results presented in **paper III** and in the transcriptome analysis of hooded seal neurons (Geßner et al., 2022), the MCT2 and MCT4 expression profile is inverted in the seal. Assuming that, although inverted, both MCT2 and MCT4 preserved their O_2-dependent regulation, it is plausible to assume that, in the hooded seal brain, a possible neuronal export of lactate resulting from a mainly glycolytic metabolism might be compensated by an increased astrocytic import via MCT2. One major implication for the neurons to be able to rely on anaerobic metabolism and shuttle the lactate to the astrocytes, is the avoidance of the above-mentioned reductive stress (Xiao and Loscalzo, 2020). If, during a hypoxic episode the neurons are mainly glycolytic, then the pyruvate produced will be reduced to lactate via LDHA, a reaction which requires the oxidation of NADH to NAD^+. The resulting increase in the NAD^+ levels guarantee the maintenance of a sustainable glycolytic rate over some time.

The results presented in **paper III** show that primary astrocytes derived from hooded seal visual cortex are enriched for both LDHA and LDHB. This is in contrast with what previously found for human astrocytes which only showed presence of LDHA (Laughton et al., 2007), and supports the rANLS hypothesis. The high expression of LDHB in astrocytes associated with high expression of MCT2, suggests the presence of a lactate shuttle from the extracellular space to the astrocytes. Via HRR analysis of immortalised astrocytes (AstroSel) we also show that these cells, which preserve the same gene expression profile as the primary hooded seal astrocytes, maintain an unchanged oxidative capacity, independently of whether glucose or

lactate is supplied. This further corroborates the hypothesis that astrocytes are fundamental for lactate oxidation in the hooded seal brain.

Such a tight mechanisms of lactate shuttling and oxidation between neurons and astrocytes might also have important implications for a seal ADL and time spent at surface. As already mentioned, the ADL corresponds to the time a seal can stay submerged without accumulating a critical amount of lactate in the blood (Kooyman et al., 1980). Dives longer than the ADL are usually associated with longer times at surface as the more lactate accumulates, the longer is needed for its concentration to go back to normal levels (Kooyman et al., 1980). However, if astrocytes in the brain are able to take up and oxidise the increased amounts of lactate exported by the neurons at reoxygenation, this might reduce the time needed for lactate levels to go back to pre-dive ones. This would be extremely beneficial as then the seal could spend longer times underwater, hunting for food, and reduce the time spent at surface between dives.

Electrophysiological studies show that hooded seal neurons have enhanced tolerance for high concentrations of lactate. Indeed, hooded seal visual cortex slices incubated with only lactate in hypoxic conditions still showed spontaneous neuronal activity, in contrast to mouse slices, in which lactate incubation caused loss of signal (Czech-Damal et al., 2014). In addition to a metabolic role, lactate may also have a role as a signalling molecule in the brain. Indeed recent evidence shows that lactate can successfully supress synaptic signalling in the hooded seal hippocampus via interaction with the lactate receptor HCAR1 (Torppa, 2023). It is therefore possible that the unusually high concentration of lactate reported in the seal brain, especially after a dive (Kooyman et al., 1983; Scholander, 1940), might be playing a neuroprotective role by contributing to the general brain hypometabolism (Torppa, 2023).

It is interesting to note that in resting harbor seals, 30% of the systemic lactate that is produced during diving, via glycolysis, is converted back to glucose between dives, possibly to enhance glycogen stores, mainly in skeletal muscle (Davis, 1983). Considering the enhanced cerebral glycogen stores, and non-significant changes in glucose levels after hypoxia and reoxygenation, both reported in the hooded seal brain (Czech-Damal et al., 2014; Martens et al., 2023), it is possible that some of the brain-derived lactate is recycled into glucose and glycogen, too.

5.7 Conclusions

In **paper I** we have established the presence of a functional molecular clockwork in the deep-diving hooded seal. We further show that mitochondrial activity is dependent on clock-phase, validating the hypothesis that a clock-mitochondria interaction exists also in hypoxia-tolerant species and that may contribute to enhanced hypoxia tolerance. According to the rANLS hypothesis, enhanced hypoxia tolerance is also given by a peculiar subdivision of the metabolic work between astrocytes and neurons in the seal brain, which we investigated in **paper II**. Our analysis show that hooded seal astrocytes have similar or possibly higher oxidative metabolic capacity as do seal neurons. Further, in **paper III** we show that seal astrocytes can rely on both glucose and lactate for energy production, thus contributing to an increased lactate oxidative capacity in seal brain.

In summary, hypoxia tolerance is not a trait which is given by one single adaptive mechanism, but it is rather due to the combined effect of several small adaptations. The work presented in this thesis shows that, in this collection of adaptive mechanisms, mitochondrial oxidative metabolism and its regulation have an important role in conferring high hypoxia tolerance.

6 Future research

6.1 Brain hypoxia tolerance

Ongoing studies on pinniped cerebral hypoxia tolerance have focused on investigating cell-specific metabolic pathways in relation to the rANLS hypothesis, and on mechanisms for regulation of neuronal activity in hypoxia. In the context of the rANLS theory, a characterisation of the cell-specific MCTs distribution in the brain is relevant. Although the results presented in **paper III** and neuronal transcriptome analysis (Geßner et al., 2022) are both suggestive of an inverted distribution of MCTs between astrocytes and neurons (compared to e.g., rodents), a direct study of MCTs in the hooded seal brain is still missing. In this respect, an astrocyte-specific transcriptome analysis would be helpful as, except for immunocytochemical and histochemical studies, a proper characterisation of pinnipeds astrocytes has not been performed yet. Similarly, although immunohistochemical studies show high localization of Ngb in hooded seal astrocytes, a quantification of Ngb content in seal astrocytes and neurons has not yet been done. For all these purposes, both existing primary cell cultures and the immortalized AstroSel lines should be exploited.

Like other hypoxia/anoxia tolerant species, the hooded seal presents high brain glycogen stores (Czech-Damal et al., 2014). Although for non-diving species it is well established that astrocytes are the site where glycogen is stored (Brown and Ransom, 2007), this has not been investigated in diving mammals. Considering the rANLS theory and assuming that neurons of a diving mammal do have a higher glycolytic capacity than have neurons of a non-diving species, it would be logical to assume that this cell type is the major site of brain glycogen stores in the seal brain. However, given the results of **paper III**, where seal astrocytes are able to oxidize both glucose and lactate, one can also hypothesised that, in the seal brain, rather than being confined only in one cell-type, glycogen might be stored and used by both astrocytes and neurons. Seeing how this has not been yet clarified, future studies should also focus on describing the dynamics of glycogen storage and usage in the seal brain.

Many physiological studies have reported a reduced signalling activity in the hooded seal brain when exposed to hypoxia (Czech-Damal et al., 2014; Geiseler et al., 2016; Ramirez et al., 2011), and lactate signalling via HCAR receptors was recently shown to play a possible role (Torppa, 2023). Despite this, no studies have yet been able to clarify whether GABA-mediated inhibition of neuronal signalling may be involved. Transcriptome analysis of hooded seal

neurons suggests that these cells have depressed glutamatergic and GABAergic synaptic activity, implying that inhibitory signalling might not be as important as in turtles (Nilsson and Lutz, 1993a). However, whether hypoxia does, in fact, enhance inhibitory signalling in the hooded seal brain remains to be investigated. Similarly, the presence of channel arrest mechanisms and suppression of ATPases activity requires further studies.

Regulation of mitochondrial metabolism also needs to be further investigated. Indeed, despite adding new knowledge on cell-specific oxidative metabolism, the results presented in **paper II** represent only one part of the story. We have indeed measured mitochondrial O_2 consumption only in normoxic conditions. Considering the diving lifestyle of the hooded seal, it would be interesting to conduct more respirometry studies in hypoxic conditions or at reoxygenation, to further investigate when and how the rANLS takes place. In addition, to fully describe the mitochondrial characteristics of both astrocytes and neurons, further studies aimed at describing their mitochondrial ultrastructure, e.g. via electron microscopy, are needed. Mitochondrial ultrastructure has, indeed, a role in determining the metabolic profile of a cell and, specifically, different organisation of the cristae mitochondriales have been reported for astrocytes and neurons in rat (Kristián et al., 2006). A differential spatial organisation of the cristae is also a determinant for the formation of mitochondrial super-complexes (Cogliati et al., 2013). Super-complexes result from the association of two or more ETS complexes (typically I, III and IV) and they not only affect mitochondrial function (Guan et al., 2022), but are also important for regulating complex I ROS production (Lopez-Fabuel et al., 2016; Maranzana et al., 2013). Although the presence of super-complexes in the heart of the anoxia-tolerant turtle was shown to not play a role in modulating mitochondrial function (Bundgaard et al., 2018; Bundgaard et al., 2019a), studies on breast cancer have demonstrated that super-complexes formation can increase hypoxia tolerance (Ikeda et al., 2019). Therefore, it would be interesting for future studies to verify whether they may have a role in conferring hypoxia-tolerance in mammals.

6.2 Circadian rhythms in hypoxia

Rhythmic changes in oxygen levels can act as a resetting cue for the mammalian molecular clock (Adamovich et al., 2017). This is the case for some species that are usually not exposed to O_2 limiting conditions, but a similar response has not yet been documented for hypoxia tolerant species. Although the results presented in "extension to paper I" show some differences in clock period and amplitude as a response to chemically simulated hypoxia (Figure 14), a

more detailed analysis of clock gene expression in actual hypoxic conditions is needed. Such measurements would give more insight on whether hypoxia can act as a resetting cue in hypoxia tolerant species as it does for non-tolerant ones (Adamovich et al., 2017; Manella et al., 2020), or whether the ability to be synchronised by oscillating O_2 levels has been lost in species which experience hypoxia on regular basis. Moreover, concomitant analysis of mitochondrial activity would also reveal whether a clock-mitochondria relationship is preserved also when O_2 is scarce.

Considering the clock-dependent change in mitochondrial complex I efficiency presented here, using seal fibroblasts, it would be interesting to investigate if similar mechanisms were also taking place in the seal brain, specifically in the astrocytes. Recent studies have revealed an important role of astrocytes in timekeeping; specifically, astrocytes located in the SCN have been shown to possess a strong molecular clock, which, alone, can determine circadian behaviour in mammals (Astiz et al., 2022; Brancaccio et al., 2019). Verifying whether astrocytes of the SCN preserve this ability also in pinnipeds, and whether they are involved in regulating the "onset" and "offset" of molecular responses to hypoxia, would give more insights into how their physiological functions are regulated, especially in relation to their rhythmic diving behaviour.

7 References

Adamovich, Y., Ladeuix, B., Golik, M., Koeners, M. P. and Asher, G. (2017). Rhythmic Oxygen Levels Reset Circadian Clocks through HIF1α. *Cell Metab.* **25**, 93–101.

Adamovich, Y., Dandavate, V. and Asher, G. (2022). Circadian clocks' interactions with oxygen sensing and signalling. *Acta Physiol.* **234**, 1–12.

Alano, C. C., Tran, A., Tao, R., Ying, W., Karliner, J. S. and Swanson, R. A. (2007). Differences among cell types in NAD+ compartmentalization: A comparison of neurons, astrocytes, and cardiac myocytes. *J. Neurosci. Res.* **85**, 3378–3385.

Almeida, A. and Medina, J. M. (1997). Different mitochondrial coupling in neurons and in astrocytes in primary culture. *Biochem. Soc. Trans.* **25**, 4–5.

Altmann, R. (1894). Die Elementarorganismen und ihre Beziehungen zu den Zellen.p. Veit, Leipzig.

Ameneiro, C., Moreira, T., Fuentes-Iglesias, A., Coego, A., Garcia-Outeiral, V., Escudero, A., Torrecilla, D., Mulero-Navarro, S., Carvajal-Gonzalez, J. M., Guallar, D., et al. (2020). BMAL1 coordinates energy metabolism and differentiation of pluripotent stem cells. *Life Sci. Alliance* **3**, 1–15.

Andersen, J. M., Skern-Mauritzen, M., Boehme, L., Wiersma, Y. F., Rosing-Asvid, A., Hammill, M. O. and Stenson, G. B. (2013). Investigating annual diving behaviour by hooded seals (cystophora cristata) within the northwest atlantic ocean. *PLoS One* **8**, e80438.

Anderson, J., Toh, Z. Q., Reitsma, A., Do, L. A. H., Nathanielsz, J. and Licciardi, P. V. (2019). Effect of peripheral blood mononuclear cell cryopreservation on innate and adaptive immune responses. *J. Immunol. Methods* **465**, 61–66.

Asher, G. and Schibler, U. (2011). Crosstalk between components of circadian and metabolic cycles in mammals. *Cell Metab.* **13**, 125–137.

Astiz, M., Delgado-garcía, L. M. and Laura, L. (2022). Astrocytes as essential time-keepers of the central pacemaker. *Glia* **70**, 808–819.

Azarias, G., Ne Perreten, H., Lengacher, S., Poburko, D., Demaurex, N., Magistretti, P. J. and Chatton, J.-Y. (2011). Glutamate Transport Decreases Mitochondrial pH and Modulates Oxidative Metabolism in Astrocytes. *J. Neurosci.* **31**, 3550–3559.

Bak, L. K. and Walls, A. B. (2018). CrossTalk opposing view: lack of evidence supporting an astrocyte-to-neuron lactate shuttle coupling neuronal activity to glucose utilisation in the brain. *J. Physiol.* **596**, 351–353.

Baydon, A. R. (2010). Cell culture technique. In *Principles and Techniques of Biochemistry and Molecular Biology* (ed. Wilson, K.) and Walker, J.), pp. 38–72. Cambridge University Press.

Bell, E. L., Klimova, T. A., Eisenbart, J., Moraes, C. T., Murphy, M. P., Budinger, G. R. S. and Chandel, N. S. (2007). The Qo site of the mitochondrial complex III is required for the transduction of hypoxic signaling via reactive oxygen species production. *J. Cell Biol.* **177**, 1029–1036.

Benz, R. and Mclaughlin, S. (1983). The molecular mechanism of action of the proton ionophore fccp (carbonylcyanide p-trifluoromethoxyphenylhydrazone). *Biophys. J.* **41**, 381–398.

Bhutta, B. S., Faysal, A. and Berim, I. (2022). Hypoxia. In *StatPearls[Internet]*, p. StatPearls Publishing.

Bittar, P. G., Charnay, Y., Pellerin, L., Bouras, C. and Magistretti, P. J. (1996). Selective distribution of lactate dehydrogenase isoenzymes in neurons and astrocytes of human brain. *J. Cereb. Blood Flow Metab.* **16**, 1079–1089.

Blix, A. S. (2018). Adaptations to deep and prolonged diving in phocid seals. *J. Exp. Biol.*

221, jeb182972.
Blix, A. S. and From, S. H. (1971). Lactate dehydrogenase in diving animals - A comparative study with special reference to the eider (Somateria mollissima). *Comp. Biochem. Physiol. -- Part B Biochem.* **40B**, 579–584.
Blix, A. S., Elsner, R. and Kjekshus, J. K. (1983). Cardiac output and its distribution through capillaries and A-V shunts in diving seals. *Acta Physiol. Scand.* **118**, 109–116.
Blix, A., Walløe, L., Messelt, E. and Folkow, L. P. (2010). Selective brain cooling and its vascular basis in diving seals. *J. Exp. Biol.* **213**, 2610–2616.
Boehme, L., Lovell, P., Biuw, M., Roquet, F., Nicholson, J., Thorpe, S. E., Meredith, M. P. and Fedak, M. (2009). Technical note: Animal-borne CTD-Satellite Relay Data Loggers for real-time oceanographic data collection. *Ocean Sci.* **5**, 685–695.
Boutilier, R. G. (2001). Mechanisms of cell survival in hypoxia and hypothermia. *J. Exp. Biol.* **204**, 3171–3181.
Boyer, P. D. (1993). The binding change mechanism for ATP synthase - some probabilities and possibilities. *Biochim. Biophys. Acta* **1140**, 215–250.
Brancaccio, M., Edwards, M. D., Patton, A. P., Smyllie, N. J., Chesham, J. E., Maywood, E. S. and Hastings, M. H. (2019). Cell autonomous clock of astrocytes drives circadian behaviour in mammals. *Science (80-.).* **363**, 187–192.
Brand, M. D. (2000). Uncoupling to survive? The role of mitochondrial inefficiency in ageing. *Exp. Gerontol.* **35**, 811–820.
Brand, M. D. and Nicholls, D. G. (2011). Assessing mitochondrial dysfunction in cells. *Biochem. J.* **435**, 297–312.
Brandt, U. (2006). Energy converting NADH:quinone oxidoreductase (complex I). *Annu. Rev. Biochem.* **75**, 69–92.
Brown, A. M. and Ransom, B. R. (2007). Astrocyte glycogen and brain energy metabolism. *Glia* **55**, 1263–1271.
Brown, S. A., Zumbrunn, G., Fleury-Olela, F., Preitner, N. and Schibler, U. (2002). Rhythms of Mammalian Body Temperature Can Sustain Peripheral Circadian Clocks. *Curr. Biol.* **12**, 1574–1583.
Buck, L. T. and Bickler, P. E. (1995). Role of adenosine in NMDA receptor modulation in the cerebral cortex of an anoxia-tolerant turtle (Chrysemys picta belli). *J. Exp. Biol.* **198**, 1621–1628.
Buck, L. T. and Pamenter, M. E. (2018). The hypoxia-tolerant vertebrate brain: Arresting synaptic activity. *Comp. Biochem. Physiol. Part - B Biochem. Mol. Biol.* **224**, 61–70.
Buhr, E. D. and Takahashi, J. S. (2013). Molecular components of the mammalian circadian clock. *Handb. Exp. Pharmacol.* **217**, 3–27.
Buhr, E. D., Yoo, S. H. and Takahashi, J. S. (2010). Temperature as a universal resetting cue for mammalian circadian oscillators. *Science (80-.).* **330**, 379–385.
Bundgaard, A., James, A. M., Joyce, W., Murphy, M. P. and Fago, A. (2018). Suppression of reactive oxygen species generation in heart mitochondria from anoxic turtles: The role of complex I S-nitrosation. *J. Exp. Biol.* **221**, jeb174391.
Bundgaard, A., Qvortrup, K., Rasmussen, L. J. and Fago, A. (2019a). Turtles maintain mitochondrial integrity but reduce mitochondrial respiratory capacity in the heart after cold acclimation and anoxia. *J. Exp. Biol.* **222**, jeb200410.
Bundgaard, A., James, A. M., Gruszczyk, A. V., Martin, J., Murphy, M. P. and Fago, A. (2019b). Metabolic adaptations during extreme anoxia in the turtle heart and their implications for ischemia-reperfusion injury. *Sci. Rep.* **9**, 2850.
Bundgaard, A., Ruhr, I. M., Fago, A. and Galli, G. L. J. (2020). Metabolic adaptations to anoxia and reoxygenation: New lessons from freshwater turtles and crucian carp. *Curr. Opin. Endocr. Metab. Res.* **11**, 55–64.

Burmester, T. and Hankeln, T. (2009). What is the function of neuroglobin? *J. Exp. Biol.* **212**, 1423–1428.

Burmester, T., Weich, B., Reinhardt, S. and Hankeln, T. (2000). A vertebrate globin expressed in the brain. *Nature* **407**, 1998–2001.

Burns, J. M., Lestyk, K. C., Folkow, L. P., Hammill, M. O. and Blix, A. S. (2007). Size and distribution of oxygen stores in harp and hooded seals from birth to maturity. *J. Comp. Physiol. B Biochem. Syst. Environ. Physiol.* **177**, 687–700.

Cadenas, S. (2018). Mitochondrial uncoupling, ROS generation and cardioprotection ☆. *Biochim. Biophys. Acta - Bioenerg.* **1859**, 940–950.

Cahn, R. D., Kaplan, N. O., Levine, L. and Zwilling, E. (1962). Nature and Development of Lactic Dehydrogenases. *Am. Assoc. Adv. Sci.* **136**, 962–969.

Capaldi, R. A. (1990). Structure and function of cytochrome c oxidase. *Annu. Rev. Biochem.* **59**, 569–596.

Capes-Davis, A. and Freshney, R. I. (2021). *Freshney's Culture of Animal Cells: A manual of Basic Technique and Specialised Applications*. Eight Edit. John Wiley & Sons, Inc.

Carrel, A. and Burrows, M. T. (1911). Cultivation of tissues in vitro and its technique. *J. Exp. Med.* **13**, 387–396.

Carroll, J., Fearnley, I. M., Skehel, J. M., Shannon, R. J., Hirst, J. and Walker, J. E. (2006). Bovine Complex I Is a Complex of 45 Different Subunits *. *J. Biol. Chem.* **281**, 32724–32727.

Carter, M. I. D., Bennett, K. A., Embling, C. B., Hosegood, P. J. and Russell, D. J. F. (2016). Navigating uncertain waters: A critical review of inferring foraging behaviour from location and dive data in pinnipeds. *Mov. Ecol.* **4**, 1–20.

Chance, B. and Williams, G. R. (1955). Respiratory enzymes in oxidative phosphorylation I. Kinetics of oxygen utilization. *J. Biol. Chem.* **217**, 383–393.

Chandel, N. S. (2021). Basics of metabolic reactions. *Cold Spring Harb. Perspect. Biol.* **13**, 1–12.

Cheng, H., Qin, Y. A., Dhillon, R., Dowell, J., Denu, J. M. and Pamenter, M. E. (2022). Metabolomic Analysis of Carbohydrate and Amino Acid Changes Induced by Hypoxia in Naked Mole-Rat Brain and Liver. *Metabolites* **12**, 56.

Chouchani, E. T., Pell, V. R., Gaude, E., Aksentijević, D., Sundier, S. Y., Robb, E. L., Logan, A., Nadtochiy, S. M., Ord, E. N. J., Smith, A. C., et al. (2014). Ischaemic accumulation of succinate controls reperfusion injury through mitochondrial ROS. *Nature* **515**, 431–435.

Chuquet, J., Quilichini, P., Nimchinsky, E. A. and Buzsáki, G. (2010). Predominant enhancement of glucose uptake in astrocytes versus neurons during activation of the somatosensory cortex. *J. Neurosci.* **30**, 15298–15303.

Ciminera, A. K., Shuck, S. C. and Termini, J. (2021). Elevated glucose increases genomic instability by inhibiting nucleotide excision repair. *Life Sci. Alliance* **4**, 1–15.

Clausen, G. and Ersland, A. (1969). The respiratory properties of the blood of the bladdernose seal (Cystophora cristata). *respir* **7**, 1–6.

Cloudsley-Thompson, J. L. (1960). Adaptive functions of circadian rhythms. *Cold Spring Harb. Symp. Quant. Biol.* **25**, 345–355.

Cogliati, S., Frezza, C., Soriano, M. E., Varanita, T., Quintana-Cabrera, R., Corrado, M., Cipolat, S., Costa, V., Casarin, A., Gomes, L. C., et al. (2013). Mitochondrial Cristae Shape Determines Respiratory Chain Supercomplexes Assembly and Respiratory Efficiency. *Cell* **155**, 160–171.

Contreras-Baeza, Y., Sandoval, P. Y., Alarcón, R., Galaz, A., Cortés-Molina, F., Alegriá, K., Baeza-Lehnert, F., Arce-Molina, R., Guequén, A., Flores, C. A., et al. (2019). Monocarboxylate transporter 4 (MCT4) is a high affinity transporter capable of

exporting lactate in high-lactate microenvironments. *J. Biol. Chem.* **294**, 20135–20147.
Cooke, S. J., Hinch, S. G., Wikelski, M., Andrews, R. D., Kuchel, L. J., Wolcott, T. G. and Butler, P. J. (2004). Biotelemetry: A mechanistic approach to ecology. *Trends Ecol. Evol.* **19**, 334–343.
Counter', C. M., Avilion3, A. A., Lefeuvrel, C. E., Stewart', N. G., Greider3, C. W., Harley2, C. B. and Bacchettil', S. (1992). Telomere shortening associated with chromosome instability is arrested in immortal cells which express telomerase activity.; Telomere shortening associated with chromosome instability is arrested in immortal cells which express telomerase activity. *EMBO J.* **1**, 1–921.
Czech-Damal, N. U., Geiseler, S. J., Hoff, M. L. M., Schliep, R., Ramirez, J. M., Folkow, L. P. and Burmester, T. (2014). The role of glycogen, glucose and lactate in neuronal activity during hypoxia in the hooded seal (Cystophora cristata) brain. *Neuroscience* **275**, 374–383.
Dahl, H. A., Johansen, A., Nilsson, G. E. and Lefevre, S. (2021). The metabolomic response of crucian carp (Carassius carassius) to anoxia and reoxygenation differs between tissues and hints at uncharacterized survival strategies. *Metabolites* **11**, 435.
Dahse, R., Fiedler, W. and Nther Ernst, G. (1997). Telomeres and telomerase: biological and clinical importance. *Clin. Chem.* **43**, 708–714.
Davis, R. W. (1983). Lactate and glucose metabolism in the resting and diving harbor seal (Phoca vitulina). 275–288.
Dawson, D. M., Goodfriend, T. L. and Kaplan, N. (1964). Lactic Dehydrogenases : Functions of the Two Types. *Am. Assoc. Adv. Sci.* **143**, 929–933.
Desquiret-Dumas, V., Leman, G., Wetterwald, C., Chupin, S., Lebert, A., Khiati, S., Le Mao, M., Geffroy, G., Kane, M. S., Chevrollier, A., et al. (2019). Warburg-like effect is a hallmark of complex I assembly defects. *Biochim. Biophys. Acta - Mol. Basis Dis.* **1865**, 2475–2489.
Díaz-García, C. M., Mongeon, R., Lahmann, C., Koveal, D., Zucker, H., Correspondence, G. Y. and Yellen, G. (2017). Neuronal Stimulation Triggers Neuronal Glycolysis and Not Lactate Uptake. *Cell Metab.* **26**, 361–374.
Dienel, G. A. (2012). Brain lactate metabolism : the discoveries and the controversies. *J. Cereb. Blood Flow Metab.* **32**, 1107–1138.
Dienel, G. A. (2019). Brain glucose metabolism: Integration of energetics with function. *Physiol. Rev.* **99**, 949–1045.
Dimova, E. Y., Jakupovic, M., Kubaichuk, K., Mennerich, D., Chi, T. F., Tamanini, F., Oklejewicz, M., Hänig, J., Byts, N., Mäkelä, K. A., et al. (2019). The Circadian Clock Protein CRY1 Is a Negative Regulator of HIF-1α. *iScience* **13**, 284–304.
Douiev, L., Miller, C., Ruppo, S., Benyamini, H., Abu-Libdeh, B. and Saada, A. (2021). Upregulation of cox4-2 via hif-1α in mitochondrial cox4-1 deficiency. *Cells* **10**, 1–16.
Drew, K. L., Harris, M. B., LaManna, J. C., Smith, M. A., Zhu, X. W. and Ma, Y. L. (2004). Hypoxia tolerance in mammalian heterotherms. *J. Exp. Biol.* **207**, 3155–3162.
Du, N.-H. and Brown, S. A. (2021). Measuring Circadian Rhythms in Human Cells.pp. 53–67.
Dunlap, J. C., Loros, J. J. and DeCoursey, P. J. (2004). *Chronobiology: Biological timekeeping*. Sinauer Associates.
Duveen, D. I. and Klickstein, H. S. (1954). *Bibliography of the works of Antoine Laurent Lavoisier, 1743-1794*. London: William Dawson & Sons Ltd. and E. Weil.
Eales, K. L., Hollinshead, K. and Tennant, D. A. (2016). Hypoxia and metabolic adaptation of cancer cells. **5**, 190.
Earle, W. . (1943). Production of malignancy in vitro. IV. The mouse fibroblast cultures and changes seen in living cells. *J. Natl. Cancer Inst.* **4**, 165–212.

Erecińska, M. and Silver, I. A. (2001). Tissue oxygen tension and brain sensitivity to hypoxia. *Respir. Physiol.* **128**, 263–276.

Fabrizius, A., Hoff, M. L. M., Engler, G., Folkow, L. P. and Burmester, T. (2016). When the brain goes diving: Transcriptome analysis reveals a reduced aerobic energy metabolism and increased stress proteins in the seal brain. *BMC Genomics* **17**, 583.

Fagernes, C. E., Stensløkken, K.-O., Røhr, Å. K., Berenbrink, M., Ellefsen, S. and Nilsson, G. E. (2017). Extreme anoxia tolerance in crucian carp and goldfish through neofunctionalization of duplicated genes creating a new ethanol-producing pyruvate decarboxylase pathway OPEN. *Sci. Rep.* **7**, 7884.

Fago, A. (2022). New insights into survival strategies to oxygen deprivation in anoxia-tolerant vertebrates. *Acta Physiol.* **235**, 1–11.

Farhat, E., Cheng, H., Romestaing, C., Pamenter, M. and Weber, J. M. (2021). Goldfish response to chronic hypoxia: Mitochondrial respiration, fuel preference and energy metabolism. *Metabolites* **11**, 187.

Fedak, M., Lovell, P., McConnell, B. and Hunter, C. (2002). Overcoming the constraints of long range radio telemetry from animals: Getting more useful data from smaller packages. In *Integrative and Comparative Biology*, pp. 3–10.

Fets, L., Driscoll, P. C., Grimm, F., Jain, A., Nunes, P. M., Gounis, M., Doglioni, G., Papageorgiou, G., Ragan, T. J., Campos, S., et al. (2018). MCT2 mediates concentration-dependent inhibition of glutamine metabolism by MOG. *Nat. Chem. Biol.* **14**, 1032–1042.

Folkow, L. P. and Blix, A. S. (1999). Diving behaviour of hooded seals (Cystophora cristata) in the Greenland and Norwegian seas. *Polar Biol.* **22**, 61–74.

Folkow, L. P., Mårtensson, P. E. and Blix, A. S. (1996). Annual distribution of hooded seals (Cystophora cristata) in the Greenland and Norwegian seas. *Polar Biol.* **16**, 179–189.

Folkow, L. P., Ramirez, J. M., Ludvigsen, S., Ramirez, N. and Blix, A. S. (2008). Remarkable neuronal hypoxia tolerance in the deep-diving adult hooded seal (Cystophora cristata). *Neurosci. Lett.* **446**, 147–150.

Folkow, L. P., Nordøy, E. S. and Blix, A. S. (2010). Remarkable development of diving performance and migrations of hooded seals (Cystophora cristata) during their first year of life. *Polar Biol.* **33**, 433–441.

Fong, G. and Takeda, K. (2008). Role and regulation of prolyl hydroxylase domain proteins. *Cell Death Differ.* **15**, 635–641.

Fukuda, R., Zhang, H., Kim, J. whan, Shimoda, L., Dang, C. V. and Semenza, G. L. L. (2007). HIF-1 Regulates Cytochrome Oxidase Subunits to Optimize Efficiency of Respiration in Hypoxic Cells. *Cell* **129**, 111–122.

Gabryelska, A., Turkiewicz, S., Karuga, F. F., Sochal, M., Strzelecki, D. and Białasiewicz, P. (2022). Disruption of Circadian Rhythm Genes in Obstructive Sleep Apnea Patients — Possible Mechanisms Involved and Clinical Implication. *Int. J. Mol. Sci.* **23**, 709.

Gandhi, G. K., Cruz, N. F., Ball, K. K. and Dienel, G. A. (2009). Astrocytes are poised for lactate trafficking and release from activated brain and for supply of glucose to neurons. *J. Neurochem.* **111**, 522–536.

Geiseler, S. J., Larson, J. and Folkow, L. P. (2016). Synaptic transmission despite severe hypoxia in hippocampal slices of the deep-diving hooded seal. *Neuroscience* **334**, 39–46.

Geßner, C., Krüger, A., Folkow, L. P., Fehrle, W., Mikkelsen, B. and Burmester, T. (2022). Transcriptomes Suggest That Pinniped and Cetacean Brains Have a High Capacity for Aerobic Metabolism While Reducing Energy-Intensive Processes Such as Synaptic Transmission. *Front. Mol. Neurosci.* **15**, 1–15.

Gey, G. O., Coffman, W. D. and Kubicek, M. T. (1952). Tissue culture studies of the proliferative capacity of cervical carcinoma and normal epithelium. *Cancer Res.* **12**, 264–265.

Gnaiger, E. (2008). Polarographic Oxygen Sensors , the Oxygraph , Respirometry To Assess. In *Mitochondrial dysfunction in drug-induced toxicity* (ed. Dykens, J.) and Will, Y.), pp. 327–348. New York: Wiley.

Gnaiger, E. (2018). MitoPathways at the Q-junction : mouse skeletal muscle fibres . *Mitochondrial Physiol. Netw.* **12.01**, 1–3.

Gnaiger, E. (2020). *Mitochondrial Pathways and Respiratory Control. An introduction to OXPHOS Analysis*. 5th ed. Innsbruck: Bioenergetics Communications 2020.

Gnaiger, E., Steinlechner-Maran, R., Méndez, G., Eberl, T. and Margreiter, R. (1995). Control of mitochondrial and cellular respiration by oxygen. *J. Bioenerg. Biomembr.* **27**, 583–596.

Guan, S., Zhao, L. and Peng, R. (2022). Mitochondrial Respiratory Chain Supercomplexes: From Structure to Function. *Int. J. Mol. Sci.* **23**, 13880.

Halestrap, A. P. and Meredith, D. (2004). The SLC16 gene family - From monocarboxylate transporters (MCTs) to aromatic amino acid transporters and beyond. *Pflugers Arch. Eur. J. Physiol.* **447**, 619–628.

Hammill, M. O. and Stenson, G. B. (2006). Abundance of the Northwest Atlantic Hooded Seals (1960-2005). *DFO Can. Sciemce Advis. Secr.*

Harris, J. J., Jolivet, R. and Attwell, D. (2012). Synaptic Energy Use and Supply. *Neuron* **75**, 762–777.

Harrison, R. G. (1906). Observations on the living developing nerve fiber. *Proc. Soc. Exp. Biol. Med.* **4**, 140–143.

Hassrick, J. L., Crocker, D. E., Teutschel, N. M., McDonald, B. I., Robinson, R. W., Simmons, S. E. and Costa, D. R. (2010). Condition and mass impact oxygen stores and dive duration in adult female northern elephant seals. *J. Exp. Biol.* **213**, 585–592.

Hawley, S. A., Pan, D. A., Mustard, K. J., Ross, L., Bain, J., Edelman, A. M., Frenguelli, B. G. and Grahame Hardie, D. (2005). Calmodulin-dependent protein kinase kinase-β is an alternative upstream kinase for AMP-activated protein kinase. *Cell Metab.* **2**, 9–19.

Hayflick, L. (1965). The limited in vitro lifetime of human diploid cell strains. *Exp. Cell Res.* **37**, 614–636.

Hazlerigg, D. G., Appenroth, D., Tomotani, B. M., West, A. C. and Wood, S. H. (2023). Biological timekeeping in polar environments: lessons from terrestrial vertebrates. *J. Exp. Biol.* **226**, jeb246308.

Heine, K. B. and Hood, W. R. (2020). Mitochondrial behaviour, morphology, and animal performance. *Biol. Rev.* **95**, 730–737.

Henderson, A. (1969). Biochemistry of hypoxia: current concepts. I. An introduction to biochemical pathways and their control. *Br. J. Anaesth.* **41**, 245–250.

Herrero-Mendez, A., Almeida, A., Fernández, E., Maestre, C., Moncada, S. and Bolaños, J. P. (2009). The bioenergetic and antioxidant status of neurons is controlled by continuous degradation of a key glycolytic enzyme by APC/C-Cdh1. *Nat. Cell Biol.* **11**, 747–754.

Hill, R. W., Wyse, G. A. and Anderson, M. (2012). Energy metabolism. In *Animal Physiology*, pp. 161–182.

Hindell, M. A., Slip, D. J. and Burton, H. R. (1991). The diving behaviour of adult male and female southern elephant seals, Mirounga leonina (Pinnipedia: Phocidae). *Aust. J. Zool.* **39**, 499–508.

Hindell, M. A., Harcourt, R., Waas, J. R. and Thompson, D. (2002). Fine-scale three-dimensional spatial use by diving, lactating female Weddell seals Leptonychotes

weddellii. *Mar. Ecol. Prog. Ser.* **242**, 275–284.
Hochachka, P. W. (1986). Defense Strategies against Hypoxia and Hypothermia. *Science (80-.).* **231**, 234–241.
Hoff, M. L. M., Fabrizius, A., Folkow, L. P. and Burmester, T. (2016). An atypical distribution of lactate dehydrogenase isoenzymes in the hooded seal (Cystophora cristata) brain may reflect a biochemical adaptation to diving. *J. Comp. Physiol. B Biochem. Syst. Environ. Physiol.* **186**, 373–386.
Hoff, M. L. M., Fabrizius, A., Czech-Damal, N. U., Folkow, L. P. and Burmester, T. (2017). Transcriptome analysis identifies key metabolic changes in the hooded seal (Cystophora cristata) brain in response to hypoxia and reoxygenation. *PLoS One* **12**, 1–21.
Hogenesch, J. B., Gu, Y. Z., Jain, S. and Bradfield, C. A. (1998). The basic-helix-loop-helix-PAS orphan MOP3 forms transcriptionally active complexes with circadian and hypoxia factors. *Proc. Natl. Acad. Sci. U. S. A.* **95**, 5474–5479.
Hughes, M. E., Hogenesch, J. B. and Kornacker, K. (2010). JTK-CYCLE: An efficient nonparametric algorithm for detecting rhythmic components in genome-scale data sets. *J. Biol. Rhythms* **25**, 372–380.
Hütter, E., Unterluggauer, H., Garedew, A., Jansen-Dürr, P. and Gnaiger, E. (2006). High-resolution respirometry-a modern tool in aging research. *Exp. Gerontol.* **41**, 103–109.
Hyvärinen, H., Holopainen, I. J. and Piironen, J. (1985). Anaerobic wintering of crucian carp (Carassius carassius L.)-I. Annual dynamics of glycogen reserves in nature. *Comp. Biochem. Physiol. Part A Physiol.* **82**, 797–803.
Ikeda, K., Horie-Inoue, K., Suzuki, T., Hobo, R., Nakasato, N., Takeda, S. and Inoue, S. (2019). Mitochondrial supercomplex assembly promotes breast and endometrial tumorigenesis by metabolic alterations and enhanced hypoxia tolerance. *Nat. Commun.* **10**, 4108.
Iommarini, L., Calvaruso, M. A., Kurelac, I., Gasparre, G. and Porcelli, A. M. (2013). Complex I impairment in mitochondrial diseases and cancer: Parallel roads leading to different outcomes. *Int. J. Biochem. Cell Biol.* **45**, 47–63.
Irving, L. (1939). Respiration in Diving Mammals. *Physiol. Rev.* **19**, 112–134.
Irving, L., Scholander, P. F. and Grinnell, S. W. (1942). The regulation of arterial blood pressure in the seal during diving. *Am. J. Physiol.* 557–566.
Itoh, Y., Esaki, T., Shimoji, K., Cook, M., Law, M. J., Kaufman, E. and Sokoloff, L. (2003). Dichloroacetate effects on glucose and lactate oxidation by neurons and astroglia in vitro and on glucose utilization by brain in vivo. *Proc. Natl. Acad. Sci. U. S. A.* **100**, 4879–4884.
Jaakkola, P., Mole, D. R., Tian, Y. M., Wilson, M. I., Gielbert, J., Gaskell, S. J., Von Kriegsheim, A., Hebestreit, H. F., Mukherji, M., Schofield, C. J., et al. (2001). Targeting of HIF-α to the von Hippel-Lindau ubiquitylation complex by O2-regulated prolyl hydroxylation. *Science (80-.).* **292**, 468–472.
Jackson, D. C. (1968). Metabolic depression and oxygen depletion in the diving turtle. *J. Appl. Physiol.* **24**, 503–509.
Jacobi, D., Liu, S., Burkewitz, K., Gangl, M. R., Mair, W. B., Lee, C., Unluturk, U., Li, X., Kong, X., Hyde, A. L., et al. (2015). Hepatic Bmal1 Regulates Rhythmic Mitochondrial Dynamics and Promotes Metabolic Fitness Article Hepatic Bmal1 Regulates Rhythmic Mitochondrial Dynamics and Promotes Metabolic Fitness. *Cell Metab.* **22**, 709–720.
Jha, K. K., Banga, S., Palejwala, V. and Ozer, H. L. (1998). SV40-Mediated Immortalization. *Exp. Cell Res.* **245**, 1–7.

Johansson, D., Nilsson, G. E. and Tornblom, E. (1995). Effects of anoxia on energy metabolism in crucian carp brain slices studied with microcalorimetry. *J. Exp. Biol.* **198**, 853–859.

Johnson, C. H., Elliott, J. A. and Foster, R. (2003). Entrainment of circadian programs. *Chronobiol. Int.* **20**, 741–774.

Kerem, D. and Elsner, R. (1973). Cerebral tolerance to asphyxial hypoxia in the harbor seal. *Respiration* **19**, 188–200.

Kierans, S. J. and Taylor, C. T. (2021). Regulation of glycolysis by the hypoxia-inducible factor (HIF): implications for cellular physiology. *J. Physiol.* **599**, 23–37.

Kim, J. W., Tchernyshyov, I., Semenza, G. L. and Dang, C. V. (2006). HIF-1-mediated expression of pyruvate dehydrogenase kinase: A metabolic switch required for cellular adaptation to hypoxia. *Cell Metab.* **3**, 177–185.

Kobayashi, M., Morinibu, A., Koyasu, S., Goto, Y., Hiraoka, M. and Harada, H. (2017). A circadian clock gene, PER2, activates HIF-1 as an effector molecule for recruitment of HIF-1α to promoter regions of its downstream genes. *FEBS J.* **284**, 3804–3816.

Koch, R. E., Buchanan, K. L., Casagrande, S., Crino, O., Dowling, D. K., Hill, G. E., Hood, W. R., McKenzie, M., Mariette, M. M., Noble, D. W. A., et al. (2021). Integrating Mitochondrial Aerobic Metabolism into Ecology and Evolution. *Trends Ecol. Evol.* **36**, 321–332.

Kooyman, G. L. (2004). Genesis and evolution of bio-logging devices: 1963-2002. *Mem. Natl. Inst. Polar Res.* 15–22.

Kooyman, G. L., Gentry, R. L. and Urguhart, D. L. (1976). Northern Fur Seal Diving Behaviour: A New Approach to its Study. *Science (80-.).* **193**, 411–412.

Kooyman, G. L., Wharenbrock, E. A., Castellini, M. A., Davis, R. W. and Sinnett, E. E. (1980). Aerobic and anaerobic metabolism during voluntary diving in Weddell seals: evidence of preferred pathways from blood chemistry and behaviour. *J. Comp. Physiol. B* **138**, 335–346.

Kooyman, G. L., Castellini, M. A., Davis, R. W. and Maue, R. A. (1983). Aerobic Diving Limits of Immature Weddell Seals. *J Comp Physiol* **151**, 171–174.

Kovacs, K. M. (2016). Cystophora cristata, hooded Seal. *IUCN Red List Threat. Species* **8235**, 1–16.

Kovacs, K. M. and Lavigne, D. M. (1986). Cystophora cristata. *Mamm. Species* 1–9.

Kristensen, T. (1984). Biology of the squid Gonatus fabricii (Lich- tenstein, 1818) from West Greenland waters. *Medd Grùn Biosci* **13**, 17.

Kristián, T., Hopkins, I. B., McKenna, M. C. and Fiskum, G. (2006). Isolation of mitochondria with high respiratory control from primary cultures of neurons and astrocytes using nitrogen cavitation. *J. Neurosci. Methods* **152**, 136–143.

Larson, J. and Park, T. J. (2009). Extreme hypoxia tolerance of naked mole-rat brain. *Neuroreport* **20**, 1634–1637.

Larson, J., Drew, K. L., Folkow, L. P., Milton, S. L. and Park, T. J. (2014). No oxygen? No problem! intrinsic brain tolerance to hypoxia in vertebrates. *J. Exp. Biol.* **217**, 1024–1039.

Laughton, J. D., Bittar, P., Charnay, Y., Pellerin, L., Kovari, E., Magistretti, P. J. and Bouras, C. (2007). Metabolic compartmentalization in the human cortex and hippocampus: Evidence for a cell- and region-specific localization of lactate dehydrogenase 5 and pyruvate dehydrogenase. *BMC Neurosci.* **8**, 1–6.

Lee, P., Chandel, N. S. and Celeste Simon, M. (2020). Cellular adaptation to hypoxia through hypoxia inducible factors and beyond. *Nat. Rev. Mol. Cell Biol.* **21**, 268–283.

Lefevre, S. and Nilsson, G. E. (2023). Two decades of research on anoxia tolerance mitochondria,-omics and physiological diversity. *J. Exp. Biol.* **226**, jeb245584.

Lenfant, C., Johansen, K. and Torrance, J. D. (1970). Gas transport and oxygen storage capacity in some pinnipeds and the sea otter. *Respir. Physiol.* **9**, 277–286.

Lenihan, C. R. and Taylor, C. T. (2013). The impact of hypoxia on cell death pathways. *Biochem. Soc. Trans.* **41**, 657–663.

Li, Y. and Deng, J. P. J. (2006). Cytochrome c oxidase subunit IV is essential for assembly and respiratory function of the enzyme complex. *J Bioenerg Biomembr* **38**, 283–291.

Liu, N., Tian, H., Yu, Z., Zhao, H., Li, W., Sang, D., Lin, K., Cui, Y., Liao, M., Xu, Z., et al. (2022). A highland-adaptation mutation of the Epas1 protein increases its stability and disrupts the circadian clock in the plateau pika. *Cell Rep.* **39**, 110816.

Lopez-Fabuel, I., Le Douce, J., Logan, A., James, A. M., Bonvento, G., Murphy, M. P., Almeida, A. and Bolaños, J. P. (2016). Complex I assembly into supercomplexes determines differential mitochondrial ROS production in neurons and astrocytes. *Proc. Natl. Acad. Sci. U. S. A.* **113**, 13063–13068.

Lutz, P. L. and Nilsson, G. E. (1997). Contrasting strategies for anoxic brain survival - glycolysis up or down. *J. Exp. Biol.* **200**, 411–419.

Lutz, P. L., Nilsson, G. E. and H.M., P. (2003). *The brain without oxygen: causes of failure-physiological and molecular mechanisms for survival*. Third. Springer Science & Business Media.

Mächler, P., Wyss, M. T., Elsayed, M., Stobart, J., Gutierrez, R., Von Faber-Castell, A., Kaelin, V., Zuend, M., San Martín, A., Romero-Gómez, I., et al. (2016). In Vivo Evidence for a Lactate Gradient from Astrocytes to Neurons. *Cell Metab.* **23**, 94–102.

Magistretti, P. J. and Allaman, I. (2018). Lactate in the brain: From metabolic end-product to signalling molecule. *Nat. Rev. Neurosci.* **19**, 235–249.

Magistretti, P. J. and Allaman, I. (2022). Brain Energy and Metabolism. In *Neuroscience in the 21st Century* (ed. D.W. Pfaff), pp. 2197–2227. Springer Science+Business Media, LLC.

Manella, G. and Asher, G. (2016). The Circadian Nature of Mitochondrial Biology. *Front. Endocrinol. (Lausanne).* **7**, 8–11.

Manella, G., Aviram, R., Bolshette, N., Muvkadi, S., Golik, M., Smith, D. F. and Asher, G. (2020). Hypoxia induces a time- And tissue-specific response that elicits intertissue circadian clock misalignment. *Proc. Natl. Acad. Sci. U. S. A.* **117**, 779–786.

Manella, G., Ezagouri, S., Champigneulle, B., Gaucher, J., Mendelson, M., Lemarie, E., Stauffer, E., Pichon, A., Howe, C. A., Doutreleau, S., et al. (2022). The human blood transcriptome exhibits time-of-day-dependent response to hypoxia: Lessons from the highest city in the world. *Cell Rep.* **40**, 111213.

Manning, A. and Dawkins, M. S. (2003). *Il comportamento animale*. Fifth Edit. (ed. Boringhieri, B.) Torino.

Manoogian, E. N. C. and Panda, S. (2016). Circadian clock, nutrient quality, and eating pattern tune diurnal rhythms in the mitochondrial proteome. *Proc. Natl. Acad. Sci. U. S. A.* **113**, 3127–3129.

Maqsood, M. I., Matin, M. M., Bahrami, A. R. and Ghasroldasht, M. M. (2013). Immortality of cell lines: Challenges and advantages of establishment. *Cell Biol. Int.* **37**, 1038–1045.

Maranzana, E., Barbero, G., Falasca, A. I., Lenaz, G. and Genova, M. L. (2013). Mitochondrial respiratory supercomplex association limits production of reactive oxygen species from complex i. *Antioxidants Redox Signal.* **19**, 1469–1480.

Marks de Chabris, N. C., Sabir, S., Perkins, G., Cheng, H., Ellisman, M. H. and Pamenter, M. E. (2023). Short communication: Acute hypoxia does not alter mitochondrial abundance in naked mole-rats. *Comp. Biochem. Physiol. -Part A Mol. Integr. Physiol.* **276**, 111343.

Martens, G. A., Folkow, L. P., Burmester, T. and Geßner, C. (2022). Elevated antioxidant defence in the brain of deep-diving pinnipeds. *Front. Physiol.* **13**, 1–18.

Martens, G. A., Geßner, C., Folkow, L. P., Creydet, M., Fischer, M. and Burmester, T. (2023). The roles of brain lipids and polar metabolites in the hypoxia tolerance of deep-diving pinnipeds. *J. Exp. Biol.* **226**, jeb245355.

Mason, S. D., Howlett, R. A., Kim, M. J., Olfert, I. M., Hogan, M. C., McNulty, W., Hickey, R. P., Wagner, P. D., Kahn, C. R., Giordano, F. J., et al. (2004). Loss of skeletal muscle HIF-1α results in altered exercise endurance. *PLoS Biol.* **2**, e288.

Mazat, J. P., Devin, A. and Ransac, S. (2020). Modelling mitochondrial ROS production by the respiratory chain. *Cell. Mol. Life Sci.* **77**, 455–465.

McKeown, S. R. (2014). Defining normoxia, physoxia and hypoxia in tumours - Implications for treatment response. *Br. J. Radiol.* **87**, 1–12.

Meir, J. U., Champagne, C. D., Costa, D. P., Williams, C. L. and Ponganis, P. J. (2009). Extreme hypoxemic tolerance and blood oxygen depletion in diving elephant seals. *Am. J. Physiol. - Regul. Integr. Comp. Physiol.* **297**, 927–939.

Merriam, C. H. (1884). The "hood" of the hooded seal, Cystophora cristata. *Science (80-.).* **4**, 514–516.

Mezhnina, V., Ebeigbe, O. P., Poe, A. and Kondratov, R. V. (2022). Circadian Control of Mitochondria in Reactive Oxygen Species Homeostasis. *Antioxidants Redox Signal.* **37**, 647–663.

Millar, A. J. (1997). Circadian rhythms: PASsing time. *Curr. Biol.* **7**, 474–476.

Mitz, S. A., Reuss, S., Folkow, L. P., Blix, A. S., Ramirez, J. M., Hankeln, T. and Burmester, T. (2009). When the brain goes diving: glial oxidative metabolism may confer hypoxia tolerance to the seal brain. *Neuroscience* **163**, 552–560.

Murdaugh, E. V., Seabury, J. C. and Mitchell, W. L. (1961). Electrocardiogram of the diving seal. *Circ. Res.* **9**, 358–361.

Murphy, M. P. (2009). How mitochondria produce reactive oxygen species. *Biochem. J.* **417**, 1–13.

Murphy, B. J. and Hochachka, P. W. (1981). Free amino acid profiles in blood during diving and recovery in the Antarctic Weddell seal. *Can. J. Zool.* **59**, 455–459.

Murphy, B., Zapol, W. M. and Hochachka, P. W. (1980). Metabolic activities of heart, lung, and brain during diving and recovery in the Weddell seal. *J. Appl. Physiol. Respir. Environ. Exerc. Physiol.* **48**, 596–605.

Neufeld-Cohen, A., Robles, M. S., Aviram, R., Manella, G., Adamovich, Y., Ladeuix, B., Nir, D., Rousso-Noori, L., Kuperman, Y., Golik, M., et al. (2016). Circadian control of oscillations in mitochondrial rate-limiting enzymes and nutrient utilization by PERIOD proteins. *Proc. Natl. Acad. Sci. U. S. A.* **113**, E1673–E1682.

Nilsson, G. E. and Lutz, P. L. (1993a). Role of GABA in hypoxia tolerance, metabolic depression and hibernation-Possible links to neurotransmitter evolution. *Comp. Biochem. Physiol. Part C, Comp.* **105**, 329–336.

Nilsson, G. E. and Lutz, P. L. (1993b). Role of GABA in hypoxia tolerance, metabolic depression and hibernation—Possible links to neurotransmitter evolution. *Comp. Biochem. Physiol. Part C Comp. Pharmacol.* **105**, 329–336.

Odden, Å., Folkow, L. P., Caputa, M., Hotvedt, R. and Blix, A. S. (1999). Brain cooling in diving seals. *Acta Physiol. Scand.* **166**, 77–78.

Ogle, M. E., Gu, X., Espinera, A. R. and Wei, L. (2012). Inhibition of prolyl hydroxylases by dimethyloxaloylglycine after stroke reduces ischemic brain injury and requires hypoxia inducible factor-1 α. *Neurobiol. Dis.* **45**, 733–742.

Ogunshola, O. O. and Antoniou, X. (2009). Contribution of hypoxia to Alzheimer's disease: Is HIF-1α a mediator of neurodegeneration? *Cell. Mol. Life Sci.* **66**, 3555–3563.

Ozer, H. L., Banga, S. S., Dasgupta, T., Houghton, J. M., Hubbard, K., Jha, K. K., Kim, S., Lenhan, M., Pang, Z., Pardinas, J. R., et al. (1996). SV40-Mediated immortalization of human fibroblasts. *Exp. Gerontol.* **31**, 303–310.

Packer, B. S., Altman, A., Cross, C. E., Victor Murdaugh, H., Linta, J. M., Robin, E. D., Altman, M. and Cross, C. E. (1969). Adaptations to diving in the harbor seal: oxygen stores and supply. *Am. J. Physiol.* **217**, 903–906.

Pajuelo Reguera, D., Čunátová, K., Vrbacký, M., Pecinová, A., Houštěk, J., Mráček, T. and Pecina, P. (2020). Cytochrome c Oxidase Subunit 4 Isoform Exchange Results in Modulation of Oxygen Affinity. *Cells* **9**, 443.

Palade, G. E. (1952). The fine structure of mitochondria. *Anat. Rec.* **114**, 427–451.

Palade, G. E. (1953). An electron microscope study of the mitochondrial structure. *J. Histochem. Cytochem.* **1**, 188–211.

Pamenter, M. E., Shin, D. S.-H., Cooray, M. and Buck, L. T. (2008). Mitochondrial ATP-sensitive K + channels regulate NMDAR activity in the cortex of the anoxic western painted turtle. *J Physiol* **586**, 1043–1058.

Pamenter, M. E., Hogg, D. W., Ormond, J., Shin, D. S., Woodin, M. A. and Buck, L. T. (2011). Endogenous GABA A and GABA B receptor-mediated electrical suppression is critical to neuronal anoxia tolerance. *Proc. Natl. Acad. Sci. U. S. A.* **108**, 11274–11279.

Pamenter, M. E., Lau, G. Y., Richards, J. G. and Milsom, W. K. (2018). Naked mole rat brain mitochondria electron transport system flux and H+ leak are reduced during acute hypoxia. *J. Exp. Biol.* **221**, jeb171397.

Panda, S., Antoch, M. P., Miller, B. H., Su, A. I., Schook, A. B., Straume, M., Schultz, P. G., Kay, S. A., Takahashi, J. S. and Hogenesch, J. B. (2002). Coordinated Transcription of Key Pathways in the Mouse by the Circadian Clock. *Cell* **109**, 307–320.

Papandreou, I., Cairns, R. A., Fontana, L., Lim, A. L. and Denko, N. C. (2006). HIF-1 mediates adaptation to hypoxia by actively downregulating mitochondrial oxygen consumption. *Cell Metab.* **3**, 187–197.

Paranjpe, D. A. and Sharma, V. K. (2005). Evolution of temporal order in living organisms.

Peek, C. B. (2020). Metabolic Implications of Circadian–HIF Crosstalk. *Trends Endocrinol. Metab.* **31**, 459–468.

Peek, C. B., Affinati, A. H., Ramsey, K. M., Kuo, H. Y., Yu, W., Sena, L. A., Ilkayeva, O., Marcheva, B., Kobayashi, Y., Omura, C., et al. (2013). Circadian clock NAD+ cycle drives mitochondrial oxidative metabolism in mice. *Science (80-.).* **342**, 1–8.

Peek, C. B., Levine, D. C., Cedernaes, J., Taguchi, A., Kobayashi, Y., Tsai, S. J., Bonar, N. A., McNulty, M. R., Ramsey, K. M. and Bass, J. (2017). Circadian Clock Interaction with HIF1α Mediates Oxygenic Metabolism and Anaerobic Glycolysis in Skeletal Muscle. *Cell Metab.* **25**, 86–92.

Pellerin, L. and Magistretti, P. J. (1994). Glutamate uptake into astrocytes stimulates aerobic glycolysis: A mechanism coupling neuronal activity to glucose utilization. *Proc. Natl. Acad. Sci. U. S. A.* **91**, 10625–10629.

Pereira-Smith, O. M. and Smith, J. R. (1988). Genetic analysis of indefinite division in human cells: Identification of four complementation groups. *Proc. Natl. Acad. Sci. U. S. A.* **85**, 6042–6046.

Perez-Pinzon, M. A., Chan, C. Y., Rosenthal, M. and Sick, T. J. (1992). Membrane and synaptic activity during anoxia in the isolated turtle cerebellum. *Am. J. Physiol. - Regul. Integr. Comp. Physiol.* **263**, R1057–R1063.

Pesta, D. and Gnaiger, E. (2012). High-Resolution Respirometry: OXPHOS protocols for human cells and permeabilized fibers from small biopsies of human muscle. In *Mitochondrial Bioenergetics: Methods and Protocols* (ed. Palmeira, C. M.) and J, M. A.), pp. 25–58. Springer Science+Business Media.

Pham, K., Parikh, K. and Heinrich, E. C. (2021). Hypoxia and Inflammation : Insights From High-Altitude Physiology. **12**, 676782.

Pierre, K. and Pellerin, L. (2005). Monocarboxylate transporters in the central nervous system: Distribution, regulation and function. *J. Neurochem.* **94**, 1–14.

Pierre, K., Pellerin, L., Debernardi, R., Riederer, B. M. and Magistretti, P. J. (2000). Cell-specific localization of monocarboxylate transporters, mct1 and mct2, in the adult mouse brain revealed by double immunohistochemical labeling and confocal microscopy. *Neuroscience* **100**, 617–627.

Pierre, Magistretti, P. J. and Pellerin, L. (2002). MCT2 is a major neuronal monocarboxylate transporter in the adult mouse brain. *J. Cereb. Blood Flow Metab.* **22**, 586–595.

Qvist, J., Hill, R. D., Schneider, R. C., Falke, K. J., Liggins, G. C., Guppy, M., Elliot, R. L., Hochachka, P. W. and Zapol, W. M. (1986). Hemoglobin concentrations and blood gas tensions of free-diving Weddell seals. *J. Appl. Physiol.* **61**, 1560–1569.

Rafiki, A., Boulland, J. L., Halestrap, A. P., Ottersen, O. P. and Bergersen, L. (2003). Highly differential expression of the monocarboxylate transporters MCT2 and MCT4 in the developing rat brain. *Neuroscience* **122**, 677–688.

Ramirez, J. M., Folkow, L. P. and Blix, A. S. (2007). Hypoxia tolerance in mammals and birds: From the wilderness to the clinic. *Annu. Rev. Physiol.* **69**, 113–143.

Ramirez, J. M., Folkow, L. P., Ludvigsen, S., Ramirez, P. N. and Blix, A. S. (2011). Slow intrinsic oscillations in thick neocortical slices of hypoxia tolerant deep diving seals. *Neuroscience* **177**, 35–42.

Ravasz, D., Bui, D., Nazarian, S., Pallag, G., Karnok, N., Roberts, J., Marzullo, B. P., Tennant, D. A., Greenwood, B., Kitayev, A., et al. (2024). Residual Complex I activity and amphidirectional Complex II operation support glutamate catabolism through mtSLP in anoxia. *Sci. Rep.* **14**, 1729.

Reczek, C. R. and Chandel, N. S. (2015). ROS-dependent signal transduction This review comes from a themed issue on Cell regulation. *Curr. Opin. Cell Biol.* **33**, 8–13.

Reinke, H. and Asher, G. (2019). Crosstalk between metabolism and circadian clocks. *Nat. Rev. Mol. Cell Biol.* **20**, 227–241.

Richardson, R. S., Newcomer, S. C. and Noyszewski, E. A. (2001). Skeletal muscle intracellular Po2 assessed by myoglobin desaturation: Response to graded exercise. *J. Appl. Physiol.* **91**, 2679–2685.

Richter, M., Piwocka, O., Musielak, M., Piotrowski, I., Suchorska, W. M. and Trzeciak, T. (2021). From Donor to the Lab: A Fascinating Journey of Primary Cell Lines. *Front. Cell Dev. Biol.* **9**, 1–11.

Rieske, J. S. (1976). Composition, structure, and function of complex III of the respiratory chain. *Biochim. Biophys. Acta* **456**, 195–247.

Rolfe, D. F. S. and Brand, M. D. (1996). Contribution of mitochondrial proton leak to skeletal muscle respiration and to standard metabolic rate. *Am. J. Physiol. - Cell Physiol.* **271**, C1380–C1389.

Rosafio, K. and Pellerin, L. (2014). Oxygen tension controls the expression of the monocarboxylate transporter MCT4 in cultured mouse cortical astrocytes via a hypoxia-inducible factor-1α-mediated transcriptional regulation. *Glia* **62**, 477–490.

Rosafio, K., Castillo, X., Hirt, L. and Pellerin, L. (2016). Cell-specific modulation of monocarboxylate transporter expression contributes to the metabolic reprograming taking place following cerebral ischemia. *Neuroscience* **317**, 108–120.

Russell, W. and Burch, R. (1959). *The principles of human experimental technique*. London: Methuen and Co.

Scheiermann, C., Kunisaki, Y. and Frenette, P. S. (2013). Circadian control of the immune

system. *Nat. Rev. Immunol.* **13**, 190–198.
Schieber, M. and Chandel, N. S. (2014). ROS function in redox signaling and oxidative stress. *Curr. Biol.* **24**, R453–R462.
Schneuer, M., Flachsbarth, S., Czech-Damal, N. U., Folkow, L. P., Siebert, U. and Burmester, T. (2012). Neuroglobin of seals and whales: Evidence for a divergent role in the diving brain. *Neuroscience* **223**, 35–44.
Schofield, C. J. and Ratcliffe, P. J. (2004). Oxygen sensing by HIF hydroxylases. *Nat. Rev. Mol. Cell Biol.* **5**, 343–354.
Scholander, P. F. (1940). Experimental investigations on the respiratory function in diving mammals and birds. *I kommisjon hos Jacob Dybwad*.
Selak, M. A., Armour, S. M., MacKenzie, E. D., Boulahbel, H., Watson, D. G., Mansfield, K. D., Pan, Y., Simon, M. C., Thompson, C. B. and Gottlieb, E. (2005). Succinate links TCA cycle dysfunction to oncogenesis by inhibiting HIF-α prolyl hydroxylase. *Cancer Cell* **7**, 77–85.
Semenza, G. L., Roth, P. H., Fang, H. M. and Wang, G. L. (1994). Transcriptional regulation of genes encoding glycolytic enzymes by hypoxia-inducible factor 1. *J. Biol. Chem.* **269**, 23757–23763.
Sharma, V. K. (2003). Adaptive Significance pf Circadian Clocks. *Chronobiol. Int.* **20**, 901–919.
Shay, J. W., Wright, W. E. and Werbin, H. (1991). Defining the molecular mechanisms of human cell immortalization. *Biochim. Biophys. Acta* **1072**, 1–7.
Shoubridge, E. A. and Hochachka, P. W. (1980). Ethanol: Novel End Product of Vertebrate Anaerobic Metabolism. *Science (80-.).* **209**, 308–309.
Smoly, J. M., Kuylenstierna, B. and Ernster, L. (1970). Topological and functional organization of the mitochondrion. *Proc. Natl. Acad. Sci. U. S. A.* **66**, 125–131.
Sokoloff, L. (1977). Relation Between Physiological Function and Energy Metabolism in the Central Nervous System. *J. Neurochem.* **29**, 13–26.
Solaini, G., Baracca, A., Lenaz, G. and Sgarbi, G. (2010). Hypoxia and mitochondrial oxidative metabolism. *BBA - Bioenerg.* **1797**, 1171–1177.
Stacey, G. and Macdonald, C. (2001). Immortalisation of Primary Cells. *Cell Biol. Toxicol.* **17**, 231–246.
Stepanova, A., Konrad, C., Guerrero-Castillo, S., Manfredi, G., Vannucci, S., Arnold, S. and Galkin, A. (2019). Deactivation of mitochondrial complex I after hypoxia–ischemia in the immature brain. *J. Cereb. Blood Flow Metab.* **39**, 1790–1802.
Steuernagel, L., Lam, B. Y. H., Klemm, P., Dowsett, G. K. C., Bauder, C. A., Tadross, J. A., Hitschfeld, T. S., del Rio Martin, A., Chen, W., de Solis, A. J., et al. (2022). HypoMap—a unified single-cell gene expression atlas of the murine hypothalamus. *Nat. Metab.* **4**, 1402–1419.
Suarez, R. K. (2012). Energy and metabolism. *Compr. Physiol.* **2**, 2527–2540.
Takahashi, J. S., Hong, H. K., Ko, C. H. and McDearmon, E. L. (2008). The genetics of mammalian circadian order and disorder: Implications for physiology and disease. *Nat. Rev. Genet.* **9**, 764–775.
Tang, B. L. (2018). Brain activity-induced neuronal glucose uptake/glycolysis: Is the lactate shuttle not required? *Brain Res. Bull.* **137**, 225–228.
Taylor, M. W. (2014). A History of Cell Culture. In *Viruses and Man: A History of Interactions*, pp. 41–52.
Taylor, B. L. and Zhulin, I. B. (1999). PAS Domains: Internal Sensors of Oxygen, Redox Potential, and Light. *Microbiol. Mol. Biol. Rev.* **63**, 479–506.
Tello, D., Balsa, E., Acosta-Iborra, B., Fuertes-Yebra, E., Elorza, A., Ordóñez, Á., Corral-Escariz, M., Soro, I., López-Bernardo, E., Perales-Clemente, E., et al.

(2011). Induction of the mitochondrial NDUFA4L2 protein by HIF-1α decreases oxygen consumption by inhibiting complex i activity. *Cell Metab.* **14**, 768–779.

Thompson, D. and Fedak, M. A. (1993). Cardiac responses of grey seals during diving at sea. *J. Exp. Biol.* **174**, 139–154.

Torppa, S. (2023). Role of the lactate receptor HCAR1 as part of neural adaptations to hypoxia in hooded seals (Cystophora cristata). *Master 's thesis* UiT-The Arctic University of Norway.

Torsvik, N., Mortensen, S. and Nedreaas, K. (1995). Fishery biology (in Norwegian). Landbruksforlaget, Aurskog.

Turek, F. W., Joshu, C., Kohsaka, A., Lin, E., Ivanova, G., McDearmon, E., Laposky, A., Losee-Olson, S., Easton, A., Jensen, D. R., et al. (2005). Obesity and metabolic syndrome in circadian Clock mutant nice. *Science (80-.).* **308**, 1043–1045.

Vacquie-Garcia, J., Lydersen, C., Biuw, M., Haug, T., Fedak, M. A. and Kovacs, K. M. (2017). Hooded seal Cystophora cristata foraging areas in the Northeast Atlantic Ocean—Investigated using three complementary methods. *PLoS One* **12**, e0187889.

Van Schaftingen, E., Lederer, B., Bartrons, R. and Hers, H. -G (1982). A Kinetic Study of Pyrophosphate: Fructose-6-Phosphate Phosphotransferase from Potato Tubers: Application to a Microassay of Fructose 2,6-Bisphosphate. *Eur. J. Biochem.* **129**, 191–195.

Van Vranken, J. G., Na, U., Winge, D. R. and Rutter, J. (2015). Protein-mediated assembly of succinate dehydrogenase and its cofactors. *Crit. Rev. Biochem. Mol. Biol.* **50**, 168–180.

Vázquez-Medina, J. P., Zenteno-Savín, T. and Elsner, R. (2006). Antioxidant enzymes in ringed seal tissues: Potential protection against dive-associated ischemia/reperfusion. *Comp. Biochem. Physiol. - C Toxicol. Pharmacol.* **142**, 198–204.

Vázquez-Medina, J. P., Zenteno-Savín, T., Elsner, R. and Ortiz, R. M. (2012). Coping with physiological oxidative stress: a review of antioxidant strategies in seals. *J. Comp. Physiol. B* **182**, 741–750.

Vogel, F., Bornhövd, C., Neupert, W. and Reichert, A. S. (2006). Dynamic subcompartmentalization of the mitochondrial inner membrane. *J. Cell Biol.* **175**, 237–247.

Voloshin, N., Tyurin-Kuzmin, P., Karagyaur, M., Akopyan, Z. and Kulebyakin, K. (2023). Practical Use of Immortalized Cells in Medicine: Current Advances and Future Perspectives. *Int. J. Mol. Sci.* **24**, 12716.

Wai, T. and Langer, T. (2016). Mitochondrial Dynamics and Metabolic Regulation. *Trends Endocrinol. Metab.* **27**, 105–117.

Walker, J. E. (1992). The Nadh: Ubiquinone oxidoreductase (complex I) of respiratory chains. *Q. Rev. Biophys.* **25**, 253–324.

Wang, G. L. and Semenza, G. L. (1993). General involvement of hypoxia-inducible factor 1 in transcriptional response to hypoxia. *Proc. Natl. Acad. Sci. U. S. A.* **90**, 4304–4308.

Wang, G. L., Jiang, B. H., Rue, E. A. and Semenza, G. L. (1995). Hypoxia-inducible factor 1 is a basic-helix-loop-helix-PAS heterodimer regulated by cellular O2 tension. *Proc. Natl. Acad. Sci. U. S. A.* **92**, 5510–5514.

Warburg, O. (1956). On respiratory impairment in cancer cells. *Science (80-.).* **124**, 269–270.

Warren, D. E., Reese, S. A. and Jackson, D. C. (2006). Tissue Glycogen and Extracellular Buffering Limit the Survival of Red-Eared Slider Turtles during Anoxic Submergence at 3°C. *Physiol. Biochem. Zool.* **79**, 736–744.

Waypa, G. B., Marks, J. D., Mack, M. M., Boriboun, C., Mungai, P. T. and Schumacker, P. T. (2002). Mitochondrial reactive oxygen species trigger calcium increases during

hypoxia in pulmonary arterial myocytes. *Circ. Res.* **91**, 719–726.
Wheaton, W. W. and Chandel, N. S. (2011). Hypoxia. 2. Hypoxia regulates cellular metabolism. *Am. J. Physiol. - Cell Physiol.* **300**, 385–393.
Wong-Riley, M. T. T. (1989). Cytochrome oxidase: an endogenous metabolic marker for neuronal activity. *Trends Neurosci.* **12**, 94–101.
Wu, Y., Tang, D., Liu, N., Xiong, W., Huang, H., Li, Y., Ma, Z., Zhao, H., Chen, P., Qi, X., et al. (2017). Reciprocal Regulation between the Circadian Clock and Hypoxia Signaling at the Genome Level in Mammals. *Cell Metab.* **25**, 73–85.
Xiao, W. and Loscalzo, J. (2020). Metabolic Responses to Reductive Stress. **32**, 1330–1347.
Yu, Y., Herman, P., Rothman, D. L., Agarwal, D. and Hyder, F. (2018). Evaluating the gray and white matter energy budgets of human brain function. *J. Cereb. Blood Flow Metab.* **38**, 1339–1353.
Zapol, W. M., Liggins, G. C., Schneider, R. C., Qvist, J., Snider, M. T., Creasy, R. K. and Hochachka, P. W. (1979). Regional blood flow during simulated diving in the conscious Weddell seal. *J. Appl. Physiol. Respir. Environ. Exerc. Physiol.* **47**, 968–973.
Zhang, J., Wang, Y. T., Miller, J. H., Day, M. M., Munger, J. C. and Brookes, P. S. (2018). Accumulation of Succinate in Cardiac Ischemia Primarily Occurs via Canonical Krebs Cycle Activity. *Cell Rep.* **23**, 2617–2628.
Zhdanov, A. V., Okkelman, I. A., Collins, F. W. J., Melgar, S. and Papkovsky, D. B. (2015). A novel effect of DMOG on cell metabolism: Direct inhibition of mitochondrial function precedes HIF target gene expression. *Biochim. Biophys. Acta - Bioenerg.* **1847**, 1254–1266.

8 Papers

Paper I

© 2024. Published by The Company of Biologists Ltd | Journal of Experimental Biology (2024) 227, jeb246990. doi:10.1242/jeb.246990

RESEARCH ARTICLE

Circadian coupling of mitochondria in a deep-diving mammal

Chiara Ciccone, Fayiri Kante, Lars P. Folkow, David G. Hazlerigg, Alexander C. West and Shona H. Wood*

ABSTRACT

Regulation of mitochondrial oxidative phosphorylation is essential to match energy supply to changing cellular energy demands, and to cope with periods of hypoxia. Recent work implicates the circadian molecular clock in control of mitochondrial function and hypoxia sensing. Because diving mammals experience intermittent episodes of severe hypoxia, with diel patterning in dive depth and duration, it is interesting to consider circadian–mitochondrial interaction in this group. Here, we demonstrate that the hooded seal (*Cystophora cristata*), a deep-diving Arctic pinniped, shows strong daily patterning of diving behaviour in the wild. Cultures of hooded seal skin fibroblasts exhibit robust circadian oscillation of the core clock genes *per2* and *arntl*. In liver tissue collected from captive hooded seals, expression of *arntl* was some 4-fold higher in the middle of the night than in the middle of the day. To explore the clock–mitochondria relationship, we measured the mitochondrial oxygen consumption in synchronized hooded seal skin fibroblasts and found a circadian variation in mitochondrial activity, with higher coupling efficiency of complex I coinciding with the trough of *arntl* expression. These results open the way for further studies of circadian–hypoxia interactions in pinnipeds during diving.

KEY WORDS: Pinniped, Hooded seal, Biological clock, Arctic, Hypoxia, Mitochondrial respiration

INTRODUCTION

The ability of animals to predict and prepare for daily changes in environmental demands relies on the presence of an intrinsic physiological system: the circadian clock. The molecular basis of the circadian clock in mammals is a transcription–translation negative feedback loop (TTFL). The positive limb of this loop depends on the dimerization of the transcriptional activators CLOCK and ARNTL (also known as BMAL1), whereas the negative limb depends on the formation of a transcriptionally repressive complex containing PER and CRY (Buhr and Takahashi, 2013). Circadian dynamics emerge through the autoregulatory effects of PER and CRY: the CLOCK/ARNTL complex activates transcription of PER and CRY, which, after dimerization, translocate into the nucleus and repress their own transcription. This creates a loop with a period of around 24 h and is therefore called circadian.

Arctic Seasonal Timekeeping Initiative (ASTI), Arctic Chronobiology and Physiology Research Group, Department of Arctic and Marine Biology, UiT – The Arctic University of Norway, Tromsø NO-9037, Norway.

*Author for correspondence (shona.wood@uit.no)

C.C., 0000-0002-0749-6198; L.P.F., 0000-0002-6580-9156; D.G.H., 0000-0003-4884-8409; A.C.W., 0000-0003-3934-5068; S.H.W., 0000-0002-8273-4045

Received 6 November 2023; Accepted 11 March 2024

One of the roles of the circadian clock is to coordinate the metabolic transcription network, presumably in order to optimize mitochondrial metabolism to the daily changes (Neufeld-Cohen et al., 2016; Turek et al., 2005). In mice, mitochondrial oxidative phosphorylation (OXPHOS) oscillates in a daily manner and in concomitance with the expression of some rate-limiting mitochondrial enzymes (Neufeld-Cohen et al., 2016). OXPHOS results from the activity of enzymatic complexes (I–IV) located on the inner mitochondrial membrane (IMM). These complexes are responsible for the transport of electrons through the IMM and are therefore referred to as the electron transport system (ETS). Complexes I and II catalyse the transfer of electrons from the two tricarboxylic acid (TCA) cycle products, NADH and $FADH_2$, to complex III via ubiquinone. The electrons are next transferred via cytochrome *c* to complex IV, where oxygen (O_2) acts as the final electron acceptor. The electron transfer process enables complexes I, III and IV to pump protons (H^+) from the mitochondrial matrix into the intermembrane space (Hosler et al., 2006), thus creating the electrochemical gradient that drives ATP production by ATP synthase, also referred to as complex V (Chance and Williams, 1956). Changes in the activity of these complexes alters mitochondrial OXPHOS and ATP production.

In mice with a dysfunctional circadian clock, the daily cycle of OXPHOS is abolished, suggesting that there is an intrinsic dependence of the mitochondrial respiration complexes on the circadian clockwork (Neufeld-Cohen et al., 2016). Deletion of *arntl* in C2C12 myotubes causes a reduction of both OXPHOS and extracellular acidification rate (an indicator of glycolytic rate), but deletion in embryonic stem cells increases OXPHOS while reducing glycolytic rate (Ameneiro et al., 2020; Peek et al., 2017). This suggests there is tissue specificity in the effect of 'circadian clock knockout' on mitochondrial responses.

O_2, the final electron acceptor of the ETS, constitutes a fundamental factor in mitochondrial regulation. In mouse and human cell cultures, hypoxia (O_2 deficiency) leads to a switch from OXPHOS-based metabolism to anaerobic glycolysis (Kim et al., 2006; Semenza et al., 1994; Wang and Semenza, 1993). In mice, this hypoxia-driven mitochondrial switch to enhanced glycolytic metabolism involves hypoxia inducible factor 1α (HIF-1α) and its interaction with the clock protein, ARNTL (Peek et al., 2017). In addition, two studies have highlighted further links between the circadian clock, mitochondrial metabolism and hypoxia (Adamovich et al., 2017; Manella et al., 2020); however, such links have only been demonstrated in rodent species that do not normally experience severe hypoxia. Therefore, it is of interest to investigate whether circadian–mitochondrial interactions are also present in a diving mammal, which through its behaviour frequently experiences episodes of hypoxia.

Diving mammals have evolved numerous hypoxia coping strategies including enhanced O_2 storage and O_2 carrying capacity, with blood volume and haemoglobin and myoglobin levels being higher than in other species (e.g. Blix, 2018; Davis, 2014). These adaptations combine with strict O_2 economy by way of cardiovascular adjustments

(bradycardia and peripheral vasoconstriction) and hypometabolism (Blix et al., 1983; Burns et al., 2007; Lenfant et al., 1970; Scholander, 1940). For the majority of dives, this means that animals are within their aerobic dive limit (ADL). Nevertheless, some deep-diving seal species [Weddell seals (*Leptonychotes weddellii*), northern elephant seals (*Mirounga angustirostris*) and hooded seals (*Cystophora cristata*)] appear to repeatedly perform dives that exceed their calculated ADL (Folkow et al., 2008; Meir et al., 2009; Qvist et al., 1986). Arterial partial O_2 pressures (tension) of 10–20 mmHg have been recorded in freely diving seals (Meir et al., 2009; Qvist et al., 1986); these values are far below what is considered as a critically low arterial partial O_2 pressure for adequate brain function (25–40 mmHg) (Erecińska and Silver, 2001). Therefore, deep-diving species are likely to experience severe hypoxia on a regular basis.

There are several reports of seasonal and daily variations in diving behaviour of different pinniped species (Bennett et al., 2001; Folkow and Blix, 1999; Nordøy et al., 2008; Photopoulou et al., 2020). Among them, the hooded seal is known for its remarkable diving capacity (Folkow and Blix, 1999): dives exceeding durations of 1 h and depths of 1600 m have been recorded (Andersen et al., 2013; Vacquie-Garcia et al., 2017), making this species a good research model for hypoxia tolerance and oxidative stress in mammals (e.g. Fabrizius et al., 2016; Folkow et al., 2008; Geiseler et al., 2016; Geßner et al., 2020; Hoff et al., 2016, 2017; Mitz et al., 2009; Vázquez-Medina et al., 2011). The hooded seal dive duration and depth are reportedly greater during the day than at night-time (Andersen et al., 2013; Folkow and Blix, 1999), suggesting that there may be a daily rhythm in exposure to severe hypoxia. We hypothesise that, in addition to other diving adaptations, a diving mammal may use circadian–mitochondrial interactions to tolerate variations in oxygen availability. However, the circadian molecular clock is yet uncharacterized in pinnipeds, and mitochondrial activity has not been measured in the deep-diving hooded seal.

Here, we provide the first molecular characterization of the circadian clock in the hooded seal and explore the clock–mitochondria relationship, showing that mitochondrial activity relates to circadian clock phase. These results open the way for further studies of circadian and (diving-induced) hypoxia interactions in pinnipeds.

MATERIALS AND METHODS

Diving behaviour analysis

Data collected by the Norwegian Polar institute in 2007 and 2008 as part of the MEOP (Marine Mammals Exploring the Ocean Pole to Pole) programme were provided by Dr M. Biuw and used for diving behaviour analysis based on dive data for 12 adult and 8 juvenile hooded seals of both sexes (Vacquie-Garcia et al., 2017, 10.21334/npolar.2017.881dbd20, file name: dive_2007.txt, dive_2008.txt). Conductivity–temperature–depth satellite relay data loggers (CTD-SRDLs) (Sea Mammal Research Unit, University of St Andrews) were glued to the fur on the back of the neck of the seals. Data were collected and transmitted for every 6-h period and included the following variables: dive duration, time of dive end, maximum depth, location (latitude and longitude), and time spent at surface after the dive. Knowing dive duration, time of dive end and time spent at surface, it was possible to infer the starting time for every single dive. Starting time was taken to represent the start of a 'diving event', which then formed the basis for analyses of diurnal changes in dive duration and depth.

Hooded seal pups perform shallower and shorter dives than adults (Folkow et al., 2010). Therefore, our analyses focused on the 12 adults (3 males and 9 females) that were present in the data set.

After having evaluated the dive duration distribution, we decided to analyse only dives between 2 min and the 95th percentile of the maximum dive duration of each individual. This allowed us to exclude outliers from further analysis.

All the following analyses were performed in RStudio (version 4.2.1). To verify the presence of a daily oscillation in hooded seal diving behaviour, a cosine curve with a 24-h period was fitted to the data through the function cosinor.lm in the package 'cosinor'. To test whether the cosine model significantly represented the data, we used the cosinor.detect function in the package 'cosinor2'. Calculations were repeated for each seal and for each month separately. The function cosinor in the package 'card' was used to define the midline statistic of rhythm (MESOR); this is a circadian rhythm-adjusted mean, which gives an estimate of the average value of an oscillating variable. The MESOR was used to identify different trends in diving duration throughout the year. Using the information about latitude and longitude, it was possible to calculate time of sunrise and sunset for each day of every month through the sunriset function in the 'maptools' package.

To compare dive durations at different times of day, we binned the data by hour and calculated the hourly mean dive duration.

Animals used for tissue sampling

Hooded seals [*Cystophora cristata* (Erxleben 1777)] were captured in their breeding colonies on the pack ice of the Greenland Sea, at ∼71°N and ∼19°W, during a research/teaching cruise with the R/V Helmer Hanssen in late March 2018, under permits of relevant Norwegian and Greenland authorities. Six live seals were brought to the Department of Arctic and Marine Biology (AMB) at UiT – The Arctic University of Tromsø, Norway, where they were maintained in a certified research animal facility [approval no. 089 by the Norwegian Food Safety Authority (NFSA)]. Seals were euthanized (in 2019, as juveniles, at age ∼10 months) for purposes other than the present study, in accordance with a permit issued by NFSA (permit no. 12268): the seals were sedated by intramuscular injection of zolazepam/tiletamine (Zoletil Forte Vet., Virbac S. A., France; 1.5–2.0 mg kg^{-1} body mass), then anaesthetized using an endotracheal tube to ventilate lungs with 2–3% isoflurane (Forene, Abbott, Germany) in air and when fully anaesthetized, they were euthanized by exsanguination via the carotid arteries.

During another research cruise in March 2019, an additional 6 weaned pups were captured (NFSA; permit no. 19305) and brought to AMB, UiT. Before culling and tissue sampling (February 2020, at age 11–12 months), the animals were exposed to 18 days of 12 h:12 h light:dark. In this experiment, we defined Zeitgeber Time 0 (ZT0) as the time when lights went on. Euthanasia was performed as explained above at ZT6 (light phase) for three seals and at ZT18 (dark phase) for the other three.

Tissue sampling

Skin biopsies were collected postmortem from the seals captured in March 2018 between the digits of the hind flipper with a biopsy punch (6 mm, 33-36-10, Miltex Inc., York) and processed for culturing of fibroblasts as described below. Samples from kidneys and liver were collected from the 6 seals held under 12 h:12 h light:dark conditions. Tissues were minced with a sterile scalpel blade and placed in 4 ml of RNAlater (AM7021, Thermo Fisher) in a 1:10 ratio. Samples were stored at 4°C for 24 h and then moved to −20°C until mRNA extraction.

Culture of hooded seal skin fibroblasts

Skin biopsies were processed as described elsewhere (Du and Brown, 2021). Briefly, biopsies were placed in collection medium [Dulbecco's modified Eagle medium (DMEM, D5796,

Journal of Experimental Biology (2024) 227, jeb246990. doi:10.1242/jeb.246990

Sigma)+50% fetal bovine serum (FBS, F7524, Sigma)+1% penicillin-streptomycin (Pen-Strep, P4458, Sigma)] and then moved into 6-well plates containing digestion medium [DMEM+10% FBS+1% amphotericin B (A2942, Sigma)] and 10% liberase (Roche, 05 401 119 001) for 8–9 h at 37°C/5% CO_2. Tissue biopsies and digestion medium were then transferred to a tube containing warm Dulbecco's phosphate buffered saline (PBS, D8537, Sigma), and plates were rinsed again with PBS to collect all the tissue fragments. Samples were centrifuged at 200 ***g*** for 5 min. The pellet was resuspended in culture medium [DMEM+20% FBS+0.1% gentamycin (15710, Invitrogen)] and placed in fresh 6-well plates. Fragments were overlaid with a Millicell Cell Culture insert (cat. PICMORG50 Millipore): 1.5 ml of culture medium was added to the interior of the insert and 0.5 ml to the exterior. Plates were incubated for about 2 weeks at 37°C/5% CO_2. Medium was changed every 3–4 days.

When cells covered approximately 80% of the plate surface (80% confluency), they were trypsinized (trypsin-EDTA solution, T4049, Sigma), resuspended in culture medium and centrifuged at 400 ***g*** for 5 min. Pelleted cells were then suspended in 3 ml of freezing medium per T75 culture flask [culture medium+10% dimethyl sulfoxide (DMSO, D5879, Sigma)] and progressively cooled in a cryocooler overnight at –80°C. Cells were then moved to liquid nitrogen for long-term storage.

A few days before the start of the experimental procedures (temperature cycling and respirometry), cells were thawed at 37°C for 1–2 min and then added to 10 ml of pre-warmed medium (DMEM+20% FBS+1% Pen-Strep). The solution was centrifuged at 300 ***g*** for 5 min. The pellet was resuspended in 12 ml of medium and transferred to a T75 culture flask. When cells reached 80% confluency, they were trypsinized and re-plated into three different plates (one T175, one T75 and one 6-well-plate) for each sampling timepoint.

Temperature cycling treatment

According to established protocols, temperature cycling was used to synchronize the circadian clock of our primary fibroblast cell cultures (Brown et al., 2002; Buhr et al., 2010). Cells were exposed to five consecutive 24 h cycles of temperature alternations between 12 h at 36.5°C and 12 h at 39.5°C. In all the temperature cycling experiments, we defined ZT0 as the time of the transition from 36.5 to 39.5°C. Cells were collected from the sixth cycle with 4-h intervals over 2 cycles (Fig. S1A). For mRNA, 6-well plates were washed with PBS and directly frozen on dry ice before storage at –80°C. For the mitochondrial O_2 consumption measurements, cells grown in T175 flasks were sampled with an 8-h interval, thus giving data around one full 24 h cycle with only one repetition for each sampling timepoint (Fig. S1A). The presence of Phenol Red in the culture medium was used as standard pH indicator in the cultures: if changes in pH were detected, the medium was changed at the end of the third cycle.

In a second experiment, cells were kept under temperature cycle for 3 cycles. Cells were sampled over a 48-h period, at 36.5°C for the first 12 h and at 39.5°C for the remaining 36 h (Fig. S1B).

mRNA extraction and cDNA conversion

For both tissues and cells, RNA was extracted using RNeasy mini kit (74104, Qiagen) following the manufacturer's instructions. Tissue samples (∼100 mg) were thawed then inserted in a low bind tube containing 600 µl RLT buffer+6 µl β-mercaptoethanol with a metal bead. The tube was shaken in a tissue lyser for 6 min at 20 shakes per second. Cell plates were taken out of the –80°C freezer and the contents of each well were collected in 350 µl of RLT buffer before being transferred to a QIAshredder column (79654, Qiagen). The column was centrifuged for 2 min at full speed and 350 µl of 70% ethanol was added to the lysate. Lysates were treated with DNase I (79254, Qiagen) and heated to 37°C for 10 min. Enzymatic reaction was stopped by adding EDTA at a final concentration of 0.05 mol l^{-1} in each tube at 75°C for 10 min. Samples were then treated with cDNA buffer and enzyme reverse transcriptase, heated for 1 h at 37°C and cooled down to 4°C. The cDNA samples were then stored at –20°C until further use.

Table 1. Primer sequences used for qPCR

Gene	Sequence	Efficiency (%)
arntl F	GTGAAGTCTATGGAGTATGTG	98.34
arntl R	GTTCTTGTGGTAAATATGCC	
per2 F	CCATAGAAGAGATTGAGAGTG	93.84
per2 R	TTGGTCAGAGATGTACAGG	
ppib F	CATCTATGGTGAACGCTTC	89.32
ppib R	TAACGGTCGTGATAAAGAAC	
tbp F	GAAGAAAGTGAACATCATGG	92.98
tbp R	GTAAGGCATCATTGGACTG	

Efficiency was calculated at 57°C. F, forward; R, reverse.

qPCR

Seal gene sequences for *arntl*, *per2* and housekeeping genes *tbp* and *ppib* were identified by aligning in BLAST dog (*Canis lupus*) gene sequences against the Weddell seal (*Leptonychotes weddellii*) genome (https://www.ncbi.nlm.nih.gov/assembly/GCF_000349705.1/). Primer specificity was confirmed by cloning PCR amplicons into Zero Blunt TOPO vector and sanger dideoxy sequencing (BigDye). Only primers with efficiency above 90% and a single product were used (Table 1). Reagents from the Promega GoTaq qPCR Master Mix kit (A6001, Promega) were used to perform qPCR. The Bio-Rad manager software was used to control the Bio-Rad CFX Connect Real_Time PCR system. The qPCR template used started with 2 min at 95°C. It then repeated 39 temperature cycles, each of: 15 s at 95°C, 15 s at 57°C and 1 min at 60°C, where fluorescence was measured. It finished with 5 s at 65°C and then a final constant temperature of 95°C. The cycle threshold (C_t) values of each gene were analysed using the $\Delta\Delta C_t$ ($2^{-\Delta\Delta C_t}$) method (Livak and Schmittgen, 2001) against housekeeping genes *ppib* and *tbp*.

Mitochondrial oxygen consumption measurements

Mitochondrial oxygen consumption was measured with two O2k high-resolution respirometers (Oroboros Instruments, Innsbruck, Austria) and data were recorded in real-time using the Oroboros DatLab software (Oroboros Instruments).

Owing to the duration of the respiration measurement protocol, and limited availability of Oroboros respirometers, it was possible to process samples only six times over 48 h. After exposure to the temperature cycling treatment, cells were collected by trypsinization, resuspended in culture medium and centrifuged at 300 ***g*** for 5 min. The pellet was then resuspended in the respiration medium MiR05 (0.5 mmol l^{-1} EGTA, 3 mmol l^{-1} $MgCl_2$, 60 mmol l^{-1} K-lactobionate, 20 mmol l^{-1} taurine, 10 mmol l^{-1} KH_2PO_4, 20 mmol l^{-1} HEPES, 110 mmol l^{-1} sucrose, 1 g l^{-1} BSA; pH 7). Cells were added to the Oxygraph chambers at a concentration of 0.6×10^6 cells ml^{-1}, with a final volume of 2.1 ml in each chamber.

After measurement of basal respiration (routine), cells were permeabilized with digitonin (3 µg ml^{-1}). Different mitochondrial states were assessed by injecting the following chemicals in the chambers: pyruvate, malate, ADP, glutamate, succinate, cytochrome *c*, rotenone, oligomycin and carbonyl cyanide

Journal of Experimental Biology (2024) 227, jeb246990. doi:10.1242/jeb.246990

Table 2. List of chemicals used during the oxygen consumption measurements and relative mitochondrial state

Chemical	Cat. no. and supplier	Final concentration	State	Description
–	–	–	Routine	Basal respiration without addition of any substrate
Digitonin	D5628, Sigma	3 µg ml^{-1}	–	Cell permeabilization
Pyruvate	P2256, Sigma	5 mmol l^{-1}	LeakN	Leak state at complex I in the absence of ADP (inactive ATP synthase); non-phosphorylating state where protons leaking through complex I are not used for ATP production
Malate	M1000, Sigma	2 mmol l^{-1}		
ADP	117105, Calbiochem	2.5 mmol l^{-1}	OXPHOS (PM-P)	Oxidative phosphorylation through complex I with pyruvate and malate as substrates
Glutamate	G1626, Sigma	10 mmol l^{-1}	OXPHOS (CI-P)	Oxidative phosphorylation through complex I with pyruvate, malate and glutamate as substrates
Succinate	S2378, Sigma	10 mmol l^{-1}	OXPHOS (CI+CII-P)	Oxidative phosphorylation through complex I and complex II with pyruvate, malate, glutamate and succinate as substrates
Cytochrome *c*	C7752, Sigma	10 µmol l^{-1}	–	Mitochondrial integrity test
Rotenone	R8875, Sigma	0.5 µmol l^{-1}	OXPHOS (CII-P)	Oxidative phosphorylation through complex II after inhibition of complex I
Oligomycin	O4876, Sigma	10 nmol l^{-1}	LeakOmy	Leak state at complex II after inhibition of ATP synthase; non-phosphorylating state
FCCP	C2920, Sigma	1 µmol l^{-1}	Uncoupled state (CII-E)	Uncoupled state measuring maximal mitochondrial capacity

p-trifluoro-methoxyphenyl hydrazone (FCCP). Optimal concentrations of both digitonin (Doerrier et al., 2018) and FCCP were determined in pilot experiments (Fig. S2). Table 2 gives an overview of the chemicals injected and the respiratory states measured. The initial O_2 concentration in the chamber was ∼200 µmol l^{-1}. Throughout the course of the experiment, the O_2 concentration decreased, down to ∼80–100 µmol l^{-1}. Fig. S3 shows an original oxygraph obtained during the mitochondrial respiration measurements.

Each experiment was done with four replicate respiratory chambers, except for ZT13 and ZT21, which have three replicates. The fourth replicate was excluded because the cells did not permeabilize; therefore, the mitochondria did not respond to the treatments.

The data obtained for each oxygraphic chamber were first normalized to the specific number of cells within that chamber (expressed as multiples of 10^6 cells) in the DatLab software (Fig. S4), and then normalized also to the routine respiration of that same chamber; this was done to eliminate any sample-specific variation. Finally, measurements at different timepoints for each mitochondrial state were normalized to cycle mean, to reveal any rhythmicity. The cycle mean was calculated as the average value for each mitochondrial state; single measurements were then divided by the cycle mean, to be represented by ratios as oscillations around 1 (Fig. S5). A significant difference between timepoints was found for all the mitochondrial states, both before and after normalization to cycle mean (one-way ANOVA).

The leak state is defined as the mitochondrial respiration in the presence of fuel substrates and in the absence of ADP. It reflects proton leak across the inner membrane that does not result in ATP production (Chance and Williams, 1956; Gnaiger, 2009; Perry et al., 2013). It can be used to determine the coupling efficiency of the different ETS enzymes through the respiratory control ratio (RCR), measured as OXPHOS/LEAK (P/L), where OXPHOS corresponds to mitochondrial respiration in the presence of substrates and saturating ADP (Chance and Williams, 1956; Gnaiger, 2009). In the literature, the RCR is preferably expressed as OXPHOS coupling efficiency ($1–RCR^{-1}$), with values between 0 and 1, where 1 corresponds to fully coupled mitochondria (Doerrier et al., 2018; Gnaiger, 2020). Accordingly, we calculated complex I coupling efficiency using this formula:

$$1 - \left(\text{LeakN} \Big/ \text{PM-P}\right), \quad (1)$$

where LeakN corresponds to leak state at complex I and PM-P refers to complex I OXPHOS, both with pyruvate and malate as substrates (Table 2).

Lentiviral vector construction

Circadian clock gene activity was recorded using the vectors pLV6-Bmal-luc (Addgene plasmid 68833) and pLV6-Per2-luc. The latter consisted of the pLV6 backbone and a mouse *per2* promoter with adjacent luciferase sequence contained in the pGL3 basic E2 vector (Addgene plasmid 48747). To ligate the Per2:luciferase reporter with pLV6 backbone, we designed a restriction cloning approach shown to be efficient in large plasmids using the QuickChange Lightning Site-Directed Mutagenesis (SDM) kit (Agilant, 210518) according to the manufacturer's instructions (Zhang and Tandon, 2012). Briefly, the SDM kit was used to create an extra BamHI cutting site 5′ on the pLV6-Bmal-luc vector. Mutated plasmid was transformed with stable competent *E. coli* (NEB, C3040H) according to the manufacturer's manual. Cells were grown on LB agar plates [40 g l^{-1} LB-agar (Sigma-Aldrich, L3147), 100 µg ml^{-1} ampicillin (Sigma-Aldrich, A9393)] and single clones were cultivated in LB broth overnight [25 g LB (Sigma-Aldrich, L3522), 100 µg ml^{-1} ampicillin]. We used a Qiagen miniprep kit (Qiagen, 27104) to extract plasmid DNA, and the mutation was confirmed through whole-plasmid sequencing (Plasmidsaurus, https://www.plasmidsaurus.com/). After the mutation was detected, the pLV6-Bmal-luc vector was digested with BamHI (NEB, R3136S) and then treated with quick CIP (NEB, M0525S) to avoid self-ligation. The digest was run on an 1% agarose gel (TAE buffer, 0.25 µg ml^{-1} EtBr) and the the QIAquick Gel extraction kit (Qiagen, 28704) was used to extract the pLV6 backbone according to the manufacturer's instructions. Because the Per2 promoter and luciferase in the pGL3-Per2-luc vector are already flanked by BamHI cutting sites, the pGL3-Per2-luc vector was directly digested with BamHI for Per2:luciferase sequence extraction.

Finally, the pLV6 backbone and the Per2:luciferase fragment were ligated with T4 DNA ligase (NEB, M0202S) according to the manufacturer's manual. Vectors extracted from transformed single colonies were sequenced by Plasmidsaurus and checked for correct ligation and sequence. The resulting vector is referred to as pLV6-Per2-luc.

Lentiviral vectors were constructed according to Du and Brown (2021). Briefly, HEK293 T cells were incubated with pMD2G

Journal of Experimental Biology (2024) 227, jeb246990. doi:10.1242/jeb.246990

Table 3. *P*-values for the fitted cosine model for each seal and month calculated through the cosinor.detected function in the cosinor2 package in RStudio

ID	Year	Month	*P*
Mj98	2007	July	6.13×10^{-5}
		August	1.27×10^{-23}
		September	*0.48*
		October	3.31×10^{-36}
		November	2.83×10^{-17}
		December	*0.26*
	2008	January	4.27×10^{-9}
		February	0.0002
		March	3.66×10^{-16}
		April	1.06×10^{-7}
		May	2.59×10^{-7}
M171	2007	August	1.74×10^{-6}
		September	2.88×10^{-6}
		October	9.10×10^{-93}
		November	1.51×10^{-19}
		December	1.29×10^{-37}
	2008	January	4.58×10^{-26}
		February	1.31×10^{-30}
		March	*0.06*
		April	1.97×10^{-28}
		May	3.78×10^{-5}
F150	2008	March	1.30×10^{-15}
		April	3.58×10^{-8}
		May	0.02
		June	*0.07*
F110	2008	March	0.0004
		April	*0.07*
		May	*0.07*
		June	*0.05*
F115	2008	March	2.85×10^{-24}
		April	9.22×10^{-114}
		May	3.34×10^{-25}
		June	*0.25*
F119	2008	March	6.80×10^{-13}
		April	5.57×10^{-150}
		May	5.59×10^{-14}
		June	0.02
F147	2008	March	1.04×10^{-19}
		April	4.17×10^{-39}
		May	9.68×10^{-30}
		June	6.50×10^{-10}
F154	2008	March	1.76×10^{-22}
		April	4.20×10^{-23}
		May	0.0001
		June	*0.58*
F175	2008	March	2.77×10^{-22}
		April	9.78×10^{-36}
		May	3.50×10^{-14}
		June	*0.90*
F180	2008	March	3.91×10^{-20}
		April	5.87×10^{-14}
		May	0.0002
		June	1.47×10^{-8}
M225	2008	March	0.80
		April	5.74×10^{-7}
		May	4.31×10^{-21}
		June	*0.10*
F93	2008	March	*0.45*
		April	2.06×10^{-49}
		May	8.77×10^{-24}
		June	*0.52*

Non-significant values ($P>0.05$) are indicated in italics.

(#12259, Addgene), psPAX2 (#12260, Addgene) and the two transfer vectors. Supernatant was collected 24 and 48 h after incubation and transfection and filtered through a 0.2 µm filter. Filtered supernatant was aliquoted and frozen at −80°C until use.

Generation of a stable cell line expressing lentiviral vector and bioluminescence recordings

Two millilitres of medium containing lentivirus was added to a T25 flask containing hooded seal fibroblasts at 50% confluency, with 3 ml of DMEM+20% FBS. Cells were incubated overnight and then the medium was changed to clean cells from the virus. After 3 days, medium was changed to DMEM+20% FBS+10 µg ml^{-1} blasticidin (R21001, Gibco) selection antibiotic (cells were passaged in a T75 flask at this point). From the T75 flask, ten 3.5-cm wells were seeded and cultured in DMEM+20% FBS+10 µg ml^{-1} blasticidin. One week before starting the temperature cycling, the medium was changed to recording medium (DMEM without Phenol Red+0.47% $NaCO_3$+1% HEPES buffer+0.25% Pen-Strep+5% FBS+10 µg ml^{-1} blasticidin+0.1 mmol l^{-1} luciferin) (Yamazaki and Takahashi, 2005). Prior to the experiment, the medium was again changed, and wells were sealed with parafilm and placed in a Photon multiplier tube (Lumicycle, Hamamatsu) for recording.

In a separate experiment, after a 2-day incubation at 37°C/5% CO_2 in recording medium, transfected cells were synchronized with dexamethasone (100 nmol l^{-1}, D4902, Sigma) for 30 min. Thereafter, cells were washed twice with PBS and the medium was changed to normal recording medium. Cells were then sealed and placed in the Photon multiplier tube for recording.

Statistical analysis

All statistical analyses were performed in RStudio using one-way ANOVA and the *post hoc* comparison Tukey HSD test. Statistical analysis of coupling efficiencies was also performed using the non-parametric Kruskal–Wallis test across all the ZTs and the Mann–Whitney *U*-test for peak and trough comparison. The analysis of circadian oscillations for clock genes mRNA expression was done using Jonckheere–Terpstra–Kendall (JTK) cycle, a non-parametric algorithm designed to detect cyclic patterns in datasets with regular intervals between measurements (Hughes et al., 2010). All data are represented as means±s.e.m. Periods of the photon multiplier tube recordings were analysed by fitting a damped sine wave in GraphPad Prism 8 (version 8.0.2). Principal component analysis (PCA) of ZTs was performed across the seven measured mitochondrial states using the prcomp function in RStudio. Ellipses were drawn with a 0.80 confidence interval.

RESULTS

Seasonal and daily variations in hooded seal diving behaviour

We used the data collected between 2007 and 2008 by the Norwegian Polar Institute (see Vacquie-Garcia et al., 2017) to perform a high-resolution time analysis of hooded seal diving behaviour. Initial analysis revealed that the maximum dive duration was 87.25 min for males (at ∼09:00 h in January 2007, adult male Mj98) and 53.25 min for females (at ∼10:00 h in April 2008, adult female F175). For most seals, cosinor analysis of diving duration data showed that there is a significant relationship between dive duration and time of the day with a 24-h period throughout the year (Table 3). Fig. 1 shows this relationship for a male adult hooded seal (ID M171, August 2007–April 2008). Although dives were

Journal of Experimental Biology (2024) 227, jeb246990. doi:10.1242/jeb.246990

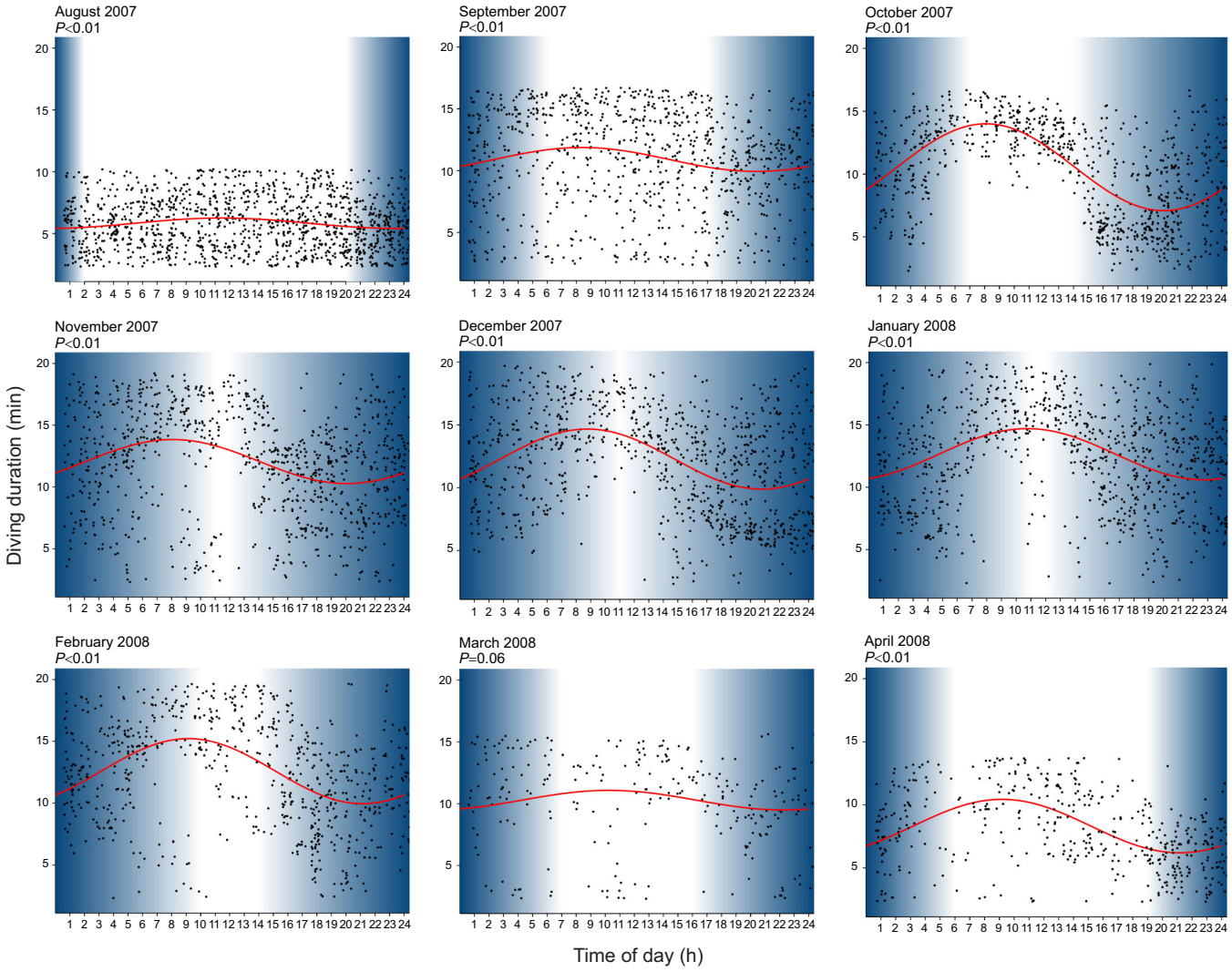

Fig. 1. Hourly and daily variations in diving durations in an adult male hooded seal (ID M171) from the Northeast Atlantic population. Data were collected between August 2007 and April 2008 (data provided by M. Biuw: 10.21334/npolar.2017.881dbd20). Only dives lasting between 2 min and the 95th percentiles of maximal duration are included. Each point represents a diving event; the red line represents the cosine curve generated through cosinor.lm in RStudio. Each panel corresponds to a different month and the respective *P*-values are indicated in the upper left. Blue and white areas represent day and night hours calculated in relation to position (latitude and longitude) and time of year.

observed in the night, the average dive duration was consistently higher during daytime (05:00–16:00 h) for most months, and very few night-time dives were longer than 1 h (Fig. 2). Therefore, by investigating the hourly distribution of diving durations, we were able to confirm the presence of a diurnal pattern in the hooded seal diving behaviour (Figs 1, 2).

Despite the limited amount of data, we also wished to investigate seasonal changes. We observed that, in accordance with previous data (Folkow and Blix, 1999), the mean value based on the daily distribution of values (MESOR) shows that dives were longer during the winter than in the summer (Fig. S6). Specifically, hourly mean dive duration was particularly short in July and August (Fig. 2) but increased again in September. In October, there was a clear pattern of shorter dives at evening and night and longer dives during the day (Fig. 2), which was persistent throughout all the winter months, until February. In March, dive duration decreased and dives were also less frequent, most likely linked to behavioural changes in connection with the breeding season (Kovacs et al., 1996).

Circadian molecular clock function in hooded seal fibroblasts and tissues

We derived primary skin fibroblasts from hooded seals and cultured them under a 24-h temperature cycle to synchronize the cells (Buhr et al., 2010). Measuring the endogenous mRNA abundance of the clock genes *arntl* and *per2*, we show a significant oscillation with a period of 24 h (JTK cycle, $P<0.0001$) and antiphase rhythms to one another: *arntl* expression peaking in middle of the low temperature phase and *per2* expression peaking in the middle of the high temperature phase (Fig. 3A). To determine whether these oscillations persist in constant conditions, we synchronized the cells using a temperature cycle and then held temperature constant for 36 h. Both *arntl* and *per2* endogenous mRNA levels continued to oscillate in anti-phase (Fig. 3B).

We then generated lentiviral reporters for *arntl* and *per2* to stably transduce our primary fibroblasts and allow real-time monitoring of clock gene expression for multiple days. After synchronization with dexamethasone, we observed significant oscillations of approximately 24 h for both *arntl* and *per2*

Journal of Experimental Biology (2024) 227, jeb246990. doi:10.1242/jeb.246990

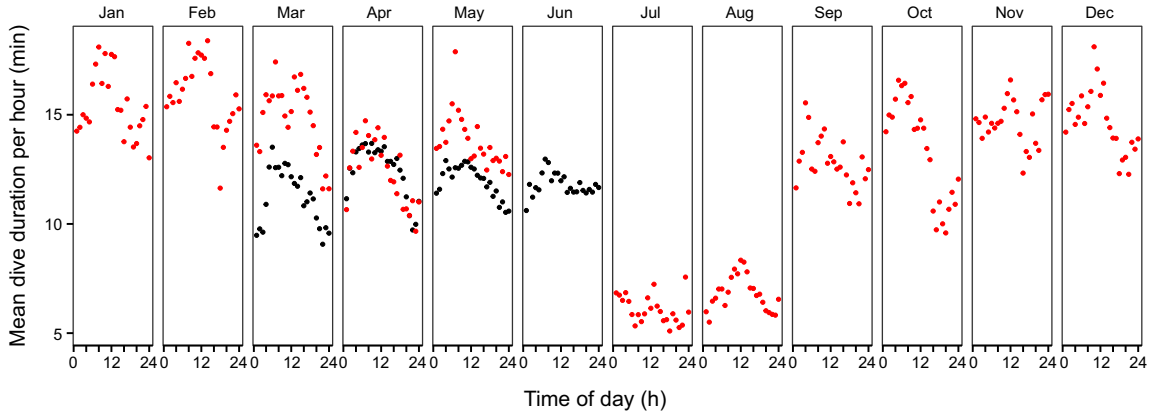

Fig. 2. Hourly mean dive duration (min) throughout the year for 12 adult hooded seals. Data from 2007 are presented in red (2 adult males); data from 2008 in black (9 adult females and 1 adult male). Only dives lasting between 2 min and 95th percentiles of maximal duration were included in the analysis. Data were binned by hour and the hourly mean dive duration was calculated.

(R^2=0.96 and 0.95, respectively) and persistent oscillations for 3 days post-synchronization (Fig. 3C). These results are consistent with a functional molecular clockwork in hooded seal fibroblasts.

We also measured endogenous *arntl* mRNA expression in liver and kidney samples collected in the mid-light (ZT6) and mid-dark phase (ZT18) from captive hooded seals held on a 12 h:12 h light:dark cycle. *Arntl* expression in the liver showed a significant

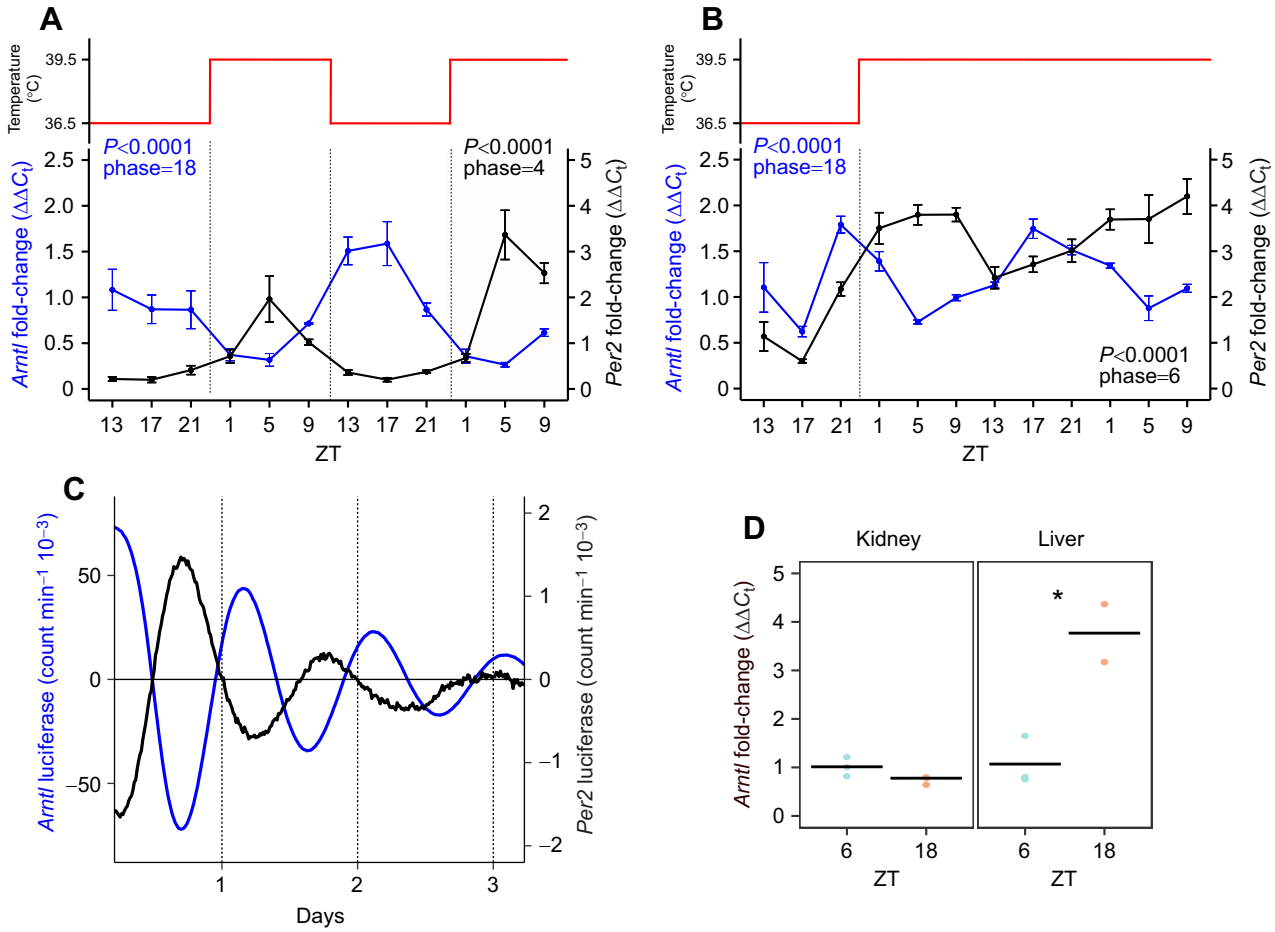

Fig. 3. Clock genes expression profile in synchronized hooded seals fibroblasts and tissues. (A) mRNA expression of core clock genes *arntl* (blue line) and *per2* (black line) in hooded seal fibroblasts synchronized by temperature cycle (°C), as represented in the upper panel. *Arntl* and *per2* mRNAs show a 24-h period and are in antiphase. *P*-values and phases were calculated through JTK cycle analysis (*n*=4). (B) mRNA expression of core clock genes *arntl* (blue line) and *per2* (black line) in hooded seal fibroblasts synchronized by temperature cycling and then left at constant temperature (upper panel). *Arntl* and *per2* mRNAs maintain a 24-h period and their antiphasic relationship also in constant conditions. *P*-values and phases were calculated through JTK cycle analysis (*n*=4). (C) Photon multiplier tube recordings of hooded seal skin fibroblasts transfected with *arntl*:luciferase (blue line) and *per2*:luciferase (black line). Cells were synchronized with dexamethasone. (D) *Arntl* mRNA expression in hooded seal kidney and liver tissue, sampled in mid-light phase (ZT6) and mid-dark phase (ZT18). **P*<0.05 (one-way ANOVA; *n*=3 except liver ZT18, where *n*=2). Data are expressed as means±s.e.m.

Journal of Experimental Biology (2024) 227, jeb246990. doi:10.1242/jeb.246990

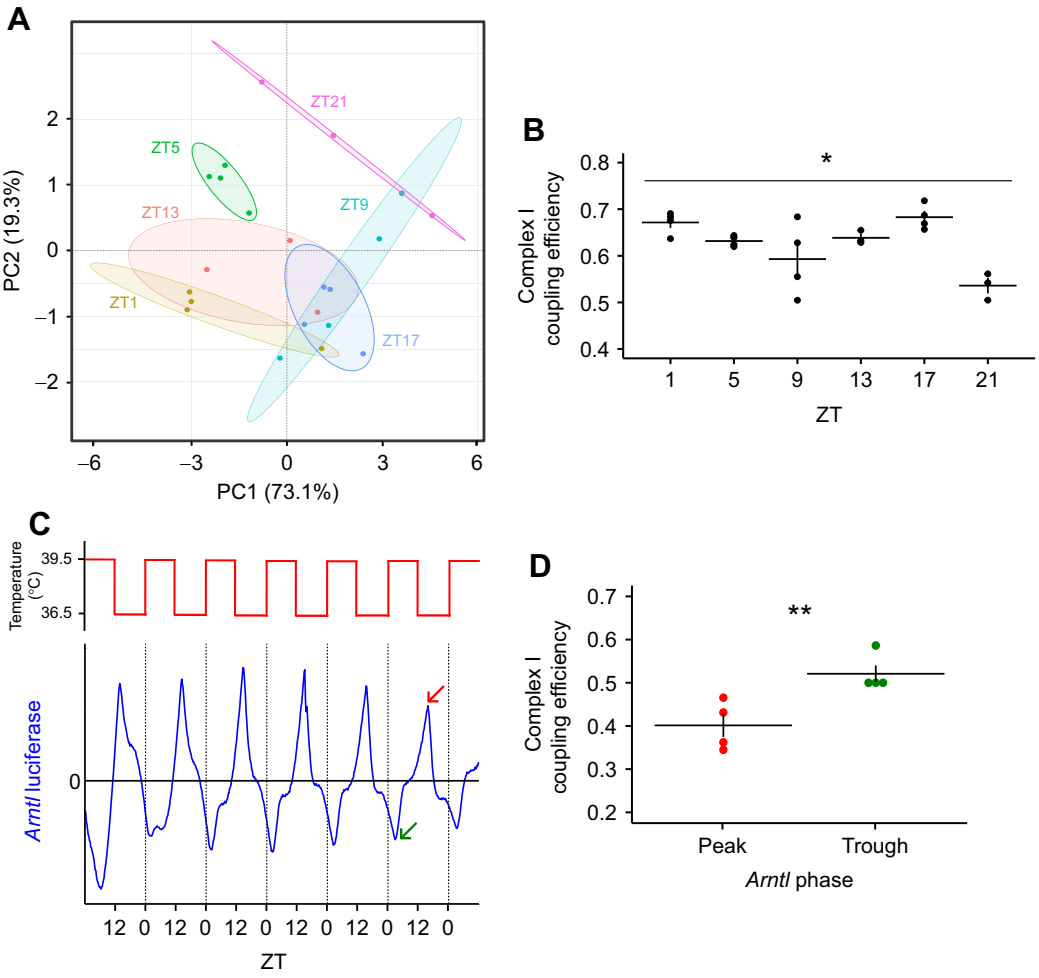

Fig. 4. Relationship between clock gene expression rhythms and mitochondrial respiration in hooded seal fibroblast cultures. (A) PCA analysis across 7 mitochondrial states [leak (LeakN, LeakOmy), OXPHOS (PM-P, CI-P, CI+CII-P, CII-P), and uncoupled state (CII-E)]. There is strong clustering at ZT5 and ZT17. Ellipses were drawn with a 0.80 confidence interval (n=4 except at ZT13 and 21, where n=3). (B) Complex I coupling efficiency [calculated as 1–(LeakN/PM-P)] at all the ZTs where oxygen consumption measurements were made. Coupling efficiency shows a time-dependent variation (one-way ANOVA: *P<0.01; Kruskal–Wallis test: P<0.05; n=4 except ZT13 and 21, where n=3). (C) Photon multiplier tube recordings of hooded seal skin fibroblasts transfected with *arntl*:luciferase and synchronized by temperature cycling (36.5–39.5°C), as indicated at the top. Recordings from the first 5 days were used to calculate expected peak (red arrow) and trough (green arrow). (D) Complex I coupling efficiency calculated as in B, at the expected peak and trough indicated in C (one-way ANOVA: P<0.001; Mann–Whitney U-test: P<0.05). Data are expressed as means±s.e.m. (**P<0.001; one-way ANOVA, n=4).

time-of-day effect, with expression at ZT18 being some 4-fold higher than at ZT6 (P<0.05; Fig. 3D).

Circadian clock phase relationship with the metabolic capacity of hooded seal mitochondria

To investigate whether there is a time-of-day variation in mitochondrial respiration, we used an O2k high-resolution respirometers (Oroboros) substrate-uncoupler-inhibitor titration (SUIT) protocol (see Table 2) with permeabilized skin fibroblasts from the hooded seal. We sampled at six different ZTs across a 48-h temperature cycling experiment (Fig. S1A). We used PCA analysis to integrate values for the seven parameters measured by the respirometers for each individual sample taken at each time-point. This generated two principal components (PC1 and PC2), which together accounted for over 90% of the overall variance for these seven parameters across the study as a whole (Fig. 4A). There was wide ZT-dependent variation, and we speculated that this variation was related to predicted phases for *arntl* and *per2* expression. Based on the endogenous mRNA expression (Fig. 3A), we focused on ZT5 (low *arntl*, high *per2* expression) and ZT17 (high *arntl*, low *per2* expression), which separated more clearly on the PCA plot (Fig. 4A). Among all the mitochondrial states, the leak state at complex I (LeakN; Table 2) was the only one to show a statistically significant difference between ZT5 and ZT17 (P=0.001). Therefore, we calculated complex I coupling efficiency using Eqn 1 across all the ZTs.

This revealed the presence of a time effect on complex I efficiency (P<0.01, one-way ANOVA; P<0.05, Kruskal–Wallis test; Fig. 4B), with the lowest values at ZT21 (0.46±0.017). High coupling efficiencies (close to 1) indicate highly coupled mitochondria (Doerrier et al., 2018; Gnaiger, 2020) and changes in coupling efficiency at complex I suggest a time-of-day effect on mitochondrial function.

To provide independent verification of the relationship between mitochondrial activity and clock phase, we collected samples from virally transduced *arntl:*luciferase-reporter-expressing hooded seal fibroblasts at phases of peak and trough *arntl* expression and processed them for respirometry analysis (Fig. 4C). Calculation of complex I coupling efficiency revealed a lower oxidative phosphorylation activity at complex I at peak *arntl* expression

(0.40±0.024) than at trough (0.52±0.017) (P<0.001, one-way ANOVA; P<0.05 Mann–Whitney U-test; Fig. 4D). Therefore, when *arntl* is at its peak, complex I is not as efficiently coupled as when *arntl* is at its trough, indicating a clock-dependent variation of complex I coupling efficiency. These differences in coupling efficiency may relate to regulation of ROS production or oxidative metabolism.

DISCUSSION

The present study confirms that under natural conditions, hooded seal diving behaviour is highly time-of-day dependent, and further demonstrates that under laboratory conditions, hooded seal cells show robust circadian characteristics, which are associated with cyclical changes in mitochondrial activity. Daily physiological and molecular changes are a key factor for determining the ability of different species to overcome the challenges imposed by a continuously changing environment. For the hooded seal, the biggest challenge is probably the restricted access to oxygen during long and deep dives.

We report that dives were consistently longer during the day and shorter at night and that there was a 24-h period in the diving duration pattern. Such daily variations are most likely related to similar patterns in the behaviour of hooded seal prey [e.g. redfish (*Sebastes* spp.) and squid (*Gonatus* spp.)], which can display diurnal vertical migrations as their prey, in turn, migrate according to the photic state in the water column (Kristensen, 1984; Torsvik et al., 1995). Even though the day–night trend is quite consistent, there is some seasonal variation, as previously reported (Andersen et al., 2013). These variations relate in part to the breeding season (late March) and the moulting season (June/July), during which adult hooded seals spend more time hauled out (Folkow and Blix, 1999; Folkow et al., 1996; Kovacs et al., 1996; Øritsland, 1959). However, dives also tend to generally be deeper and longer in winter than in summer (Folkow and Blix, 1999). Although the ultimate causation for diel patterning (i.e. prey availability) is clear, the proximate mechanisms dictating the time-of-day dependent diving behaviour is unknown; this led us to investigate whether a circadian clock–mitochondria coupling might be present in hooded seal cells.

Here, we show that circadian changes in *arntl* expression in hooded seal fibroblasts coincide with a significant change in the coupling efficiency of complex I. When *arntl* expression is at its trough, complex I coupling efficiency is high. In support of this view, we show, by two independent methods, that primary hooded seal skin fibroblasts display antiphase circadian oscillations of the clock genes *arntl* and *per2*, a result consistent with other characterizations of the mammalian circadian clock (Buhr and Takahashi, 2013). These oscillations are circadian because they persist under constant conditions (temperature, in this study) and with a period of approximately 24 h (Dunlap et al., 2004). We also show that the activity of complex I varies according to time of day and to the circadian clock phase defined by *arntl*.

Diurnal oscillations in complex I activity have been documented in mice liver (Jacobi et al., 2015; Neufeld-Cohen et al., 2016) and in human skeletal muscle (van Moorsel et al., 2016). In the human cell line HepG2, *arntl* expression regulates complex I activity by a process of acetylation and deacetylation through the NAMPT-NAD-SIRT1/3 machinery (Cela et al., 2016).

Finally, we show a time-of-day difference in *arntl* gene expression in the hooded seal liver, consistent with previous recordings in freshly isolated mice livers (Jacobi et al., 2015; Manella et al., 2020). However, we observed no difference in the kidneys, but we were limited to only two time-points so no strong conclusions regarding tissue-specific circadian rhythmicity can be drawn. We wanted to consider those organs specifically, because they are known to undergo substantial reduction in their arterial blood supply (by >80%) – and, hence, in the supply of blood-borne O_2 – in connection with long-duration diving in seals (e.g. Blix et al., 1983; Zapol et al., 1979). Therefore, the liver and kidney appear to be particularly hypoxia-/ischemia-tolerant (e.g. Hochachka et al., 1988), from which follows that a potentially tissue-dependent circadian clock phasing and interaction with mitochondria may be expected to be found in these particular tissues. However, further studies are needed to investigate this.

In summary, we have identified a circadian clock phase-dependent change in complex I coupling efficiency, demonstrating for the first time a mitochondria–clock interaction in the hooded seal. This change in coupling efficiency is determined by clock-dependent changes in complex I leak state and may represent a switch from an OXPHOS-based metabolism to less oxidative metabolism. But it could also be interpreted as a protective mechanism, to modulate the amount of reactive oxygen species (ROS) produced by the mitochondria through regulation of complex I leak (Brand, 2000; Cadenas, 2018). We speculate that the existence of mitochondria–circadian clock coupling that regulates either ROS production or oxidative metabolism may enhance the ability of seals to tolerate long-duration dives, by providing additional hypoxia tolerance mechanisms at the time it is needed the most – i.e. during the day, when they forage at greater depths and for longer durations (Fig. 1). However, a functional link remains to be determined. Our findings suggest that future experiments should take circadian clock phase into account, when investigating mitochondrial responses to hypoxia and the role of HIF-1 in diving mammals.

Acknowledgements

We thank the animal technicians of the Arctic Chronobiology and Physiology group for all the help with the animal handling: Hans Lian, Hans-Arne Solvang and Renate Thorvaldsen. We also thank Dr Martin Biuw for his help in the initial stages of the dive data analyses, and Dr Daniel Appenroth for his work on the lentiviral reporter.

Competing interests

The authors declare no competing or financial interests.

Author contributions

Conceptualization: C.C., D.G.H., A.C.W., S.H.W.; Methodology: C.C., F.K., A.C.W.; Software: C.C.; Validation: F.K.; Formal analysis: C.C., D.G.H., A.C.W.; Investigation: C.C., F.K., A.C.W., S.H.W.; Resources: L.P.F., S.H.W.; Data curation: C.C.; Writing - original draft: C.C., D.G.H.; Writing - review & editing: C.C., F.K., L.P.F., D.G.H., A.C.W., S.H.W.; Visualization: C.C., D.G.H., A.C.W.; Supervision: L.P.F., D.G.H., A.C.W., S.H.W.; Project administration: L.P.F., S.H.W.; Funding acquisition: S.H.W., D.G.H.

Funding

The work was supported by grants from the Tromsø Forskningsstiftelse (TFS) starter grant TFS2016SW and the TFS infrastructure grant (IS3_17_SW) awarded to S.H.W., the Arctic Seasonal Timekeeping Initiative (ASTI) grant and Universitetet i Tromsø strategic funds support to D.G.H. Open Access funding provided by Universitetet i Tromsø. Deposited in PMC for immediate release.

Data availability

Code used for the analysis and the data are available at https://github.com/ShonaWood/SealClock.

ECR Spotlight

This article has an associated ECR Spotlight interview with Chiara Ciccone.

References

Adamovich, Y., Ladeuix, B., Golik, M., Koeners, M. P. and Asher, G. (2017). Rhythmic oxygen levels reset circadian clocks through HIF1α. *Cell Metab.* **25**, 93-101. doi:10.1016/j.cmet.2016.09.014

Ameneiro, C., Moreira, T., Fuentes-Iglesias, A., Coego, A., Garcia-Outeiral, V., Escudero, A., Torrecilla, D., Mulero-Navarro, S., Carvajal-Gonzalez, J. M.,

Guallar, D. et al. (2020). BMAL1 coordinates energy metabolism and differentiation of pluripotent stem cells. *Life Sci. Alliance* **3**, 1-15. doi:10.26508/lsa.201900534
Andersen, J. M., Skern-Mauritzen, M., Boehme, L., Wiersma, Y. F., Rosing-Asvid, A., Hammill, M. O. and Stenson, G. B. (2013). Investigating annual diving behaviour by hooded seals (*Cystophora cristata*) within the Northwest Atlantic Ocean. *PLoS One* **8**, e80438. doi:10.1371/journal.pone.0080438
Bennett, K. A., McConnell, B. J. and Fedak, M. A. (2001). Diurnal and seasonal variations in the duration and depth of the longest dives in southern elephant seals (*Mirounga leonina*): possible physiological and behavioural constraints. *J. Exp. Biol.* **204**, 649-662. doi:10.1242/jeb.204.4.649
Blix, A. S. (2018). Adaptations to deep and prolonged diving in phocid seals. *J. Exp. Biol.* **221**, jeb182972. doi:10.1242/jeb.182972
Blix, A. S., Elsner, R. and Kjekshus, J. K. (1983). Cardiac output and its distribution through capillaries and A–V shunts in diving seals. *Acta Physiol. Scand.* **118**, 109-116. doi:10.1111/j.1748-1716.1983.tb07250.x
Brand, M. D. (2000). Uncoupling to survive? The role of mitochondrial inefficiency in ageing. *Exp. Gerontol.* **35**, 811-820. doi:10.1016/S0531-5565(00)00135-2
Brown, S. A., Zumbrunn, G., Fleury-Olela, F., Preitner, N. and Schibler, U. (2002). Rhythms of mammalian body temperature can sustain peripheral circadian clocks. *Curr. Biol.* **12**, 1574-1583. doi:10.1016/S0960-9822(02)01145-4
Buhr, E. D. and Takahashi, J. S. (2013). Molecular components of the mammalian circadian clock. *Handb. Exp. Pharmacol.* **217**, 3-27. doi:10.1007/978-3-642-25950-0_1
Buhr, E. D., Yoo, S.-H. and Takahashi, J. S. (2010). Temperature as a universal resetting cue for mammalian circadian oscillators. *Science (80-.).* **330**, 379-385. doi:10.1126/science.1195262
Burns, J. M., Lestyk, K. C., Folkow, L. P., Hammill, M. O. and Blix, A. S. (2007). Size and distribution of oxygen stores in harp and hooded seals from birth to maturity. *J. Comp. Physiol. B Biochem. Syst. Environ. Physiol.* **177**, 687-700. doi:10.1007/s00360-007-0167-2
Cadenas, S. (2018). Mitochondrial uncoupling, ROS generation and cardioprotection. *Biochim. Biophys. Acta Bioenerg.* **1859**, 940-950. doi:10.1016/j.bbabio.2018.05.019
Cela, O., Scrima, R., Pazienza, V., Merla, G., Benegiamo, G., Augello, B., Fugetto, S., Menga, M., Rubino, R., Fuhr, L. et al. (2016). Clock genes-dependent acetylation of complex I sets rhythmic activity of mitochondrial OxPhos. *Biochim. Biophys. Acta Mol. Cell Res.* **1863**, 596-606. doi:10.1016/j.bbamcr.2015.12.018
Chance, B. and Williams, R. (1956). The respiratory chain and oxidative phosphorylation. *Adv. Enzymol. Relat. Areas Mol. Biol.* **17**, 65-134. doi:10.1002/9780470122624.ch2
Davis, R. W. (2014). A review of the multi-level adaptations for maximizing aerobic dive duration in marine mammals: from biochemistry to behavior. *J. Comp. Physiol. B Biochem. Syst. Environ. Physiol.* **184**, 23-53. doi:10.1007/s00360-013-0782-z
Doerrier, C., Garcia-souza, L. F., Krumschnabel, G., Gnaiger, E. and Wohlfarter, Y. (2018). High-resolution FluoRespirometry and OXPHOS protocols for human cells, and isolated mitochondria. *Methods Mol. Biol.* 1782, 31-70. doi:10.1007/978-1-4939-7831-1_3
Du, N.-H. and Brown, S. A. (2021). Measuring circadian rhythms in human cells. *Methods Mol. Biol.* **2130**, 53-67. doi:10.1007/978-1-0716-0381-9_4
Dunlap, J. C., Loros, J. J. and DeCoursey, P. J. (2004). *Chronobiology: Biological Timekeeping*. Sinauer Associates.
Erecińska, M. and Silver, I. A. (2001). Tissue oxygen tension and brain sensitivity to hypoxia. *Respir. Physiol.* **128**, 263-276. doi:10.1016/S0034-5687(01)00306-1
Fabrizius, A., Hoff, M. L. M., Engler, G., Folkow, L. P. and Burmester, T. (2016). When the brain goes diving: transcriptome analysis reveals a reduced aerobic energy metabolism and increased stress proteins in the seal brain. *BMC Genomics* **17**, 583. doi:10.1186/s12864-016-2892-y
Folkow, L. P. and Blix, A. S. (1999). Diving behaviour of hooded seals (*Cystophora cristata*) in the Greenland and Norwegian seas. *Polar Biol.* **22**, 61-74. doi:10.1007/s003000050391
Folkow, L. P., Mårtensson, P. E. and Blix, A. S. (1996). Annual distribution of hooded seals (*Cystophora cristata*) in the Greenland and Norwegian seas. *Polar Biol.* **16**, 179-189. doi:10.1007/BF02329206
Folkow, L. P., Ramirez, J. M., Ludvigsen, S., Ramirez, N. and Blix, A. S. (2008). Remarkable neuronal hypoxia tolerance in the deep-diving adult hooded seal (*Cystophora cristata*). *Neurosci. Lett.* **446**, 147-150. doi:10.1016/j.neulet.2008.09.040
Folkow, L. P., Nordøy, E. S. and Blix, A. S. (2010). Remarkable development of diving performance and migrations of hooded seals (*Cystophora cristata*) during their first year of life. *Polar Biol.* **33**, 433-441. doi:10.1007/s00300-009-0718-y
Geiseler, S. J., Larson, J. and Folkow, L. P. (2016). Synaptic transmission despite severe hypoxia in hippocampal slices of the deep-diving hooded seal. *Neuroscience* **334**, 39-46. doi:10.1016/j.neuroscience.2016.07.034
Geßner, C., Stillger, M. N., Mölders, N., Fabrizius, A., Folkow, L. P. and Burmester, T. (2020). Cell culture experiments reveal that high S100B and clusterin levels may convey hypoxia-tolerance to the hooded seal (*Cystophora cristata*) brain. *Neuroscience* **451**, 226-239. doi:10.1016/j.neuroscience.2020.09.039
Gnaiger, E. (2009). Capacity of oxidative phosphorylation in human skeletal muscle. New perspectives of mitochondrial physiology. *Int. J. Biochem. Cell Biol.* **41**, 1837-1845. doi:10.1016/j.biocel.2009.03.013
Gnaiger, E. (2020). *Mitochondrial Pathways and Respiratory Control. An Introduction to OXPHOS Analysis*, 5th edn. Innsbruck: Bioenergetics Communications.
Hochachka, P. W., Castellini, J. M., Hill, R. D., Schneider, R. C., Bengtson, J. L., Hill, S. E., Liggins, G. C. and Zapol, W. M. (1988). Protective metabolic mechanisms during liver ischemia: transferable lessons from long-diving animals. *Mol. Cell. Biochem.* **84**, 77-85. doi:10.1007/BF00235195
Hoff, M. L. M., Fabrizius, A., Folkow, L. P. and Burmester, T. (2016). An atypical distribution of lactate dehydrogenase isoenzymes in the hooded seal (*Cystophora cristata*) brain may reflect a biochemical adaptation to diving. *J. Comp. Physiol. B Biochem. Syst. Environ. Physiol.* **186**, 373-386. doi:10.1007/s00360-015-0956-y
Hoff, M. L. M., Fabrizius, A., Czech-Damal, N. U., Folkow, L. P. and Burmester, T. (2017). Transcriptome analysis identifies key metabolic changes in the hooded seal (*Cystophora cristata*) brain in response to hypoxia and reoxygenation. *PLoS One* **12**, e0169366. doi:10.1371/journal.pone.0169366
Hosler, J. P., Ferguson-Miller, S. and Mills, D. A. (2006). Energy transduction: proton transfer through the respiratory complexes. *Annu. Rev. Biochem.* **75**, 165-187. doi:10.1146/annurev.biochem.75.062003.101730
Hughes, M. E., Hogenesch, J. B. and Kornacker, K. (2010). JTK-CYCLE: an efficient nonparametric algorithm for detecting rhythmic components in genome-scale data sets. *J. Biol. Rhythms* **25**, 372-380. doi:10.1177/0748730410379711
Jacobi, D., Liu, S., Burkewitz, K., Gangl, M. R., Mair, W. B., Lee, C., Unluturk, U., Li, X., Kong, X., Hyde, A. L. et al. (2015). Hepatic Bmal1 regulates rhythmic mitochondrial dynamics and promotes metabolic fitness. *Cell Metab.* **22**, 709-720. doi:10.1016/j.cmet.2015.08.006
Kim, J. W., Tchernyshyov, I., Semenza, G. L. and Dang, C. V. (2006). HIF-1-mediated expression of pyruvate dehydrogenase kinase: a metabolic switch required for cellular adaptation to hypoxia. *Cell Metab.* **3**, 177-185. doi:10.1016/j.cmet.2006.02.002
Kovacs, K. M., Lydersen, C., Hammill, M. and Lavigne, D. M. (1996). Reproductive effort of male hooded seals (*Cystophora cristata*): estimates from mass loss. *Can. J. Zool.* **74**, 1521-1530. doi:10.1139/z96-166
Kristensen, T. (1984). Biology of the squid *Gonatus fabricii* (Lichtenstein, 1818) from West Greenland waters. *Medd Grùn Biosci.* **13**, 17.
Lenfant, C., Johansen, K. and Torrance, J. D. (1970). Gas transport and oxygen storage capacity in some pinnipeds and the sea otter. *Respir. Physiol.* **9**, 277-286. doi:10.1016/0034-5687(70)90076-9
Livak, K. J. and Schmittgen, T. D. (2001). Analysis of relative gene expression data using real-time quantitative PCR and the 2 C T method. *Methods* **25**, 402-408. doi:10.1006/meth.2001.1262
Manella, G., Aviram, R., Bolshette, N., Muvkadi, S., Golik, M., Smith, D. F. and Asher, G. (2020). Hypoxia induces a time- and tissue-specific response that elicits intertissue circadian clock misalignment. *Proc. Natl. Acad. Sci. USA* **117**, 779-786. doi:10.1073/pnas.1914112117
Meir, J. U., Champagne, C. D., Costa, D. P., Williams, C. L. and Ponganis, P. J. (2009). Extreme hypoxemic tolerance and blood oxygen depletion in diving elephant seals. *Am. J. Physiol. Regul. Integr. Comp. Physiol.* **297**, 927-939. doi:10.1152/ajpregu.00247.2009
Mitz, S. A., Reuss, S., Folkow, L. P., Blix, A. S., Ramirez, J. M., Hankeln, T. and Burmester, T. (2009). When the brain goes diving: glial oxidative metabolism may confer hypoxia tolerance to the seal brain. *Neuroscience* **163**, 552-560. doi:10.1016/j.neuroscience.2009.06.058
Neufeld-Cohen, A., Robles, M. S., Aviram, R., Manella, G., Adamovich, Y., Ladeuix, B., Nir, D., Rousso-Noori, L., Kuperman, Y., Golik, M. et al. (2016). Circadian control of oscillations in mitochondrial rate-limiting enzymes and nutrient utilization by PERIOD proteins. *Proc. Natl. Acad. Sci. USA* **113**, E1673-E1682. doi:10.1073/pnas.1519650113
Nordøy, E. S., Folkow, L. P., Potelov, V., Prischemikhin, V. and Blix, A. S. (2008). Seasonal distribution and dive behaviour of harp seals (*Pagophilus groenlandicus*) of the White Sea-Barents Sea stock. *Polar Biol.* **31**, 1119-1135. doi:10.1007/s00300-008-0453-9
Øritsland, T. (1959). The hooded seal (in Norwegian). *Fauna Oslo* **12**, 70-90.
Peek, C. B., Levine, D. C., Cedernaes, J., Taguchi, A., Kobayashi, Y., Tsai, S. J., Bonar, N. A., McNulty, M. R., Ramsey, K. M. and Bass, J. (2017). Circadian clock interaction with HIF1α mediates oxygenic metabolism and anaerobic glycolysis in skeletal muscle. *Cell Metab.* **25**, 86-92. doi:10.1016/j.cmet.2016.09.010
Perry, C. G. R., Kane, D. A., Lanza, I. R. and Neufer, P. D. (2013). Methods for assessing mitochondrial function in diabetes. *Diabetes* **62**, 1041-1053. doi:10.2337/db12-1219
Photopoulou, T., Heerah, K., Pohle, J. and Boehme, L. (2020). Sex-specific variation in the use of vertical habitat by a resident Antarctic top predator: sex-specific variation in diving. *Proc. R. Soc. B Biol. Sci.* **287**, 20201447. doi:10.1098/rspb.2020.1447
Qvist, J., Hill, R. D., Schneider, R. C., Falke, K. J., Liggins, G. C., Guppy, M., Elliot, R. L., Hochachka, P. W. and Zapol, W. M. (1986). Hemoglobin

concentrations and blood gas tensions of free-diving Weddell seals. *J. Appl. Physiol.* **61**, 1560-1569. doi:10.1152/jappl.1986.61.4.1560

Scholander, P. F. (1940). *Experimental Investigations on the Respiratory Function in Diving Mammals and Birds*. I kommisjon hos Jacob Dybwad.

Semenza, G. L., Roth, P. H., Fang, H. M. and Wang, G. L. (1994). Transcriptional regulation of genes encoding glycolytic enzymes by hypoxia-inducible factor 1. *J. Biol. Chem.* **269**, 23757-23763. doi:10.1016/S0021-9258(17)31580-6

Torsvik, N., Mortensen, S. and Nedreaas, K. (1995). *Fishery Biology (in Norwegian)*. Aurskog: Landbruksforlaget.

Turek, F. W., Joshu, C., Kohsaka, A., Lin, E., Ivanova, G., McDearmon, E., Laposky, A., Losee-Olson, S., Easton, A., Jensen, D. R. et al. (2005). Obesity and metabolic syndrome in circadian Clock mutant nice. *Science* **308**, 1043-1045. doi:10.1126/science.1108750

Vacquie-Garcia, J., Lydersen, C., Biuw, M., Haug, T., Fedak, M. A. and Kovacs, K. M. (2017). Hooded seal *Cystophora cristata* foraging areas in the Northeast Atlantic Ocean — investigated using three complementary methods. *PLoS One* **12**, e0187889. doi:10.1371/journal.pone.0187889

van Moorsel, D., Hansen, J., Havekes, B., Scheer, F. A. J. L., Jörgensen, J. A., Hoeks, J., Schrauwen-Hinderling, V. B., Duez, H., Lefebvre, P., Schaper, N. C. et al. (2016). Demonstration of a day–night rhythm in human skeletal muscle oxidative capacity. *Mol. Metab.* **5**, 635-645. doi:10.1016/j.molmet.2016.06.012

Vázquez-Medina, J. P., Olguín-Monroy, N. O., Maldonado, P. D., Santamaría, A., Königsberg, M., Elsner, R., Hammill, M. O., Burns, J. M. and Zenteno-Savín, T. (2011). Maturation increases superoxide radical production without increasing oxidative damage in the skeletal muscle of hooded seals (*Cystophora cristata*). *Can. J. Zool.* **89**, 206-212. doi:10.1139/Z10-107

Wang, G. L. and Semenza, G. L. (1993). General involvement of hypoxia-inducible factor 1 in transcriptional response to hypoxia. *Proc. Natl. Acad. Sci. USA* **90**, 4304-4308. doi:10.1073/pnas.90.9.4304

Yamazaki, S. and Takahashi, J. S. (2005). Real-time luminescence reporting of circadian gene expression in mammals. *Methods Enzymol.* **393**, 288-301. doi:10.1016/S0076-6879(05)93012-7

Zapol, W. M., Liggins, G. C., Schneider, R. C., Qvist, J., Snider, M. T., Creasy, R. K. and Hochachka, P. W. (1979). Regional blood flow during simulated diving in the conscious Weddell seal. *J. Appl. Physiol.: Respir. Environ. Exerc. Physiol.* **47**, 968-973.

Zhang, G. and Tandon, A. (2012). Quantitative assessment on the cloning efficiencies of lentiviral transfer vectors with a unique clone site. *Sci. Rep.* **2**, 1-8. doi:10.1038/srep00415

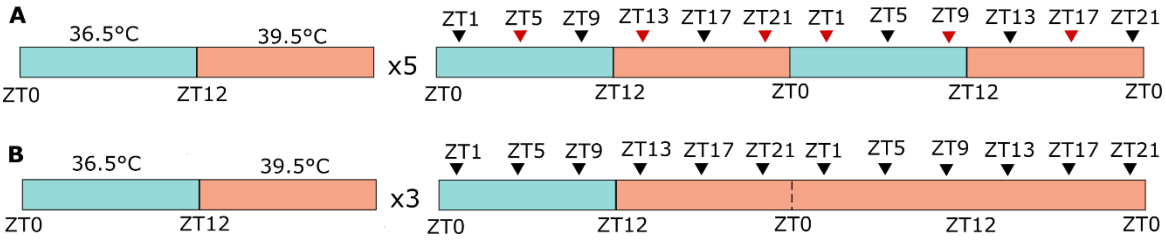

Fig. S1. Experimental design of temperature treatments used on hooded seal skin fibroblasts. A) Temperature cycling treatment: cells were exposed to 5 temperature cycles before being collected every 4 hours. Sampling start is indicated by arrow heads. Black arrow heads represent RNA sampling, red arrow heads represent RNA and mitochondrial oxygen consumption sampling. **B)** Constant temperature treatment: cells were exposed to 3 cycles of cycling temperature and then sampled at constant temperature. Only samples for RNA extraction were taken in this experiment. ZT= Zeitgeber Time.

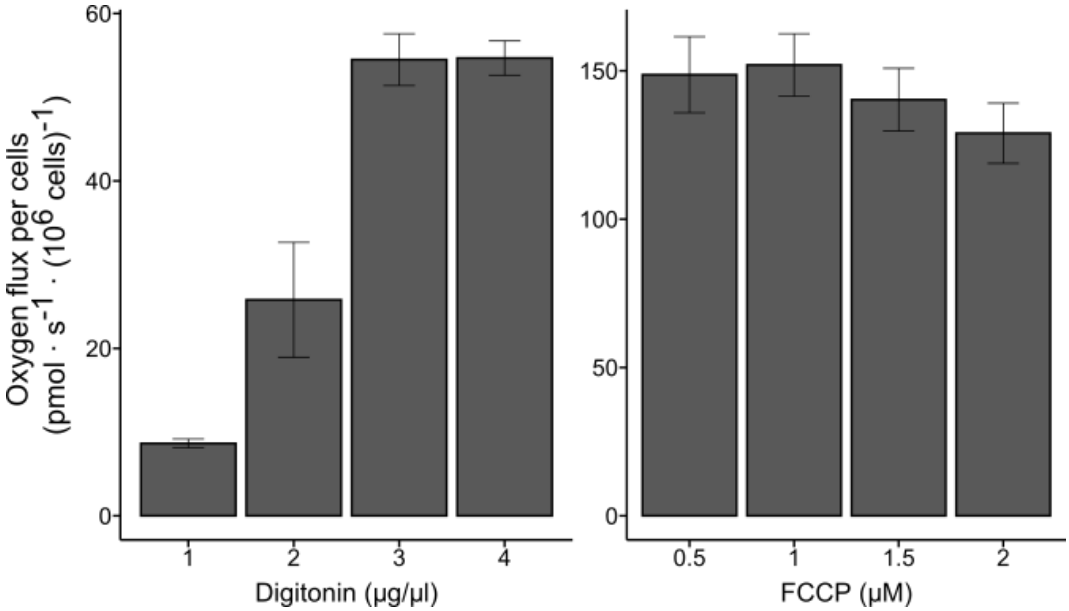

Fig. S2. Optimal concentration of digitonin and FCCP. Prior to the main experiments, the optimal concentrations of digitonin and FCCP were determined in separate pilot experiments. For digitonin, the SUIT-010 (Doerrier et al., 2018) was followed: optimal concentration was assumed when maximal O_2 flux was recorded in the chamber. For FCCP, cells were treated with multiple FCCP titrations until O_2 flux started to decrease. Data are represented as mean ± SEM and expressed as picomoles of O_2 per second per million cell (10^6 cells).

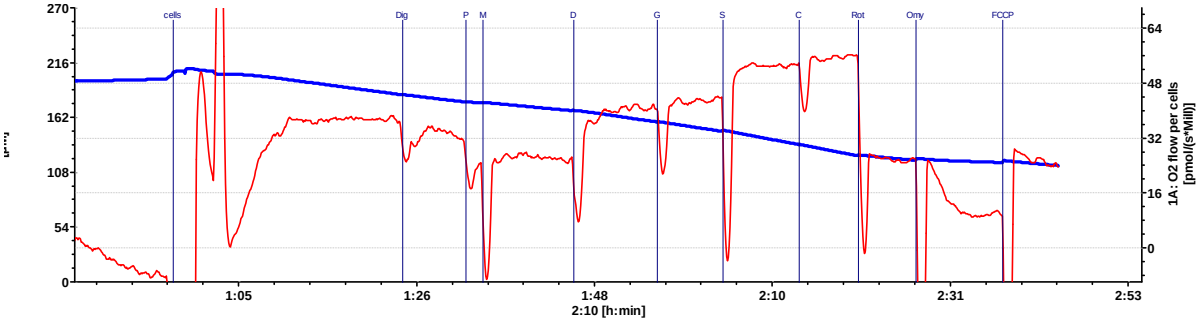

Fig. S3. Original oxygraph from mitochondrial respiration measurements. The oxygraph shows the real time changes in O_2 flow per cell (pmol • s^{-1} • $(10^6$ cells$)^{-1}$) in red and the O_2 concentration in the Oroboros oxygraphic chamber (µM) in blue. Vertical blue lines represent injections following the SUIT protocol explained in Table 2. Cells: insertion of cell sample in the oxygraphic chamber; Dig: digitonin; P: pyruvate; M: malate; D: ADP; G: glutamate; S: succinate; C: cytochrome c; Rot: rotenone; Omy: oligomycin; FCCP: uncoupler.

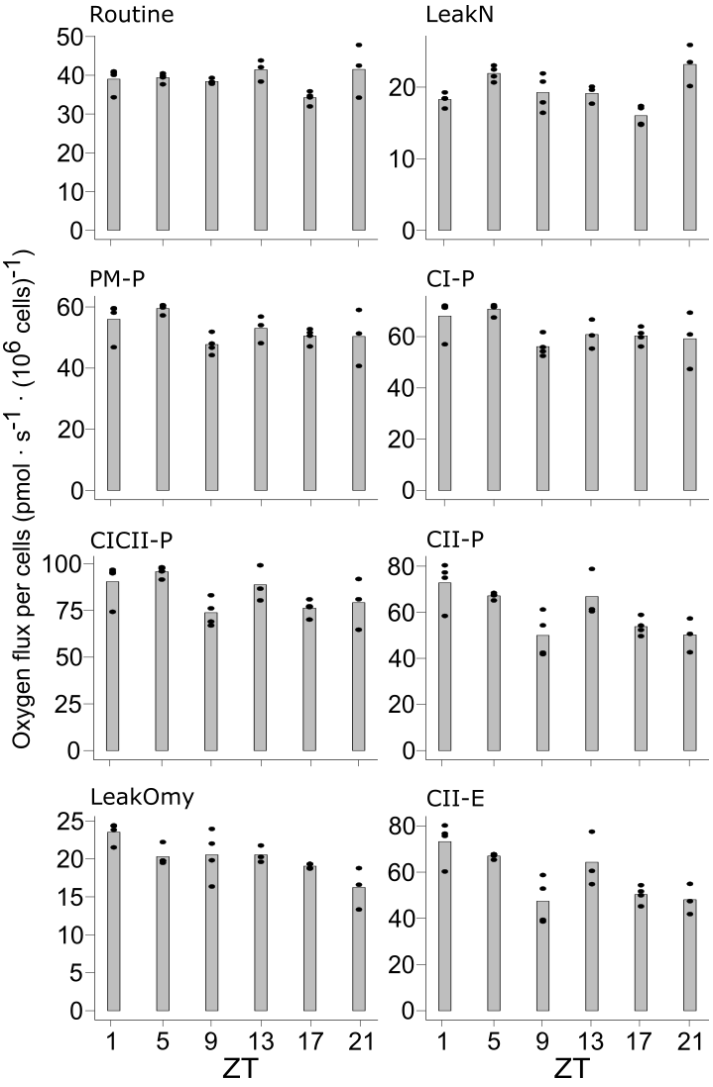

Fig. S4. Average oxygen flux per each mitochondrial state. The average measures for each mitochondrial state are shown in the figure as picomoles (pmol) of O_2 per second per million cell (10^6). Routine: basal respiration before addition of any substrate; LeakN: leak state at complex I in the presence of pyruvate and malate; PM-P: OXPHOS through complex I in the presence of pyruvate, malate and ADP; CI-P: OXPHOS through complex I in the presence of pyruvate, malate, glutamate and ADP; CICII-P: OXPHOS through complex I and complex II in the presence of pyruvate, malate, glutamate, succinate and ADP; CII-P: OXPHOS through complex II after inhibition of complex with rotenone I; LeakOmy: leak state at complex II after inhibition of ATP synthase with oligomycin; CII-E: uncoupled state measuring maximal mitochondrial capacity after addition of FCCP.

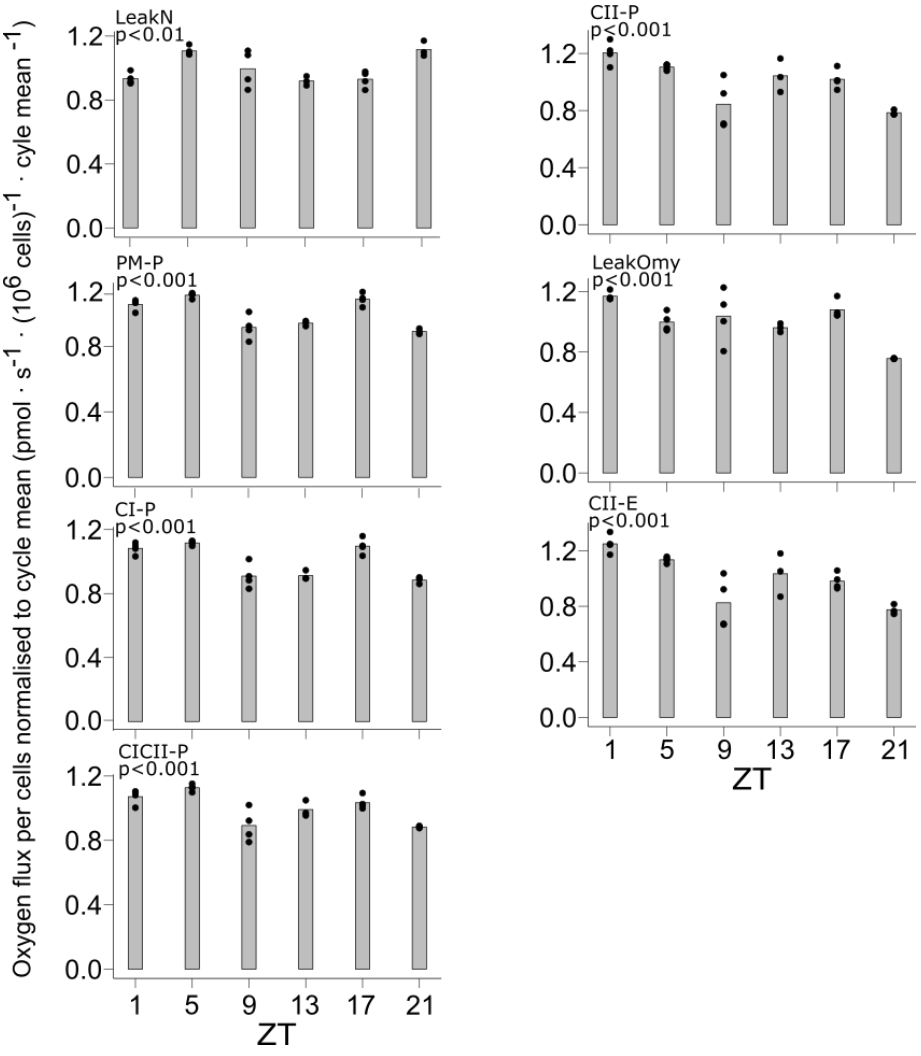

Fig. S5. Mitochondrial states normalised to cycle mean. Respiratory rates were first normalised to million cells (10^6) in DatLab software. Then, they were normalised to 'Routine respiration', defined as basal respiration without addition of any substrate (Table 2). Finally, the cycle mean was calculated and used to normalise the respiratory rate, expressed as a ratio of the mean, and represented as oscillations around the value 1. P-values are indicated as calculated across all the ZTs with one-way ANOVA. (Total n=22, with n=4 for each ZT except at ZT13, 21 where n=3). LeakN: leak state at complex I in the presence of pyruvate and malate; PM-P: OXPHOS through complex I in the presence of pyruvate, malate and ADP; CI-P: OXPHOS through complex I in the presence of pyruvate, malate, glutamate and ADP; CICII-P: OXPHOS through complex I and complex II in the presence of pyruvate, malate, glutamate, succinate and ADP; CII-P: OXPHOS through complex II after inhibition of complex with rotenone I; LeakOmy: leak state at complex II after inhibition of ATP synthase with oligomycin; CII-E: uncoupled state measuring maximal mitochondrial capacity after addition of FCCP.

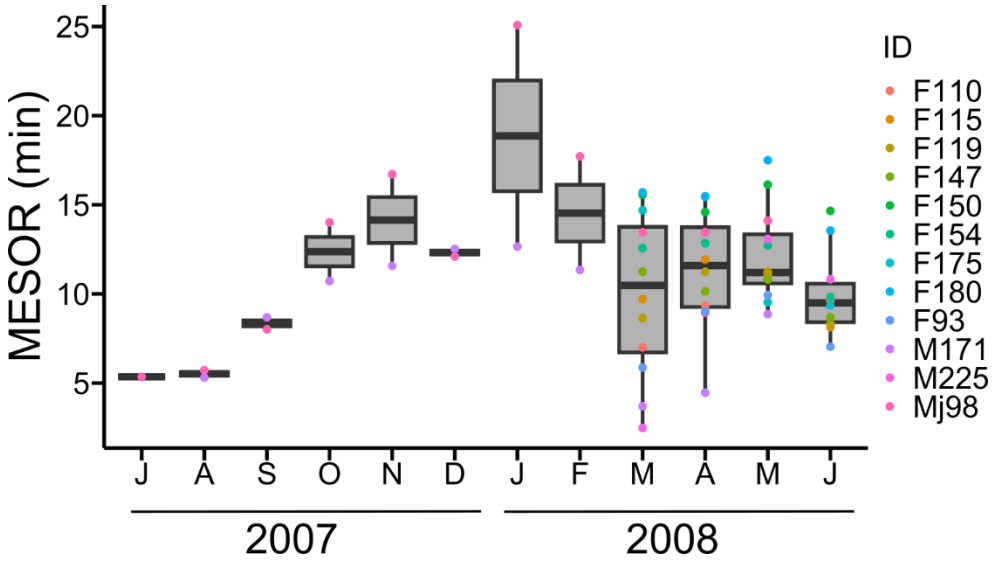

Fig. S6. Dive duration MESOR calculated for each seal and for each month from July 2007 until June 2008. In the legend, the seals IDs are listed with the gender (F=female, M=male) and their body weight. Only dives lasting between 2 min and 95 percentiles of maximal duration were considered in the analysis.

Paper II

Paper III